

สถาบันวิจัย จุฬาภรณ์ สถาบันบัณฑิต ศึกษาจุฬาภรณ์

มหาวิทยาลัย มหิดล มหาวิทยาลัย บูรพา มหาวิทยาลัย ธรรมศาสตร์

Center of Excellence on Environmental Health and Toxicology

Proceedings of The 17th Annual Conference on Highlighting Environmental Health Issues: Research towards Solutions



The Center of Excellence on Environmental Health and Toxicology's

Annual Academic Conference 2025 on the topic of

"Highlighting Environmental Health Issues: Research towards Solutions"

Saturday September 20th, 2025

Chulabhorn Research Institute Convention Center, Bangkok

Saturday, September 20th, 2025

08.30 - 09.00 AM Registration

09.00 - 09.10 AM Opening by Professor Emeritus Khunying Mathuros Ruchirawat

Director of Center of Excellence on Environmental Health and Toxicology

09.10 AM - 12.45 PM Roundtable discussion: Environmental Health Issues covered by the Center of Excellence's Research Framework

Group 1 Environmental pollutants that impact on human health and solutions to the issues

Air pollutants by Dr. Supat Wangwongwatana and Associate Professor Dr. Panida Navasumrit

Hazardous metals by *Professor Dr. Prayad Pokethitiyook Associate Professor Dr. Piyajit Watcharasit* and *Dr. Thitirat Ngaotepprutaram*

PFAS by Dr. Phum Tachachartvanich and Dr. Tawit Suriyo

Session moderators: Dr. Jakkaphan Nanuam

Group 2 Risk factors for liver cancer and AI screening tools

by Dr. M.L. Siritida Rabibhadana Dr. Benjarath Pupacdi Javed and Dr. Chalermpol Punnotok Session moderators: Assistant Professor Dr. Puey Ounjai

Group 3 Anti-microbial resistance (AMR)

by Dr. Nisanart Charoenlap and Dr. Punyawee Dulyayangkul

Session moderators: Associate Professor Dr. Rojana Sukchawalit

Group 4 Development of chemicals/therapeutics for treatment of disease

by Associate Professor Dr. Charnsak Thongsornkleeb and Dr. Charlermchai Artpradit Session moderators: Assistant Professor Dr. Puey Ounjai

*12.45 - 14.00 PM Lunch and Poster Presentation

14.00 - 15.30 PM Roundtable discussion: Role of the Center of Excellence in Capacity Building by

- Professor Emeritus Dr. M.R. Jisnuson Svasti

Director of Laboratory of Biochemistry, Chulabhorn Research Institute (CRI)

- Professor Dr. Sompong Klaynonsruang

Director of Thailand Science Research and Innovation (TSRI)

- Associate Professor Dr. Piniti Ratananukul

Vice Rector, Chulabhorn Graduate Institute (CGI)

- Mr. Ekapong Musikacharoen

Director of the Division for Science, Research and Innovation Promotion and Coordination, MHESI

Session moderator: Dr. Poonsakdi Ploypradith

15.30 - 16.45 PM Research presentations (oral) by lecturer/students from the 4 academic units

16.45 – 17.00 PM The website/expert dataset of the Hub of Talents on Environmental Health by Dr. Daam Settachan

17.00 - 17.30 PM Awards ceremony for poster presentations

Closing by Professor Emeritus Khunying Mathuros Ruchirawat

^{*}poster presenters ready at their posters at 13.15 PM

Center of Excellence on Environmental Health and Toxicology (EHT) Trends in Environmental Health (2025)

Organizing Committee

Chairperson

Prof. Dr. Khunying Mathuros Ruchirawat Director, EHT

Committee Members

Prof. Dr. Suchart Upatham
 Prof. Dr. Pornchai Matangkasombut
 Prof. Dr. Skorn Mongkolsuk
 Advisor, EHT
 Advisor, EHT

4. Assoc. Prof. Dr. Jutamaad Satayavivad Deputy Director, EHT

5. Assoc. Prof. Nardtida Tumrasvin Assistant Management Director, EHT

6. Prof. Dr. Prayad Pokethitiyook Representative, Faculty of Science,

Mahidol University

7. Prof. Dr. Somsak Ruchirawat Representative,

Chulabhorn Graduate Institute

8. Assoc. Prof. Dr. Panida Navasumrit Representative,

Chulabhorn Research Institute

9. Assoc. Prof. Dr. Prayoon Fongsatitkul Representative, Faculty of Public Health,

Mahidol University

10. Asst. Prof. Dr. Bhumiphat Pachana Representative, Faculty of Science,

Burapha University

Scientific Committee

1.	Assoc. Prof. Dr. Panida Navasumrit	Chulabhorn Research Institute/
		Chulabhorn Graduate Institute
2.	Assoc. Prof. Dr. Piyajit Watcharasit	Chulabhorn Research Institute/
		Chulabhorn Graduate Institute
3.	Dr. Poonsakdi Ploypradith	Chulabhorn Research Institute/
		Chulabhorn Graduate Institute
4.	Prof. Dr. Prasat Kittakoop	Chulabhorn Research Institute/
		Chulabhorn Graduate Institute
5.	Assoc. Prof. Dr. Paiboon Vattanaviboon	Chulabhorn Research Institute/
		Chulabhorn Graduate Institute
6.	Assoc. Prof. Dr. Mayuree Fuangthong	Chulabhorn Research Institute/
		Chulabhorn Graduate Institute
7.	Dr. Phum Tachachartvanich	Chulabhorn Research Institute/
		Chulabhorn Graduate Institute
8.	Prof. Dr. Prayad Pokethitiyook	Faculty of Science,
		Mahidol University
9.	Asst. Prof. Dr. Puey Ounjai	Faculty of Science,
		Mahidol University
10.	Assoc. Prof. Dr. Suphaphat	Faculty of Public Health,
	Kwonpongsagoon	Mahidol University
11.	Prof. Dr. Ubolluk Rattanasak	Faculty of Science, Burapha University
10		•
12.	Assoc. Prof. Pachoenchoke Jintasaeranee	Faculty of Science, Burapha University
13	Asst. Prof. Dr. Chantima Piyapong	Faculty of Science,
13.	Asst. 1101. Dr. Chantina 1 Tyapong	Burapha University

Logistics Committee

1. Mr. Preecha Sowanthip Manager of Central Facility, EHT

Mrs. Sasiwimol Hoontrakul Academic Officer, EHT
 Ms. Photjaman Nilbai Financial Officer, EHT

4. Ms. Pusadee Nokthong Coordinating Officer, EHT

5. Ms. Thitipat La-Ongnual Coordinating Officer, Faculty of Science,

Mahidol University, EHT

6. Ms. Preeyapatra Boonma Coordinating Officer, Faculty of Public Health,

Mahidol University, EHT

7. Ms. Phunyisa Boonkunth Coordinating Officer, Faculty of Science,

Burapha University, EHT

8. Ms. Thitirat Luangwong Database Administrator,

Hub of Talents in Environmental Health, EHT

9. Ms. Waraporn Nilbai Secretary & Project Coordinator,

Hub of Talents in Environmental Health, EHT

10. Ms. Wandee Sirapat Academic Officer,

Chulabhorn Research Institute

11. Mrs. Rungnapa Rungsa Coordinating Officer,

Chulabhorn Research Institute

12. Ms. Chalida Sangsawat Coordinating Officer,

Chulabhorn Research Institute

13. Mrs. Nattha Khamto Coordinating Officer,

Chulabhorn Research Institute

14. Mr. Pornthep Pongsao Educational Technologist,

Chulabhorn Research Institute

15. Mr. Pakorn Ontham Educational Technologist,

Chulabhorn Research Institute

Abbreviations

CGI = Chulabhorn Graduate Institute CRI = Chulabhorn Research Institute

PH = Faculty of Public Health, Mahidol University

SCBI = Environmental Biology / Biology, Faculty of Science, Mahidol University

SCTX = Toxicology, Faculty of Science, Mahidol University

EHT = Center of Excellence on Environmental Health and Toxicology

PERDO = S&T Postgraduate Education and Research Development Office

CONTENTS

IMPACTS OF CHEMICALS AND CLIMATE CHANGE ON HUMAN HEALTH AND DISEASE DEVELOPMENT AND FACTORS MODULATING SUCH IMPACTS	Pages
A MECHANISTIC STUDY OF POLYHALOGENATED CARBAZOLES (PHCZS) ON ADIPOGENESIS IN ADIPOSE-DERIVED MESENCHYMAL STEM CELLS (AD-MSCs)	1
Nattharat Donchalermsak, M.Sc. Student, (CGI)	
ASSESSMENT OF CYTOTOXICITY INDUCED BY NON-PSYCHOTROPIC CANNABINOID COMPOUND ON CHOLINOCEPTOR MODULATION IN CHOLANGIOCARCINOMA CELLS	5
Phetdalyvone Khounnorath, M.Sc. Student, (CGI)	
CARBON FOOTPRINT ASSESSMENT OF BAKED AND FRIED SNACK PRODUCTS USING A LIFE CYCLE APPROACH	9
Anuttara Sukkhapan, M.Sc. Student, (PH)	
EFFECTS OF ARSENIC EXPOSURE ON INSULIN-MEDIATED EXPRESSION OF <i>SCYL3</i> , <i>CDK8</i> , and <i>DEP-1/PTPRJ</i> IN DIFFERENTIATED HUMAN NEUROBLASTOMA SH-SY5Y CELLS	14
Tanawit Tapnan, M.Sc. Student, (CGI)	
EFFECTS OF PRENATAL EXPOSURE TO AMBIENT MICROPLASTICS: MATERNAL EXPOSURE AND ALTERED TELOMERE LENGTH AND MITOCHONDRIAL DNA COPY NUMBER IN NEWBORNS	18
Kusala Sithumini Sirirathna Kankanmalage, M.Sc. Student, (CGI)	
INVESTIGATION OF THE IMPACT OF <i>PLNS</i> , <i>PLNR</i> , AND <i>PLNP</i> ON ANTIBIOTIC RESISTANCE AND VIRULENCE IN <i>Stenotrophomonas maltophilia</i>	23
Phatcharin Laosena, M.Sc. Student, (CGI)	
PRELIMINARY STUDY OF POLLEN AND $PM_{2.5}$: SEASONAL OVERLAP AND IMPLICATIONS FOR ALLERGY PREVENTION	28
Lilian Haidvogl, M.Sc. Student, (SCTX)	
THE EFFECT OF ARSENIC EXPOSURE ON EXTRACELLULAR MATRIX REMODELING IN CHOLANGIOCARCINOMA MICROENVIRONMENT	33
Chilean Chheang, M.Sc. Student, (CGI)	
THE EVALUATION OF GREENHOUSE GAS EMISSIONS IN PRIMARY COFFEE CULTIVATION AND PRIMARY PROCESSING	37
Nutrada Wichanuchit, M.Sc. Student, (PH)	
TRANSCRIPTOMIC INSIGHTS INTO PA2806 DISRUPTION REVEAL ALTERED STRESS AND VIRULENCE BALANCE IN Pseudomonas aeruginosa PAO1	43
Duong Do Van, M.Sc. Student, (CGI)	

DEVELOPMENT OF BIOLOGICALLY ACTIVE COMPOUNDS FOR CONTROL, PREVENTION AND TREATMENT OF ENVIRONMENTAL HEALTH PROBLEMS/DISEASES	Pages
GREEN BANANA FLOUR AND PROBIOTIC SYNERGIES: UNLOCKING THE FUNCTIONAL FOOD POTENTIAL OF THAI BANANAS	47
Natchaya Chatsaengsupawong, M.Sc. Student, (SCBI)	
MELATONIN-MEDIATED MODULATION OF HYPOXIA-INDUCED NEUROINFLAMMATION IN SH-SY5Y HUMAN NEUROBLASTOMA CELLS	52
Kultasnim Kado, Ph.D. Student, (CGI)	
MODULATION OF GLYCOSYLATION PROFILE IN CHO-DERIVED MONOCLONAL ANTIBODY PRODUCTION USING MONOSACCHARIDE ANALOGUE	56
Diana Atsieno, M.Sc. Student, (CGI)	
PRODUCTION OF AN ANTIBODY AGAINST Burkholderia pseudomallei	60
Adiati Bintari Ayuningtias, M.Sc. Student, (CGI)	
PROTECTIVE EFFECTS OF MELATONIN ON ERASTIN-INDUCED FERROPTOSIS NEUROTOXICITY IN MURINE HIPPOCAMPAL HT-22 CELLS	65
Anuttree Boontor, (CRI)	
RUTIN: AN ANTI- INFLAMMATORY AGENT FOR MANGANESE INDUCED INFLAMMATION IN RAW 264.7 CELLS	70
Oneshi De Silva, M.Sc. Student, (CGI)	
SAFETY AND TOXICITY OF FOOD, DRUGS AND OTHER CHEMICALS INCLUDING BIOFUELS	
ECOLOGICAL RISK ASSESSMENT OF MICROPLASTICS POLLUTION IN THAILAND	75
Dr. Bongkotrat Suyamud, (PH)	
ENVIRONMENT / HEALTH IMPACT ASSESSMENT AND MANAGEMENT	
ASSESSING RECYCLING OF BEVERAGE CARTONS IN THAILAND: A PASSIVE COLLECTION SYSTEM	79
Sudthinee Wichenwan, M.Sc. Student. (PH)	

ENVIRONMENT / HEALTH IMPACT ASSESSMENT AND MANAGEMENT (Continued)	Pages
HEALTH RISK ASSESSMENT OF NICKEL AND CHROMIUM CONTAINING PARTICLES IN ARC WELDING FACTORY	84
Kanoot Jaikla, M.Sc. Student, (PH)	
INFECTIOUS WASTE GENERATION, KNOWLEDGE, ATTITUDE AND PRACTICE OF PERSONNELS TO THE INFECTIOUS WASTE MANAGEMENT IN SUB-DISTRICT HEALTH PROMOTION HOSPITAL OF THE RAYONG PROVINCIAL ADMINISTRATIVE ORGANIZATION	89
Thidarat Ouengsakuncharoen, M.Sc. Student, (PH)	
MICROPLASTICS IN EVERYDAY DIET: QUANTIFYING CONTAMINATION IN SOFT DRINKS AND SEAFOOD IN THAILAND	93
Dr. Anh Tuan Ta, (PH)	
THE ASSESSMENT OF HEALTH RISKS FROM CHEMICAL AND MICROBIOLOGICAL CONTAMINATION IN WATER USE: A CASE STUDY OF HUAI SO MUNICIPALITY, CHIANG KHONG DISTRICT, CHIANG RAI PROVINCE	96
Aim-on Khanmee, M.Sc. Student, (PH)	
THE EFFECTIVENESS OF FOOD HANDLER TRAINING COURSES ON HYGIENE AND SANITATION COMPETENCIES OF FOOD HANDLERS IN NONTHABURI MUNICIPALITY	101
Jenjira Duangsonsaeng, M.Sc. Student, (PH)	

Impacts of chemicals and climate change on human health and disease development and factors modulating such impacts



A MECHANISTIC STUDY OF POLYHALOGENATED CARBAZOLES (PHCZS) ON ADIPOGENESIS IN ADIPOSE-DERIVED MESENCHYMAL STEM CELLS (AD-MSCs)

Nattharat Donchalermsak¹, Phum Tachachartvanich^{2,3}, Panida Navasumrit^{2,3}, and Mathuros Ruchirawat^{2,3}

¹Environmental Toxicology Program, Chulabhorn Graduate Institute, Bangkok, Thailand, 10210 ²Environmental Toxicology Laboratory, Chulabhorn Research Institute, Bangkok, Thailand, 10210 ³Center of Excellence on Environmental Health and Toxicology (EHT) OPS, Thailand, 10210

Abstract:

Obesity is a metabolic disease characterized by high body mass index (BMI) and excessive body fat. The prevalence of obesity has rapidly increased in over the past decades. Evidence suggests that the etiology of obesity is associated with environmental exposure to obesogens, chemicals that can promote adiposity by reprograming adipocyte development. Various obesogens have been reported to promote obesity via the activation of peroxisome proliferator-activated receptor gamma (PPARγ), a master regulator of adipogenesis. In this study, we investigated the effect of emerging environmental polyhalogenated carbazoles (PHCZs) on adipocyte differentiation in human adipose-derived mesenchymal stem cells (AD-MSCs). Cells were treated with several PHCZs at environmentally relevant concentrations ranging from 0.05 - $15~\mu M$. As a result, PHCZs significantly promoted adipogenesis. We further investigated the molecular mechanism underlying PHCZ-induced adipogenesis by using a selective PPARy inhibitor. Intriguingly, the level of PHCZ-induced human adipocyte differentiation was completely mitigated by the treatment of a selective PPARy inhibitor (GW9662) suggesting that PHCZs promoted adipogenesis through the direct activation of the PPARy signaling pathway. Moreover, the gene expression profile of 15 adipogenesis related genes confirmed the role of PPARy in PHCZ-induced adipocyte differentiation. Altogether, our findings uncovered a group of novel environmental obesogens promoted adipogenesis at environmentally relevant concentrations and provided implications on metabolic effects posed by environmental chemicals.

Keywords: Polyhalogenated carbazole, obesogen, adipogenesis, endocrine disruptor, peroxisome proliferator-activated receptor gamma

Introduction:

Obesity is a multifactorial disease affecting millions of people worldwide across all age groups. The etiology of obesity is not only an imbalance between calorie intake and energy expenditure but also the exposure to some endocrine disruptors. An obesogen, a subset of endocrine disrupting chemicals (EDCs), is an exogenous chemical that mimics the structure of endogenous hormones, which can disrupt the homeostasis mechanism and ultimately promotes lipid accumulation and metabolic dysfunction. $PPAR\gamma$, a master regulator of adipogenesis, is a ligand-activated transcription factor that regulates adipose tissue growth and development via the induction of adipogenesis, a process of adipocyte differentiation.

Polyhalogenated carbazoles (PHCZs) are emerging contaminants frequently detected in various environmental matrices. Despite the similarity in terms of chemical structure to dioxin, the toxicity of PHCZs has been studied and confirmed as EDCs (Delfosse et al., 2015). However, the roles of these chemicals as novel obesogens have not yet been investigated. Accordingly, human adipose-derived mesenchymal stem cells (AD-MSCs) were used as a study model to investigate the adipogenic effect of PHCZs and its mechanism of action.

Methodology:

Cell line and cell culture

Adipose derived mesenchymal stem cell (ATCC® SCRC-4000TM) was obtained from American Type Culture Collection (ATCC).

Lipid staining

To assess the effect of PHCZs on adipocyte differentiation in AD-MSCs. Cells were treated with differentiation cocktails containing DMSO as a vehicle control, rosiglitazone: a positive control, 3,6-dibromocarbazole (3,6-BCZ), 3,6-dichlorocarbazole (3,6-CCZ), and 3-bromo-9-phenylcarbazole (3-B-9-PCZ) at concentrations ranging from 0.05 to 15 μ M for 16 days. To further investigate the roles of these chemicals in adipogenesis promotion through the PPAR γ signaling pathway, the test compounds were co-treated with GW9662 during the whole differentiation process. After incubation period, cells were fixed with 3.7% paraformaldehyde then stained with DAPI (nuclei) and BODIPY (lipid droplet).

Gene expression assay

The total RNA of PHCZs-treated AD-MSCs was extracted and converted into cDNA. The expression of genes relevant to PPARγ and adipogenesis was assessed using RT-qPCR.

Results and discussion:

PHCZ-induced adipogenic effect in AD-MSCs

As expected, AD-MSCs treated with rosiglitazone, a potent PPAR γ agonist had a significant increase in lipid accumulation in a concentration-dependent manner, indicating that the experimental model used in the present study was valid. Likewise, 3-B-9-PCZ, 3,6-BCZ and 3,6-CCZ also exhibited lipid accumulation in a similar manner to rosiglitazone (**Figures 2A-2D**). We also observed a significant decrease in lipid accumulation of structurally similar chemicals: 3,6-BCZ and 3,6-CCZ likely due to a cytotoxicity as shown in (**Figures 1B and 1C**). Interestingly, PHCZs exhibited the relatively strong potential in promoting adipogenesis when compared to other previously reported environmental obesogens like bisphenol analogs and flame retardants (Sun et al., 2025) as the PHCZs at the lowest concentration of 0.05 μ M can significantly promote adipogenesis. While other emerging contaminants such as bisphenol analogs exhibited the adipogenesis at 1–10 μ M. While rosiglitazone and 3-B-9-PCZ did not elicit any significant cytotoxic effects, the two PHCZs: 3,6-BCZ and 3,6-CCZ notably induced cytotoxicity at a concentration range of 10 to 15 μ M.

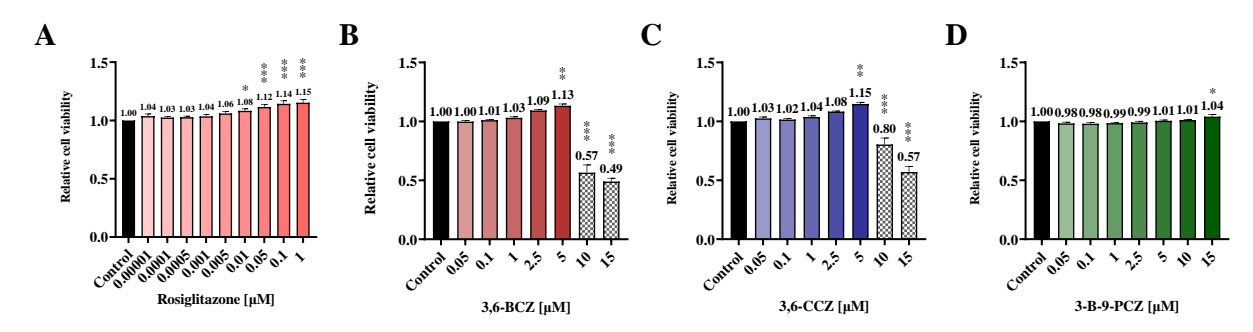


Figure 1 Effect of PHCZs exposure on viability of AD-MSCs treated with rosiglitazone, 3,6-BCZ, 3,6-CCZ, and 3-B-9-PCZ.

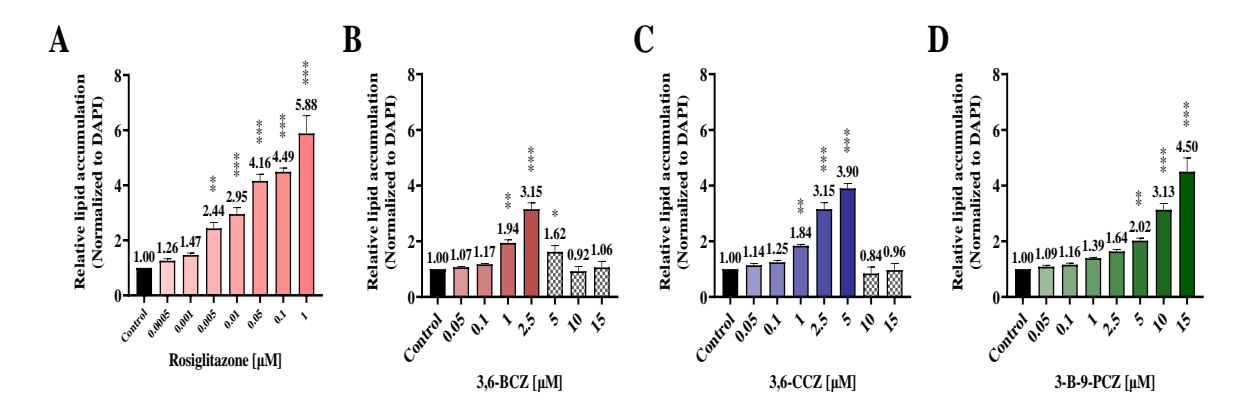


Figure 2 Effect of PHCZs exposure on adipogenesis of AD-MSCs treated with rosiglitazone, 3,6-BCZ, 3,6-CCZ, and 3-B-9-PCZ.

Effects of pharmacologic inhibition on PPARγ-dependent adipogenesis in AD-MSCs.

The results demonstrated that AD-MSCs exhibited a notable increase in lipid accumulation in groups treated with 3,6-BCZ, 3,6-CCZ, and 3-B-9-PCZ. As expected, the treatment of the PPARγ selective inhibitor GW9662 decreased PHCZ-induced adipogenic effects, indicating that PHCZs induce adipogenesis through activation of PPARγ (**Figure 3**).

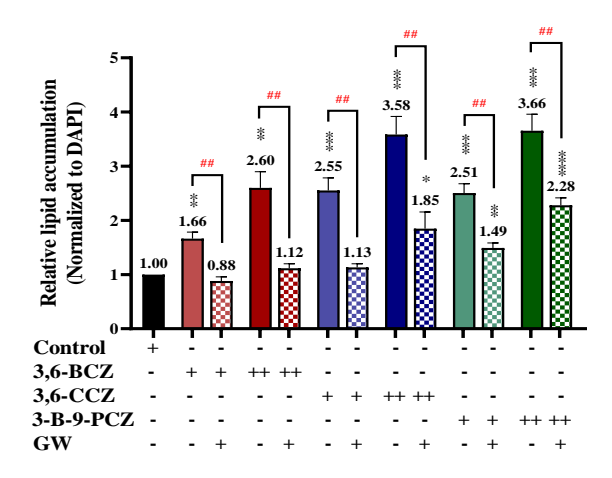


Figure 3 Effect of PPAR γ signaling selective inhibitor on PHCZ-induced adipogenesis in AD-MSCs. Cells were treated with various concentrations of treatment, including 0.2% v/v DMSO as a vehicle control, 1-2.5 μ M 3,6-BCZ, 2.5-5 μ M 3,6-CCZ, and 10-15 μ M 3-B-9-PCZ, in the presence and absence of GW9662.

Expression of adipogenic-mediated gene expression

At the transcription level, PHCZs showed a significant alteration in the expression of adipogenic and *PPARG*-mediated genes. The rosiglitazone treatment, as a positive control, notably increased the expression of genes associated with fatty acid oxidation (*MCAD*), fatty acid transport (*LPL* and *ACSL1*), cholesterol metabolism (*LXRA*), lipogenesis (*SCD1* and *FASN*), and adipocyte differentiation (*FABP4*, *ADIPOQ*, *CAP*, *PLIN4*, *PPARA* and *PPARG*). While GW9662 co-treatment showed a notable reduction in the aforementioned gene expression. As expected, 3,6-BCZ, 3,6-CCZ, and 3-B-9-PCZ also elevated in gene expression of adipocytes treated with only PHCZs, which were significantly mitigated by the treatment with GW9662. (**Figure 4**).

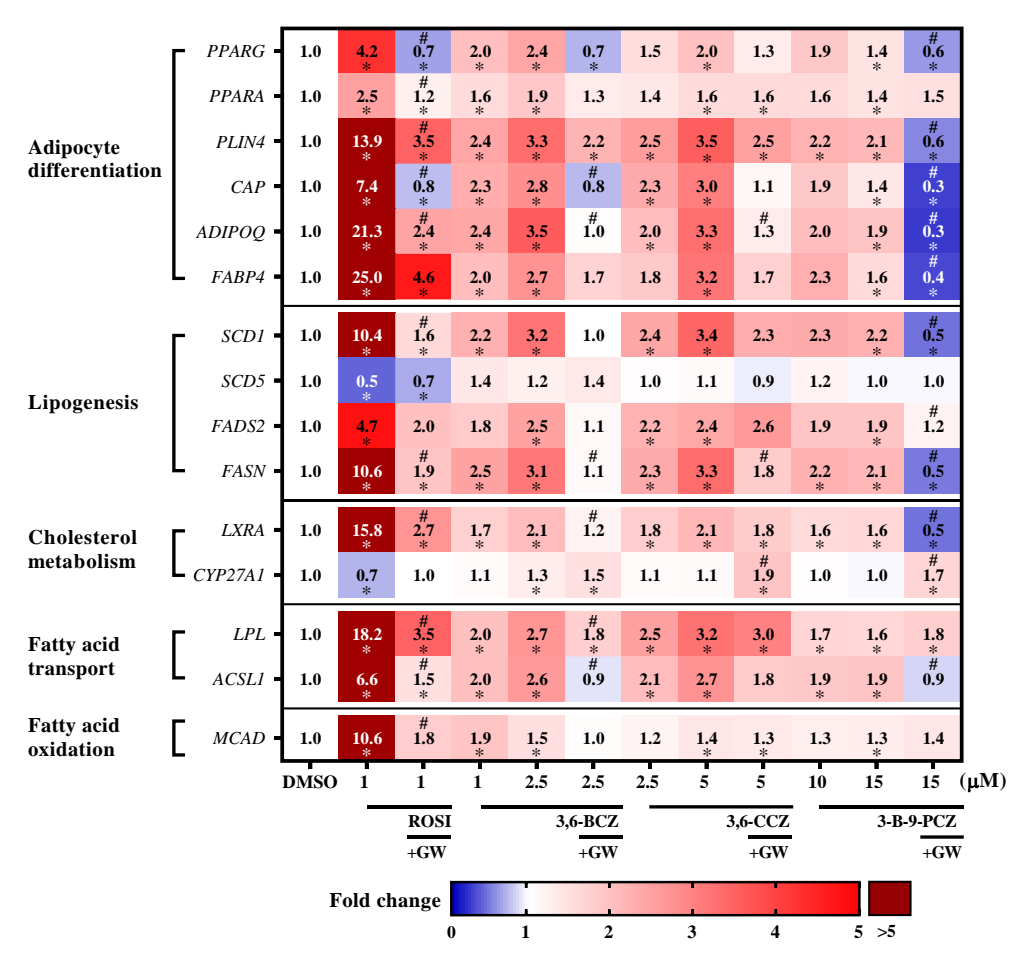


Figure 4 Heatmap displaying the expression of genes related to adipocyte differentiation, lipogenesis, cholesterol metabolism, fatty acid transport, and fatty acid oxidation in AD-MSCs treated with rosiglitazone, 3,6-BCZ, 3,6-CCZ, and 3-B-9-PCZ with and without GW9662.

Conclusion:

Collectively, PHCZs: 3,6-BCZ, 3,6-CCZ, and 3-B-9-PCZ exhibit the adipogenesis in AD-MSCs through the activation of PPARγ signaling pathway.

References:

- 1. Delfosse, V., Maire, A. I., Balaguer, P., and Bourguet, W. (2015). A structural perspective on nuclear receptors as targets of environmental compounds. *Acta Pharmacologica Sinica*, 36(1), 88-101. doi:10.1038/aps.2014.133
- Sun, Z., Zhang, S., Liang, J., Li, C., Yang, X., Liu, Q. S., Zhou, Q., Shi, J., Zhao, B., and Jiang, G. (2025). Effects of multiple novel bisphenol S analogs on adipogenesis in 3T3-L1 cells. *Journal of Hazardous Materials*, 489, 137689. doi:10.1016/j.jhazmat.2025.137689

ASSESSMENT OF CYTOTOXICITY INDUCED BY NON-PSYCHOTROPIC CANNABINOID COMPOUND ON CHOLINOCEPTOR MODULATION IN CHOLANGIOCARCINOMA CELLS

<u>Phetdalyvone Khounnorath</u>¹, Jantamas Kanitwithayanun^{2,3,4}, Nedsai Uddin Babar³, Noppawan Rittapai³, and Jutamaad Satayayiyad^{2,3,4}

¹Applied Biological Sciences: Environmental Health program, Chulabhorn Graduate Institute, Bangkok, Thailand

²Environmental Toxicology program, Chulabhorn Graduate Institute, Bangkok, Thailand ³Laboratory of Pharmacology, Chulabhorn Research Institute, Bangkok, Thailand ⁴Center of Excellence Environmental Health and Toxicology (EHT), OPS, MHESI, Thailand

Abstract:

Cholangiocarcinoma (CCA) is a bile duct cancer with poor prognosis. Both cannabinoid receptors (CBs) and acetylcholine receptors (AChRs) are expressed in CCA cells. HU-308, a selective CB2 agonist, is a non-psychotropic synthetic cannabinoid with anti-inflammatory, analgesic, anti-hypertension properties. However, its cellular toxicity in cancer remains poorly understood. While cannabinoid-cholinergic interactions affect memory, little is known about CBs mediated growth inhibition in cancer cells. This study investigated *in vitro* cytotoxicity of HU-308 in CCA cells, focusing on its molecular mechanisms and the modulation of cholinoceptors including M3-mAChR and α7-nAChR. **Method:** KKU-100, a human CCA cell line, was treated with HU-308 for 24 h. The effects on cell viability, cholinoceptors expression and apoptosis level were evaluated by MTT viability assay, Western immunoblotting, and flow cytometry, respectively.

The results: HU-308 (50-200 μ M) showed a reduction in cell viability which was mitigated by pre- and co-treatment with a selective CB2 antagonist (AM630 10 nM), confirming CB2 involvement. Apoptotic cells were significantly increased after HU-308 treatment compared to control group. Moreover, the intrinsic pro-apoptotic Bax protein has a trend towards increasing, while anti-apoptotic Bcl2 protein was decreased by HU-308 treatment. Additionally, α 7-nAChR protein expression was reduced, but M3-mAChR did not show any reduction.

In conclusion: HU-308, a selective CB2 agonist, exerted cytotoxic effects in KKU-100 cells through activation of the intrinsic apoptotic pathway and downregulation of α 7-nAChR which may, at least in part, offer a potential effective on anticancer effects in CCA cells.

Keywords: Cannabinoid receptor subtype 2 (CB2), cytotoxicity, cholangiocarcinoma, apoptosis, cholinoceptor.

Introduction:

Cannabinoids are active compounds original discovered in *Cannabis sativa* L., commonly as marijuana. These compounds primarily interact cannabinoid receptor type 1 (CB1), located mainly in central nervous system; and cannabinoid receptor type 2 (CB2), found predominantly in immune cells and peripheral tissues (1). CB2 represents a promising therapeutic target due to its anti-cancer properties without psychoactive side effects. HU-308 is a synthetic selective CB2 agonist, has demonstrated anti-inflammatory, anti-hypertensive, anti-osteoporotic, and analgesic activities (2). Crucially, HU-308 exhibits anti-cancer

mechanism by inhibiting forskolin-stimulated cAMP production in CB2-transfected cells, where cAMP inhibition triggers death pathways that induce cytotoxic effects and inhibit cancer cell growth. This evidence suggests that selective CB2 agonist like HU-308 could serve as effective cancer therapeutics while avoiding psychotropic effects associated with CB1 activation.

Cholangiocarcinoma (CCA) is a cancer arising from bile ducts epithelial cells that frequently invade blood vessels and metastasis to other parts of the body. Consequently, patients are typically diagnosed at advanced stages, limiting treatment options resulting in high fatality rates. Currently, several studies have demonstrated an increase in CB1 and CB2 expressions in various human malignancies including CCA. Increase expression of these receptors is associated with increased disease progression. However, little is known about the role of CBs in CCA cells. Previous study reported that THC and cannabinol could trigger apoptosis in human CCA cell line (HuCCT1, from intrahepatic bile ducts) by suppressing the AKT and MAPK signaling pathway, contribute to reduced cell proliferation.

Cholinergic neuron is a specific neuronal cell that produces acetylcholine (ACh). It has been reported that cholinoceptors including M3-mAChR and α 7-nAChR were found highly expressed in CCA (3, 4). α 7-nAChR and M3-mAChR expressions play a crucial role in cancer-related characteristic, including promoting proliferation, inhibiting apoptosis and enhancing metastasis (5). However, the specific function of CBs in suppressing tumor growth in CCA cells, along with their interactions with cholinergic components, remains poorly understood. Therefore, this study focuses on evaluating the *in vitro* cytotoxicity of HU-308, a non-psychotropic cannabinoid compound and selective CB2 agonist, on KKU-100 cells growth and the possible mechanisms underlying their effects as well as the modulation of cholinoceptors including M3-mAChR and α 7-nAChR were also investigated.

Methodology:

Cell culture

CCA cell line derived from Thai CCA patient as KKU-100 was cultured in Dulbecco's Modified Eagle Medium (DMEM) supplemented with 10% fetal bovine serum (FBS), 1%L-Glutamine, 1% antibiotics (100 U/mL of penicillin and 100 $\mu g/mL$ of streptomycin) and maintained under a humidified atmosphere containing 5% CO $_2$ at 37 $^{\circ}$ C in an incubator.

Cell viability assay

KKU-100 cells were seeded in 96-well plate at a density of 10,000 cells per well. After 24 h, cells were treated with HU-308 at concentrations 1, 10, 25, 50, 100, and 200 μM or medium as control for 24 h. For antagonist treatment, KKU-100 cells were pre-treated with 10 nM AM630, a CB2 antagonist, for 30 min before being co-treated with HU-308 (50, 100, and 200 μM) for 24 h. At the end of incubation time, MTT solution was added, then incubated for 4 h. Thereafter, the absorbance was measured at 570 nm using a microplate reader.

Protein preparation and Western blotting

The collected cells were lysed with lysis buffer, then sonicated and centrifuged at 14,000 rpm for 20 min at 4°C and the supernatant was collected. Protein concentrations were determined using Bradford reagent. Protein sample (30 µg) was electrophoresed onto a 7.5 or 10% SDS-polyacrylamide gel. Then, the separated protein bands were transferred onto a nitrocellulose membrane. After that, the membrane was blocked with 5% skim milk in TBST buffer for 1 h at RT, followed by overnight incubation with the specific primary

antibodies: Bax, Bcl2, PARP-1, M3-mAChR, and α 7-nAChR. The proteins bands were visualized by using enhanced chemiluminescence (ECL) and quantified using the ChemiDoc Imaging Machine with the ChemiDoc system, Bio-rad. The signal of each immunoblot sample was normalized with β -actin.

Cell apoptosis assay

To determine the apoptotic effect of HU-308 on KKU-100 cells, cells were seeded in 6-well plate with a density of 6×10^5 cells per well. Thereafter, the cells were treated with various concentrations of HU-308 (10, 25, 50, and 100 μ M) for 24 h. At the end of the experiment, cells were harvested and stained with Annexin V conjugated with fluorescein isothiocyanate (FITC) and propidium iodine (PI) for 15 min. Apoptotic cells were analyzed by flow cytometry, and the percentages of healthy, early apoptotic, late apoptotic and necrotic populations were quantified with the FlowJo v10 software.

Statistical analysis

All results are expressed as mean \pm standard errors (SEM). Unless otherwise specified, statistical analysis for multiple comparisons was performed using one-way analysis of variance (ANOVA). A p-value<0.05 was considered statistically significant. Calculation of inhibitory concentration at 50% (IC50) and all statistical analyses were performed using GraphPad Prism 8.

Results and discussion:

MTT assay results revealed that treatment with 50, 100, and 200 μ M HU-308 for 24 h significantly inhibited KKU-100 cell growth in concentrations-dependent manner (50 μ M, 1.29-fold; 100 μ M 1.90-fold and 200 μ M, 3.83-fold) compared to control. The reduction of KKU-100 cell viability following HU-308 treatment (50, 100, and 200 μ M) was reversed by pre- and co-treatment with AM630, a selective CB2 antagonist, at 10 nM. The IC50 of HU-308 treatment alone was 155 μ M. Notably, when HU-308 was combined with 10 nM AM630, the IC50 value shifted to 177 μ M. These results suggested that the growth inhibitory effect of HU-308 on KKU-100 cells may, at least in part, involved CB2 receptor activation.

Next experiment was performed whether the reduction of cell viability was associated with cell apoptosis by using flow cytometry analysis. The result found a concentration-response increase in total apoptotic cells (both early and late) following 24 h treatment with HU-308 at 10, 25, 50 and 100 μ M. The percentage of early apoptotic cells increased significantly by 1.89-, 2.29-, 3.19-, and 6.24-fold respectively, compared to the control. Similarly, the percentage of late apoptotic cells was significantly elevated by 1.05-, 1.36-, 1.59-, and 1.99-fold, respectively. These findings indicated that the mechanism by which HU-308 inhibits KKU-100 cell growth involved the induction of cell apoptosis.

To further investigate the mechanisms underlying HU-308-induced apoptosis, protein expression levels were analyzed. The result showed an upregulation of Bax, a key proapoptotic protein and cleaved PARP-1, indicate as marker of apoptosis. Conversely, the expression of Bcl2, an anti-apoptotic protein and cell survival marker, was significantly downregulated. Additionally, the Bax/Bcl2 ratio was significantly increased with concentration-dependent manner. These results indicate that HU-308 induced KKU-100 cell death may be associated with intrinsic apoptotic signaling pathways. Regarding the cholinergic receptor expression, the α 7-nAChR showed significantly decreased with HU-308 at 50 μ M for 24 h, while no significant reduction was observed in M3-mAChR. This result suggested that HU308 induced growth inhibitory effect in KKU100 cells may be mediated, at least in part, through the downregulation of α 7-nAChR.

Conclusion:

These findings demonstrate that activation of CB2 by HU-308, a selective CB2 agonist, induces cytotoxic effects in KKU-100 cells through activation of the intrinsic apoptotic pathway. Additionally, HU-308 significantly downregulated α 7-nAChR expression, a receptor known to play a role in cancer progression. Together, these results suggest that HU-308 may exert its effects via mechanisms involving both enhanced apoptosis and reduced expression of the cholinoceptor α 7-nAChR in KKU-100 cells.

References:

- 1. Bie B, Wu J, Foss JF, Naguib M. An overview of the cannabinoid type 2 receptor system and its therapeutic potential. Curr Opin Anaesthesiol. 2018;31(4):407-14.
- 2. Hanus L, Breuer A, Tchilibon S, Shiloah S, Goldenberg D, Horowitz M, et al. HU-308: a specific agonist for CB(2), a peripheral cannabinoid receptor. Proc Natl Acad Sci U S A. 1999;25):14228-33.
- 3. Chen S, Kang X, Liu G, Zhang B, Hu X, Feng Y. α7-Nicotinic Acetylcholine Receptor Promotes Cholangiocarcinoma Progression and Epithelial–Mesenchymal Transition Process. Digestive Diseases and Sciences. 2019;64(10):2843-53.
- 4. Feng Y, Hu X, Liu G, Lu L, Zhao W, Shen F, et al. M3 muscarinic acetylcholine receptors regulate epithelial-mesenchymal transition, perineural invasion, and migration/metastasis in cholangiocarcinoma through the AKT pathway. Cancer Cell Int. 2018;18:173.
- 5. Singh S, Pillai S, Chellappan S. Nicotinic acetylcholine receptor signaling in tumor growth and metastasis. J Oncol. 2011;2011:456743.

CARBON FOOTPRINT ASSESSMENT OF BAKED AND FRIED SNACK PRODUCTS USING A LIFE CYCLE APPROACH

Anuttara Sukkhapan¹, Chaowalit Warodomrungsimun^{1,2}, Withida Patthanaissaranukool^{1,2}, Chatchawal singhakant^{1,2} and Supawadee Polprasert^{1,2}

¹Department of Environmental Health Sciences, Faculty of Public Health, Mahidol University, Bangkok, Thailand ²Center of Excellence on Environmental Health and Toxicology (EHT), OPS, MHESI, Thailand

Abstract:

Climate change and environmental sustainability have become urgent global concerns, primarily driven by human activities such as energy consumption and industrial expansion, which are the main contributors to greenhouse gas (GHG) emissions. This study aims to analyze and compare the carbon footprint of crispy snack products produced as baked and fried processes using the Life Cycle Assessment (LCA) approach within a cradle-to-gate system boundary. The assessment was conducted using data from a snack manufacturing facility located in Nakhon Pathom Province, Thailand. The functional unit was set at 13 grams per snack package. GHG emissions were calculated in terms of carbon dioxide equivalent (CO2e) across all production stages, from raw material acquisition to the final product. The results show that the fried snack products generate significantly higher GHG emissions compared to the baked products. This is mainly due to the use of wheat flour and tapioca starch, along with coal as the primary energy source in the production process. The baking process, on the other hand, demonstrated greater energy efficiency and lower emissions. These findings provide valuable insights for the development of policies and strategies aimed at reducing the environmental impacts of the food industry in Thailand, promoting sustainable production, and enhancing international trade competitiveness.

Keyword: Life cycle assessment, greenhouse gases, global warming potential, allocation

Introduction:

Climate change and environmental sustainability have become pressing global concerns in the contemporary era, largely due to increasing pollution in various forms air, water, waste disposal, and transportation. Human activities, particularly energy consumption and industrial expansion, have significantly contributed to increase greenhouse gas (GHG) emissions, which in turn disrupt ecosystems and accelerate global warming. Climate change is widely recognized as one of the greatest challenges of the twenty-first century. According to the Sixth Assessment Report (AR6) of the Intergovernmental Panel on Climate Change (IPCC), human activities are the primary cause of the increase in GHG emissions, resulting in a rise of more than 1.1°C in global average temperature compared to pre-industrial levels. This figure is projected to reach 1.5°C within the next two decades if no decisive mitigation measures are undertaken [1]. The consequences include more frequent and severe extreme weather events, greater risks to the global economy, social systems, and food security.

In response to this crisis, the global community has sought cooperative solutions through international agreements. The Paris Agreement, adopted at COP21, established the target of keeping the increase in global temperature well below 2 °C and pursuing efforts to limit it to 1.5 °C. More recently, COP26, held in Glasgow in 2021, reaffirmed the urgency of reducing fossil usage, expanding renewable energy, and supporting developing nations in adapting to and mitigating climate impacts. Many countries, including Thailand, have

announced long-term commitments to achieve carbon neutrality by 2050 and net-zero GHG emissions by 2065. Meanwhile, trade-related measures have emerged as influential drivers of change. The European Union's Carbon Border Adjustment Mechanism (CBAM), currently applies to several industries and is expected to expand to agricultural and food products in the future. This development has prompted agri-food industries worldwide to accelerate efforts in reducing GHG emissions across supply chains to safeguard their competitiveness in international markets. At the same time, consumers in developed nations increasingly demand safe, high-quality food produced with minimal environmental impact.

A key instrument in assessing environmental performance is the measurement of a product's carbon footprint, which refers to the total GHG emissions generated throughout its life cycle. Life Cycle Assessment (LCA), standardized under ISO 14040 and 14044, is a widely accepted methodology for evaluating the Carbon Footprint of Products (CFP). It encompasses the entire process, from raw material acquisition, transportation, and production to energy use and waste management. LCA provides insights into the main sources of emissions and identifies opportunities for improvement, such as adopting clean energy, modernizing production technologies, or sourcing sustainable raw materials. The adoption of carbon footprint measurement not only enhances transparency and accountability but also strengthens the credibility of businesses. Environmentally responsible enterprises often referred to as "green businesses" tend to gain advantages in international trade, as reducing emissions has become a decisive factor influencing both business strategies and consumer preferences. Beyond compliance, carbon footprint analysis serves as an essential tool for innovation, product development, and sustainable marketing[3].

The food industry, broadly defined as the sector that transforms agricultural products, including crops, livestock, and fisheries into food through processing and preservation technologies, plays a central role in producing safe, reliable, and convenient food on a large scale. Within this sector, the snack industry is particularly resource- and energy-intensive. Crispy snack production, for instance, can rely on frying or baking methods, which differ substantially in terms of energy use and GHG emissions. A comparison of the carbon footprints associated with these two processes therefore provides critical insights into their respective environmental impacts, offering guidance for producers seeking more sustainable manufacturing methods.

This study aims to analyze the carbon footprint of crispy snack products both baked and fried processes as a means of enhancing environmental performance. Despite the increasing significance of carbon footprint assessment, research applying the LCA methodology to snack products in Thailand remains scarce. To address this gap, the present study focuses on a case of a snack production facility located in Nakhon Pathom Province. The assessment applies the cradle-to-gate system boundary, covering all processes from raw material acquisition to the final production stage. Greenhouse gas emissions are quantified in terms of carbon dioxide equivalent (CO₂e). The analysis is intended to identify major emission sources and propose strategies for reducing environmental impacts. The findings are expected to provide valuable guidance for formulating policies and strategies to reduce environmental burdens in both existing and future food production facilities, not only in Nakhon Pathom but also across Thailand.

Methodology:

This study is analytical research. To assess the environmental impacts and product carbon footprint of crispy snack production based on life cycle assessment (LCA) principles.

Life Cycle Assessment

This research study was conducted using guidelines from the ISO 14040, 14044 standard series for Product Life Cycle Assessment (LCA)[4], which is a tool for analyzing and evaluating environmental impacts. The steps involved are: 1) setting goals and scope, 2) environmental inventory analysis, 3) environmental impact assessment, 4) carbon footprint assessment of the product, and 5) Interpretation.

To study the use of resources, energy, and waste and determine the functional units of the product and specification of functional units. The assessment result of greenhouse gas emissions must be in the form of CO₂eq unit of operation. Scope in this study consider as "Cradle to Gate" study focuses solely on the process from raw material acquistion to the finished product. This includes sub-processes such as incoming raw material, production process, packaging material, electricity and thermal power generation systems, water systems, and waste management and functional Unit (FU) 13 grams of crispy snack product (1 packet) **According to Figure 1.**

Within the factory, Allocation methods are required when two or more products or co-products share the same production processes. For this study was estimated on the basic of mass allocation.

Raw material acquisition

Wheat flour/Cassava starch

Palm Oil

Seasoning

Transportation

Fuel (Fosil, LPG)

Flying, Mixing seasoning, Packing

Fried crispy snack Production

Baked crispy snack Production

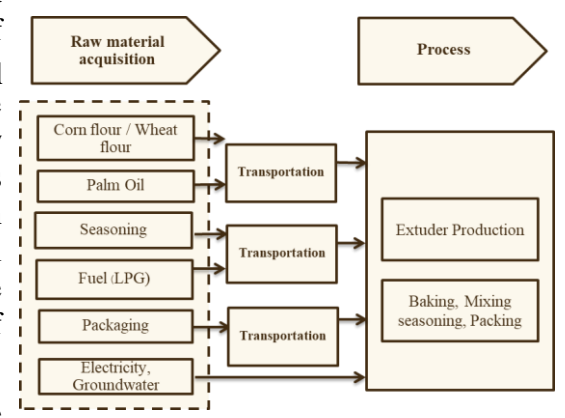


Figure 1 The cradle-to-gate system boundary boundaries of Baked and fried crispy snack

Environmental impact assessment, Life cycle inventory (LCI) results in this study are classified into only global warming potential (GWP). Total GHG emission expressed as $kgCO_2e$ were determined as $CF = \Sigma$ (Activity data_i x Ef_i) where: Activity data_i = life cycle value of i, unit and EF_i = emission factor of i, $kgCO_2e$ /unit which used Thailand National Guidance on Carbon Footprint Calculation for Products[2].

Results and Discussion:

Carbon footprint of Baked crispy snack production

The production process of baked snack products involves several sequential stages, including raw material reception, dough preparation through the mixing of flour with water, extrusion, cutting, drying using liquefied petroleum gas (LPG), seasoning, and packaging. For the life cycle inventory (LCI), both primary and secondary data were employed. Primary data were collected through on-site measurements; however, their direct application is constrained by several limitations. Firstly, the data are not product-specific, as the factory manufactures multiple product types using shared resources and utility systems, making it difficult to allocate resource consumption to an individual product. Secondly, precise

measurements of raw material inputs and product outputs are required to establish reliable mass balances, which are not consistently available. Thirdly, verification of the mass balance is essential to ensure data completeness and accuracy. Lastly, pollutant emission data are generally reported in aggregated form across water, electricity, and waste streams, without differentiation by production stage, thereby hindering the identification of specific processes that contribute most significantly to environmental impacts. The proportions in the production process between baked and fried crispy snacks are 7.59% and 31.16%, respectively.

The analysis of the data reveals that the raw materials acquistion the carbon emissions are presented in Table1. In terms of energy use during the production process, Electricity consumption (in process) 0.003 kg CO₂-eq/kWh, Natural gas consumption (LPG gas) 0.010 kg CO₂-eq/t. The analysis revealed that the raw materials contributing most significantly to greenhouse gas emissions are wheat flour, corn starch, and palm oil, whereas salt and sugar exhibit relatively low environmental impacts. In the production process, electricity and liquefied petroleum gas (LPG) are the primary sources of carbon emissions. Although their individual emission factors (EFs) are not particularly high, the total emissions become substantial due to the large quantities consumed. These factors collectively contribute to a significant carbon footprint of the final product.

Carbon footprint of fried crispy snack production

The production process of fried snack products comprises raw material incoming, dough preparation through mixing flour with solution water, crude rice production, Frying, mixing seasoning, and packaging. The analysis of the data reveals that the raw materials acquistion the carbon emissions are presented in Table 1

In terms of energy use during the production process, Electricity consumption (in process) 0.046 kg CO₂-eq/kWh, Fuel consumption 0.205 kg CO₂-eq/t. These results indicate that the carbon footprint of the fried snack product is primarily influenced by both high-impact raw materials and energy-intensive processing stages. Among the raw materials, cassava starch and wheat flour contribute the highest greenhouse gas emissions, attributable to the upstream agricultural practices and processing operations required for their production. Palm oil also presents a considerable impact due to the environmental burden associated with its cultivation. Conversely, ingredients such as salt, sugar, and seasoning contribute minimally to overall emissions due to their low emission factors and relatively small quantities used in the formulation.

Table 1 Carbon emission of baked and fried crispy snack production

Baked production	carbon emissions	Fried production	carbon emissions
	kg CO2-eq/t-product		kg CO ₂ -eq/t-product
Wheat flour	0.035,	Wheat flour	0.743
Corn flour	0.030	Cassava starch	0.979
Salt	2.98E-06	Salt	2.44E-05
sugar	0.004	sugar	0.027
Plam oil	0.032	Plam oil	0.154
Seasoning	0.009	Seasoning	0.005

Conclusion:

The comparative assessment of the carbon footprint between baked and fried crispy snack products highlights significant differences in their environmental impacts, primarily resulting from raw material acquisition and production processes. The production of fried snacks generates substantially higher greenhouse gas emissions, particularly due to the use of high-impact ingredients such as cassava starch and wheat flour, as well as the use of fuel as a primary energy source during processing. In contrast, baked snacks demonstrate a lower carbon footprint per unit, attributed to the use of raw materials with lower emission factors (EFs) and reduced energy consumption, such as the use of LPG gas for drying and lower electricity usage. However, data limitations, especially in the production of baked snacks, need to be addressed through accurate mass balance tracking, appropriate allocation of shared resources, and process-specific pollutant reporting to enhance the reliability of the Life Cycle Assessment (LCA) results. Overall, the study underscores the potential for reducing environmental impacts in the snack food industry through product reformulation, enhanced process efficiency, and systematic energy optimization, which collectively represent promising strategies for lowering the carbon footprint of food manufacturing.

Acknowledgments:

The authors would like to express their gratitude to the Department of Environmental Health Sciences, Faculty of Public Health, Mahidol University for instrument and technical support. Also, the authors would like to thank the Center of Excellence on Environmental Health and Toxicology (EHT), OPS, Ministry of Higher Education, Science, Research, and Innovation for their excellent technical support.

References:

- 1. United Nations Framework Convention on Climate Change. (2021). COP26 Glasgow climate pact. UNFCCC.
- 2. Thailand Greenhouse Gas Management Organization. (2021). Carbon footprint of products guidelines. TGO.
- 3. Shamraiz, A., Kuan W, T., Ahmad, R., Mushtaq, K. Environmental impacts and improvement implications for industrial meatballs manufacturing: scenario in a developing country. The International Journal of Life Cycle Assessment (2023).
- 4. International Organization for Standardization. (1997). Environmental management Life cycle assessment Principles and framework (ISO 14040).

EFFECTS OF ARSENIC EXPOSURE ON INSULIN-MEDIATED EXPRESSION OF *SCYL3*, *CDK8*, AND *DEP-1/PTPRJ* IN DIFFERENTIATED HUMAN NEUROBLASTOMA SH-SY5Y CELLS

<u>Tanawit Tapnan</u>^{1,2}, Naphada Leelaprachakul^{1,2}, Daranee Visitnontachai¹, Piyajit Watcharasit^{1,2,3}, and Jutamaad Satayavivad^{1,2,3}

¹Laboratory of Pharmacology, Chulabhorn Research Institute, Thailand ²Environmental Toxicology Program, Chulabhorn Graduate Institute, Thailand ³Center of Excellence on Environmental Health and Toxicology (EHT), OPS, MHESI, Thailand

Abstract:

We previously reported that prolonged arsenic exposure results in impairment of insulin signaling, decreases insulin biosynthesis and secretion in neurons. The insulin receptor (IR) can move to the nucleus and influence gene expression; we hypothesized that arsenic might alter insulin-mediated gene expression in neurons. Here, we examined the basal expression of insulin-mediated genes and their corresponding proteins, namely SCYL3, CDK8, and DEP-1/ PTPRJ, in human neuroblastoma SH-SY5Y cells that have been differentiated and treated with NaAsO₂ using qRT-PCR and immunoblotting. The findings indicated that the mRNA and protein levels of SCYL3 and CDK8 were significantly decreased in cells treated with NaAsO2 for 1, 3, and 5 days. Meanwhile, DEP-1/ PTPRJ mRNA levels were significantly reduced at every time point measured; however, the protein levels were decreased significantly only after 3 and 5 days of arsenic treatment. Furthermore, NaAsO₂ reduced the expression of HCF-1, an IR transcriptional co-regulator, suggesting that alterations in HCF-1 levels could play a role in the downregulation of insulin-mediated genes. The results from the present study indicate that arsenic disrupts the basal expression of insulin-mediated genes and their corresponding proteins in neuronal cells, at least in part by modulating the transcriptional co-regulator HCF-1.

Keywords: Arsenic, Insulin signaling, Insulin-mediated gene expression, Neurons

Introduction:

Chronic arsenic exposure is currently a global health concern due to its widespread presence and harmful effects (1). Our previous studies demonstrated that prolonged arsenic exposure impairs insulin signaling and decreases insulin biosynthesis in neurons (2, 3). The insulin receptor (IR) has been shown to translocate to the nucleus, which plays a role in regulating gene expression (4). Notably, IR interacts with different target genes depending on the cell type and physiological context, such as *SCYL3* in neurons, *CDK8* in hepatocytes (4), and *DEP-1/PTPRJ*, a protein tyrosine phosphatase, which negatively regulates IR signaling in peripheral tissues (5). Based on these findings, we hypothesize that arsenic may impair neuronal insulin signaling by disrupting nuclear IR functions and altering insulin-mediated gene expression.

Methodology:

Cell culture and treatment: Human neuroblastoma SH-SY5Y cells were cultured in a mixture of Ham's F12 and Minimum Essential Medium (MEM) at a 1:1 ratio, supplemented with 10 % FBS, 100 U/mL penicillin, 100 U/mL streptomycin, and 2 mM L-glutamine. To induce the differentiation of SH-SY5Y cells, the culture medium was switched to the differentiation medium consisting of 1% FBS and 10 μ M retinoic acid. The cells were

maintained in differentiation medium for 3 days prior to treatment. Differentiated SH-SY5Y cells were subsequently treated with 1, 5, and 10 µM NaAsO₂ for the indicated time.

qRT-PCR: At the end of treatment, RNA was extracted using an RNA extraction kit. The qRT-PCR was conducted, and the relative mRNA level was determined using the $2^{-\Delta\Delta Ct}$ method using β -actin as a reference gene.

Immunoblotting: At the end of treatment, whole cell lysates were prepared. The samples were separated using SDS-PAGE and subsequently transferred onto a nitrocellulose membrane. The membrane was blocked with 5% skim milk. Following this, the membrane was incubated with a primary antibody. Thereafter, the membrane was incubated with an appropriate secondary antibody. Protein bands were visualized using ECL and captured with the ChemidocTM Touch Imaging System along with Image LabTM Software (Bio-Rad, USA).

Results and Discussion:

Arsenic effects on basal transcription levels of insulin-mediated genes

We examined the effect of arsenic on the basal transcription levels of insulin-mediated genes in differentiated SH-SY5Y cells treated with 5 µM NaAsO₂ for 1, 3, or 5 days. The transcription levels of these insulin-mediated genes, namely *SCYL3*, *CDK8*, and *DEP-1/PTPRJ*, were measured by qRT-PCR. Across all time points, NaAsO2 treatment significantly downregulated the expression of these genes (Fig. 1A-C). These findings indicate that arsenic exposure reduces the basal expression of insulin-mediated genes. Given that arsenic impairs neuronal insulin signaling (2, 3), these findings suggest that prolonged arsenic exposure could disrupt basal transcriptional regulation of insulin-mediated genes in neurons.

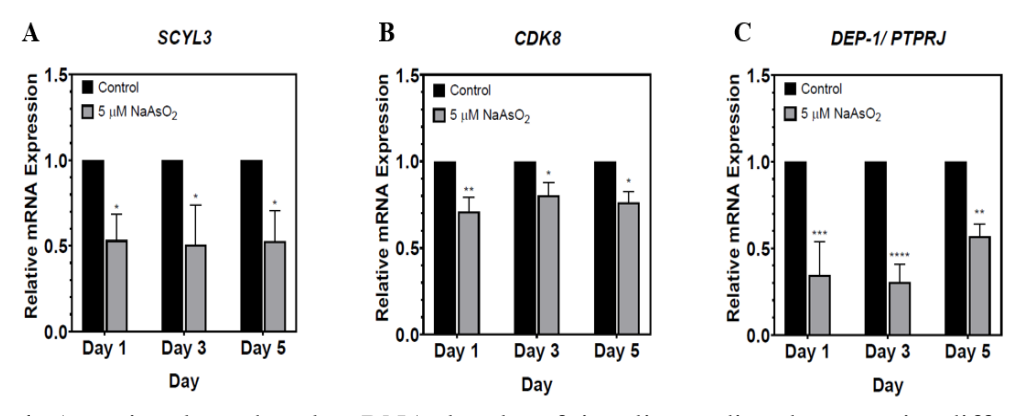


Figure 1 Arsenic alters basal mRNA levels of insulin-mediated genes in differentiated SH-SY5Y cells

Differentiated SH-SY5Y cells were treated with 5 μ M NaAsO₂ for 1, 3, or 5 days. The relative mRNA expression levels of *SCYL3* (A), *CDK8* (B), and *DEP-1/PTPRJ* (C) were analyzed by qRT-PCR, and expression levels were calculated using the $2^{-\Delta\Delta Ct}$ method and normalized to β -actin.

Arsenic effects on basal levels of proteins derived from insulin-mediated genes

To further investigate the effect of arsenic on basal levels of proteins that their expression is mediated by insulin, we examined protein levels in differentiated SH-SY5Y cells following arsenic treatment using immunoblotting. The results showed that SCYL3 and CDK8 levels were significantly decreased following NaAsO₂ treatment at all time points (Figure 2A, 2B). Although DEP-1/PTPRJ mRNA expression was reduced at all time points, a significant reduction in DEP-1/PTPRJ protein levels was only observed after 3 and 5 days of arsenic treatment, suggesting possible post-transcriptional or translational regulation (Figure 2A, 2B). These findings indicate that arsenic reduces the protein levels of SCYL3, CDK8, and DEP-1/PTPRJ which are derived from the insulin-mediated genes (Figure 2A, 2B).

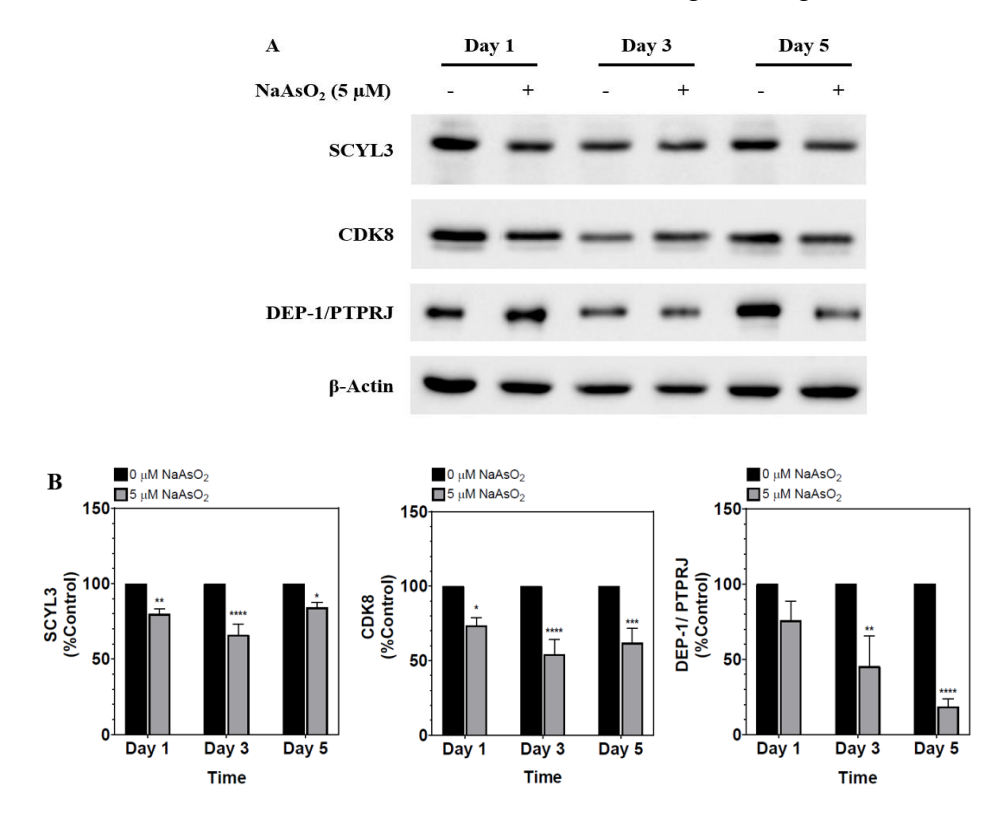


Figure 2 Arsenic alters the basal levels of proteins derived from insulin-mediated genes in differentiated SH-SY5Y cells

(A) Representative SCYL3, CDK8, DEP-1/PTPRJ, and β -Actin immunoblots are shown. (B) The quantitative levels of SCYL3, CDK8, and DEP-1/PTPRJ in cell lysates from cells treated with 5 μ M NaAsO2 for 1, 3, and 5 days are calculated as a percentage of the control.

Arsenic effects on the level of IR transcriptional coregulator, Host Cell Factor-1 (HCF-1)

We next investigated whether arsenic affected the levels of HCF-1 in differentiated. SH-SY5Y cells. The level of HCF-1 was measured in whole cell lysate of cells treated with 1, 5, or $10\,\mu\text{M}$ NaAsO₂ for 3 days, or with $5\,\mu\text{M}$ NaAsO₂ for 1, 3, or 5 days by immunoblotting. The results revealed a significant reduction in HCF-1 following treatment with $5\,\mu\text{M}$ NaAsO₂ for 3 or 5 days (Fig. 3A, 3B). Interestingly, treatment with $1\,\mu\text{M}$ NaAsO₂ for 3 days significantly increased HCF-1 level (Fig. 3C, 3D), whereas treatment with 5 or $10\,\mu\text{M}$ NaAsO₂ for 3 days significantly reduced it (Fig. 3C, 3D). These findings suggest that arsenic may modulate insulin-mediated gene expression by altering HCF-1 levels under basal conditions.

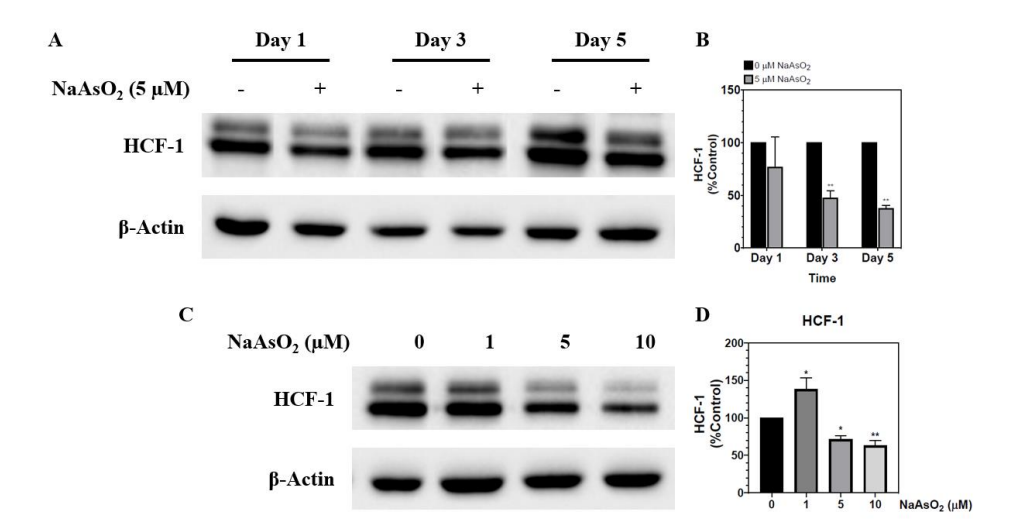


Figure 3 Arsenic decreases HCF-1 levels in differentiated SH-SY5Y cells Representative immunoblots of HCF-1 (A, C) are shown. The quantitative levels of HCF-1 in cell lysates from cells treated with 5 μ M NaAsO₂ for 1, 3, and 5 days (B), and 1, 5, and 10 μ M NaAsO₂ for 3 days (D) are calculated as a percentage of the control.

Conclusion:

Taken together, this study demonstrates that arsenic may reduce the basal expression of insulin-mediated genes, SCYL3, CDK8, and DEP-1/ PTPRJ, along with their corresponding protein levels in neuronal cells, by modulating the transcriptional co-regulator HCF-1.

References:

- 1. Lucio M, Barbir R, Vučić Lovrenčić M, Canecki Varžić S, Ljubić S, Smirčić Duvnjak L, et al. Association between arsenic exposure and biomarkers of type 2 diabetes mellitus in a Croatian population: A comparative observational pilot study. Science of the Total Environment. 2020;720:137575.
- 2. Niyomchan A, Visitnonthachai D, Suntararuks S, Ngamsiri P, Watcharasit P, Satayavivad J. Arsenic impairs insulin signaling in differentiated neuroblastoma SH-SY5Y cells. Neurotoxicology. 2018;66:22-31.
- 3. Wisessaowapak C, Watcharasit P, Satayavivad J. Arsenic disrupts neuronal insulin signaling through increasing free PI3K-p85 and decreasing PI3K activity. Toxicology Letters. 2021;349:40-50.
- 4. Hancock ML, Meyer RC, Mistry M, Khetani RS, Wagschal A, Shin T, et al. Insulin Receptor Associates with Promoters Genome-wide and Regulates Gene Expression. Cell. 2019;177(3):722-36.e22.
- 5. Chopra S, Kadiri OL-J, Ulke J, Hauffe R, Jonas W, Cheshmeh S, et al. DEP-1 is a brain insulin receptor phosphatase that prevents the simultaneous activation of counteracting metabolic pathways. Cell Reports. 2024;43(12).

EFFECTS OF PRENATAL EXPOSURE TO AMBIENT MICROPLASTICS: MATERNAL EXPOSURE AND ALTERED TELOMERE LENGTH AND MITOCHONDRIAL DNA COPY NUMBER IN NEWBORNS

<u>Kusala Sirirathna¹</u>, Panida Navasumrit^{1,2,3}, Wanrada Jiranuntawut², Chalida chompoobut² and Mathuros Ruchirawat^{1,2,3}

¹Applied Biological Sciences Program, Chulabhorn Graduate Institute, Bangkok 10210, Thailand, ²Laboratory of Environmental Toxicology Chulabhorn Research Institute, Bangkok 10210, Thailand, ³Center of Excellence on Environmental Health and Toxicology (EHT), OPS, Bangkok 10210, Thailand

Abstract:

Ambient microplastics (MPs), particularly from traffic emissions, are increasingly recognized for their contribution to environmental pollution and potential health risks. Growing evidence suggests that maternal exposure to harmful agents during pregnancy can adversely impact fetal development and increase the likelihood of childhood health problems. This study aimed to investigate the effects of prenatal exposure to traffic-related airborne MPs on maternal and fetal exposure and their implications on telomere length (TL) and mitochondrial DNA copy number (mtDNA-CN) in newborns. In addition, an *in vitro* cell-based study was conducted to confirm the effects of MPs on alterations of TL and mtDNA-CN in umbilical cord-derived mesenchymal stem cells (UC-MSCs).

The study was conducted in high- and low-traffic congested areas. A total of 101 subjects were recruited from pregnant subjects consisting 50 and 51 from high- and lowtraffic locations, respectively. Pyrolysis GC-MS/MS was used to determine the concentrations of MPs and characterize polymers. Maternal and fetal exposure to MPs was assessed in urine and placental tissue, respectively. In the high-exposed group, the concentrations of MPs were significantly increased in maternal urine by 1.33-fold (8.72 vs. 6.53 mg/g creatinine, p<0.05) and in placental tissues (21.03 vs 16.14 mg/g tissue, p<0.01), compared to the low-traffic exposed group. Polyethylene (PE) and polyethylene terephthalate (PET) were predominant polymers which was in consistent with previous ambient air analyses from this study. Relative TL and mtDNA-CN was determined using quantitative real-time PCR in cord blood. A significant shortening of telomeres was observed in cord blood from high-exposed newborns, compared to those from low-exposed groups (1.2-fold, p<0.05). In addition, newborns from the high traffic-exposed group had a significantly lower mtDNA-CN in cord blood (1.2-fold, p < 0.05). Levels of TL and mtDNA-CN were significantly negatively associated with exposure to MPs. *In vitro* experiments confirmed that PE treatment caused a concentration-dependent reduction in both TL and mtDNA-CN in UC-MSCs.

In conclusion, this study demonstrates that prenatal exposure to traffic-related ambient MPs increases maternal and fetal exposure to MPs. Furthermore, the high-traffic exposed group had shortened TL and reduced mtDNA-CN in cord blood. This could potentially result in genomic instability in newborns. Therefore, this study highlights the importance of being aware of *in utero* exposure to ambient MPs which may lead to increase the health risk of disease development in newborns.

Keywords: Microplastics, air pollution, prenatal exposure, telomere length, mitochondrial DNA copy number

Introduction:

Microplastics (MPs), plastic particles smaller than 5 mm, have become a persistent environmental pollutant due to their durability and widespread presence across ecosystems. With plastic production rapidly increasing, over 170 trillion MPs are now estimated to contaminate the world's oceans; a number expected to triple by 2040 without intervention (1). MPs are classified as primary (intentionally produced for consumer and industrial products) or secondary (resulting from the degradation of larger plastics) (2). Their small size enables them to enter the food chain, bioaccumulate, and exert toxic effects on both wildlife and humans. Human exposure occurs primarily through ingestion, inhalation, and skin contact, with airborne MPs raising particular concern for their ability to penetrate biological barriers and reach internal organs (3). Exposure to MPs poses potential health hazards to humans, including the risk of cancer, immunotoxicity, cardiovascular diseases, inflammation and adverse effects on pregnancy (2). Of increasing concern is prenatal exposure, as studies show MPs can cross the placental barrier, potentially affecting fetal development by interfering with DNA integrity and genomic instability (4).

Exposure to air pollutants has been associated with increased oxidative stress that may lead to telomere length (TL) shortening and decreased mitochondrial DNA copy number (mtDNA-CN) (5). Telomeres are repetitive, non-coding nucleotide sequences located at the end of chromosomes which can maintain genome integrity and chromosome stability. Mitochondria are multifunctional organelles that are involved in a variety of cellular functions, including energy metabolism, cell proliferation, and apoptosis and are required for maintaining nuclear genome stability. Dysfunctions of mitochondria cause telomere shortening, while telomere damage leads to dysfunctions of mitochondria and the reprogramming of mitochondrial biosynthesis. Environmental exposure may affect the TL of newborns, which is considered as an early biomarker indicating susceptibility to later life diseases (6).

Given these risks, this study aims to evaluate prenatal MP exposure and its potential impact on newborns by measuring MP levels in maternal urine and assessing telomere length and mitochondrial DNA copy number in cord blood. *In vitro* studies using human stem cells are also employed to support and strengthen the findings, contributing to a better understanding of MP-related developmental toxicity and public health implications.

Objectives:

This study aims to assess prenatal exposure to traffic-related MPs on maternal and fetal exposure and the impact of MPs exposure on telomere length and mitochondrial DNA in newborns,

Methodology:

Study locations

This study was conducted in high- and low-traffic congested areas in Bangkok, Thailand. The initial criteria for selecting the study sites involve assessing traffic density. The high-traffic site was located in Klongsan District along Somdej Chaophraya Road, while the low-traffic site was located in peri-Bangkok at Buddhamontol 3 Road.

Sample collection

A total of 101 healthy pregnant women, aged between 20 and 40 years, were recruited during their first trimester from areas with different traffic densities. To ensure consistent in environmental exposure, all participants had to live in the study area for at least one year. Urine samples were collected from participants in both high- and low-exposure groups using 50 mL tubes and stored at -20 °C until analysis. After the birth of a live infant, cord blood samples were obtained and stored at -80 °C until further analysis.

Part 1 Assessment of Prenatal Exposure to Microplastics and Associated Health Risks Determination of MPs in maternal urine samples and placental tissue

To analyze maternal exposure to MPs, 5 mL of maternal urine was filtered through dry-filter membranes (MN GF-3) with a pore size of 0.6 µm using a vacuum pump and filter funnel setup. The membranes were then dried at 70 °C for 4 hours. Subsequently, the filters were cut and placed into sample cups for analysis using Pyrolysis GC-MS/MS.

To assess fetal exposure to MPs, placental tissues (1 gm) were cut into small pieces and dried at 100°C. The samples were grinded and analyzed using Pyrolysis GC-MS/MS.

Determination of telomere length in cord blood

Genomic DNA was extracted from cord blood samples using the DNeasy Blood/Tissue Kit. Telomere length was determined using the monochrome multiplex quantitative PCR technique on the CFX-96 Touch Real-Time PCR Detection System. This method simultaneously amplified telomere (T) and albumin (S) gene sequences; targets differing in copy number and melting temperature in a single reaction. The relative telomere length was calculated as the ratio of T to S (T/S ratio).

Determination of mitochondrial copy number in cord blood

Mitochondrial DNA copy number (mtDNA-CN) was quantified by measuring mitochondrial DNA levels relative to a nuclear single-copy gene; β -Globin. Genomic DNA was isolated from cord blood using the DNeasy Blood/Tissue Kit, and quantitative real-time PCR was conducted using the CFX-96 Touch Real-Time PCR Detection System.

Part 2 *In vitro* study the effect of PE treatment on TL and mtDNA-CN in UC-MSCs Determination of cytotoxicity of polyethylene (PE) in UC-MSCs

UC-MSCs were used to investigate the effects of PE-induced cytotoxicity and genomic damage. Cytotoxicity was assessed using the MTT assay by measuring absorbance at 570 nm on a SpectraMax plate reader.

Determination of TL and mtDNA-CN in UC-MSCs treated with PE

UC-MSCs were treated with PE particles, and following 24 hours of incubation, genomic DNA was isolated. The relative expression of TL and albumin genes was quantified using the monochrome multiplex quantitative PCR technique. Mitochondrial DNA copy number (mtDNA-CN) was determined by comparing the relative amounts of mitochondrial DNA to a nuclear single-copy reference gene, β -Globin, using quantitative real-time PCR.

Statistical evaluation

The Mann-Whitney U test was used to evaluate statistical differences between groups. A p-value < 0.05 was considered the difference with a statistical significance.

Results and Discussion:

1. Maternal exposure to microplastics

Characterization and concentrations of total MPs and various MP polymers, including polyethylene (PE), polyethylene terephthalate (PET), polystyrene (PS), polycaprolactam (N6), nylon (N66), polymethyl methacrylate (PMMA), polyvinyl chloride (PVC), and styrene-butadiene rubber (SBR) were determined in maternal urine. The total concentration of urinary MPs was higher in pregnant subjects from high-traffic areas, compared to those from low-traffic areas. In the first trimester, the predominant MP polymers detected included PE, PET, N6, N66, PVC, and SBR. During the second and third trimesters, PE, PET, N6, N66, and PVC remained the major polymers identified. Notably, in the second trimester, MP levels in the high-traffic exposure group were significantly 1.33-fold higher (p<0.05) than those in the low-traffic exposure group (8.72 vs. 6.53 mg/g creatinine). The elevated levels of MPs in the urine of high- exposed pregnant subjects reflect increased maternal exposure and are consistent with previously collected data showing higher concentrations of airborne MPs in high-traffic areas.

2. Fetal exposure to MPs

Consistent with the presence of MPs in maternal urine, MPs were detected in placental tissue suggesting transplacental transfer and fetal exposure. The detected MPs polymers in placental tissues included PE, ABS, PET, N6, N66, PVC, SBR, and PS. In line with higher levels of MPs in high-exposed maternal urine, the concentrations of total MPs in placental tissue were significantly increased by 1.3-fold in the high-exposed group, compared to those from the low-exposed group (21.03 vs 16.14 µg/g dry weight, p<0.01).

3. Telomere length and mitochondrial DNA copy number in newborns

Telomere length in cord blood samples from the high- exposed group was significantly lower than those from the low-exposed group, with an approximate 1.2-fold (2.08 vs 1.78, p < 0.05). The reduced telomere length observed in high-traffic regions may be attributed to elevated oxidative stress and DNA damage, both of which are known to contribute to telomere shortening.

Similarly, mtDNA-CN in cord blood was significantly 1.2-fold lower in the high-exposed group the low-exposed group (0.59 vs 0.51, p < 0.05). This was in line with the telomere length trends. These results suggest that prenatal exposure to MPs may affect genomic instability during fetal development.

The univariate regression analysis indicated that levels of TL or mtDNA-CN were significantly negatively associated with total MPs and PE polymer (p<0.05). These results suggested that the shortened TL and decreased mtDNA-CN were in part mediated by prenatal exposure to MPs and PE.

4. In vitro study the effect of PE treatment on TL and mtDNA-CN in UC-MSCs

To confirm the aforementioned biological effects of shortened TL and decreased mtDNA-CN in cord blood, in *vitro* cell-based studies were conducted in umbilical cord tissue-derived MSCs cell line (UC-MSCs). The effects of PE treatment alone on TL and mtDNA-CN were determined in UC-MSCs.

4.1 Cytotoxicity of PE in UC-MSCs

The UC-MSCs were cultured and treated with various concentrations of PE (0-10 mg/mL for 24 hours). The results from the MTT assay showed no significant reduction in cell viability, even at the highest dose $(10 \, \text{mg/mL})$, indicating an absence of acute cytotoxic

effects under the tested conditions. Flow cytometry analysis revealed an increased side scattering intensity of the treated cells suggesting the cellular uptake of PE particles. However, the 24-hour exposure period may have been insufficient to elicit measurable cytotoxic responses.

4.2 The effects of PE on TL and mtDNA-CN in UC-MSCs

Analysis of relative TL and mtDNA-CN in UC-MSCs treated with PE (0-5 mg/ml, 24 hours) showed a dose-dependent reduction of TL and mtDNA-CN in treated cells. These results suggest that PE exposure can induce genomic instability in fetal stem cells.

Conclusions:

This study reported that increased maternal and fetal exposure to MPs was observed in high-traffic exposed groups suggesting that traffic emissions contribute to prenatal exposure to MPs. Prenatal exposure to MPs, particularly PE polymer was associated with shortened telomere length and decreased mtDNA-CN in cord blood. An *in vitro* study which showed shortened TL and decreased mtDNA-CN in PE-treated UC-MSCs supports the observations in prenatal exposure. These results suggest that exposure to traffic-related MPs can cause genomic instability which may potentially increase the health risk of developing diseases later in life. Therefore, implementing policies to enhance air quality and minimize microplastic exposure, especially among pregnant women and newborns is essential to protect public health.

References:

- 1. Eriksen M, Cowger W, Erdle LM, Coffin S, Villarrubia-Gómez P, Moore CJ, et al. A growing plastic smog, now estimated to be over 170 trillion plastic particles afloat in the world's oceans-Urgent solutions required. PLoS One. 2023;18(3):e0281596.
- 2. Osman AI, Hosny M, Eltaweil AS, Omar S, Elgarahy AM, Farghali M, et al. Microplastic sources, formation, toxicity and remediation: a review. Environmental Chemistry Letters. 2023;21(4):2129-69.
- 3. Sarkar S, Diab H, Thompson J. Microplastic Pollution: Chemical Characterization and Impact on Wildlife. Int J Environ Res Public Health. 2023;20(3).
- 4. Ragusa A, Svelato A, Santacroce C, Catalano P, Notarstefano V, Carnevali O, et al. Plasticenta: First evidence of microplastics in human placenta. Environment International. 2021;146:106274.
- Hautekiet, P., Nawrot, T.S., Janssen, B.G., Martens, D.S., De Clercq, E.M., Dadvand, P., Plusquin, M., Bijnens, E.M., Saenen, N.D., Child buccal telomere length and mitochondrial DNA content as biomolecular markers of ageing in association with air pollution. Environ. Int. 2021; 147, 106332.
- Jiang Y, Xu Z, Wang M, Liu H, Li Y, Xu S. Association Between Prenatal Exposure to Organochlorine Pesticides and Telomere Length in Neonatal Cord Blood. Toxics. 2024 Oct 23;12(11):769.

INVESTIGATION OF THE IMPACT OF PLNS, PLNR, AND PLNP ON ANTIBIOTIC RESISTANCE

AND VIRULENCE IN Stenotrophomonas maltophilia

<u>Phatcharin Laosena¹</u>, Nisanart Charoenlap^{2,3}, Wirongrong Whangsuk², Skorn Mongkolsuk^{2,3}, and Paiboon Vattanaviboon^{1,2,3,*}

¹Program in Applied Biological Science Environmental Health, Chulabhorn Graduate Institute, Bangkok, Thailand,

²Laboratory of Biotechnology, Chulabhorn Research Institute, Bangkok, Thailand, ³Center of Excellence on Environmental Health and Toxicology (EHT), OPS, MHESI, Bangkok, Thailand,

*Correspondence: E-mail: Phatcharin@cgi.ac.th

Abstract:

Stenotrophomonas maltophilia is an emerging multidrug-resistant opportunistic pathogen that poses a serious challenge in clinical settings. The resistance of this organism is mainly driven by intrinsic mechanisms including the production of β-lactamases, multidrug efflux pumps, and biofilm formation. These traits make infections difficult to treat. Among its virulence factors, type IV pili (T4P) are critical for surface attachment, twitching motility, and biofilm development. The regulatory systems that control these functions and their possible link to antimicrobial resistance in S. maltophilia remain poorly characterized. This study investigated the function of a putative major pilin gene (plnP) and its associated two-component regulatory system, a sensor kinase (plnS) and a response regulator (plnR). Clean deletions of plnP, plnS, and plnR were generated in the S. maltophilia K279a. Deletion of plnS and plnR increased resistance to a wide range of antibiotics. These resistance phenotypes were not observed in the $\Delta plnP$. In addition, both $\Delta plnS$ and $\Delta plnR$ showed enhanced growth rates and biofilm formation compared with the wild type. Notably, only the $\Delta plnR$ retained twitching motility. Collectively plnP is likely not the major pilin in S. maltophilia. Instead, plnS and plnR act as key regulators that modulate both antimicrobial resistance and virulence-associated traits. The findings underscore the critical role of plnS and plnR, which are likely significant to the regulatory networks in shaping biological traits with direct clinical relevance in this pathogen.

Keywords: *Stenotrophomonas maltophilia*, multidrug resistance, biofilm formation, Type IV pili, two-component system, antibiotic resistance, virulence

Introduction:

The growing crisis of antibiotic resistance poses a serious threat to global health. One of the emerging multidrug-resistant organisms is S. maltophilia. This bacterium has gained attention for its inherent resistance and its ability to thrive in both clinical and environmental settings. 1,2 S. maltophilia is a Gram-negative, rod-shaped bacterium. It can be found in diverse environments and frequently establishes colonization in hospital environment, especially water outlets, ventilators, and medical devices. This ecological adaptability makes it a potential link between environmental sources and hospital-acquired infections. In clinical settings, S. maltophilia causes opportunistic infections, particularly in immunocompromised patients and those using invasive medical equipment such as ventilators. The bacterium is resistant to multiple antibiotics including β -lactams, aminoglycosides, and carbapenems. β β Most resistance genes are chromosomally encoded, contributing to its intrinsic high-level resistance to antibiotics. The bacterium produces

 β -lactamases, multidrug efflux pumps, and the ability to form robust biofilms. ³ Biofilm formation plays a critical role by protecting bacterial cells from both antibiotic and host immune responses. ⁴

Type IV pili (T4P) plays important role in virulence of *S. maltophilia*. They mediate adhesion, twitching motility, and early biofilm formation.⁵ In *S. maltophilia* K279a, plnP encodes the putative major pilin subunit; plnS encodes the sensor kinase and plnR encodes the σ^{54} -dependent response regulator. Previous studies in *Pseudomonas*, *Xanthomonas*, and *Acidovorax* indicated that PlnSR regulate T4P expression.^{6–8} In *S. maltophilia*, the studies in strain K279a showed that mutations in the pilin gene plnP after antibiotic exposure are associated with antibiotic resistance⁹ but the genetic regulation of T4P and its contribution to antibiotic resistance remain unclear.

In this study *plnP*, *plnS*, and *plnR* were functionally characterized in term of bacterial virulence factors (growth characteristic, motility, biofilm formation) and antibiotic resistance in *S. maltophilia*.

Methodology:

This study employed clean deletion mutagenesis to construct knockouts of *plnP*, *plnS*, and *plnR* in *S. maltophilia* strain K279a. Mutant constructs were generated using the NEBuilder HiFi DNA Assembly Cloning Kit. Antibiotic susceptibility was determined using the Kirby–Bauer disk diffusion method.¹⁰ Twitching motility was examined on semi-solid agar.¹¹ Biofilm formation was measured with a crystal violet staining assay following a microtiter plate protocol.¹² Growth characteristics were assessed by monitoring OD₆₀₀ in 96 well plate.¹³

Results, Discussion and Conclusion:

Clean deletions of plnP, plnS, and plnR were generated in S. maltophilia K279a. Expression analysis revealed that plnS and plnR regulate the expression of plnP. Interestingly, only the $\Delta p lnR$ mutant exhibited twitching motility, whereas the $\Delta p lnP$ and plnP overexpression showed non-motile phenotype similar to the wild type (Figure 1). These findings collectively support the conclusion that K279a possesses functional pili enabling its motility ability, while plnP is likely not the predominant pilin subunit in S. maltophilia. PlnR acted as a suppressor of motility, which suggests indirect control through alternative pilin loci or other regulatory networks. ¹⁴ Notably, mutants lacking *plnS* or *plnR* also displayed increased growth (Figure 2), more robust biofilm formation (Figure 3), and higher resistance to multiple antibiotics (Figure 4). In contrast the plnP showed no change in growth (Figure 2), biofilm formation (Figure 3), or antibiotic susceptibility compared with the wild type (Figure 4). These results indicate that PlnSR regulates multiple physiological traits in S. maltophilia in a non-canonical manner. Loss of PlnSR signaling shifted physiology toward enhanced biofilm development and multidrug resistance, thereby promoting persistence traits that complicate both environmental survival and clinical treatment outcomes. Overall, PlnSR functions as a regulatory signal in S. maltophilia, coordinating motility, biofilm formation, and antibiotic resistance in ways that differ from Pseudomonas aeruginosa and other Gram-negative bacteria. 16,17 Understanding this regulatory network will support the monitoring and control of this multidrug-resistant pathogen.

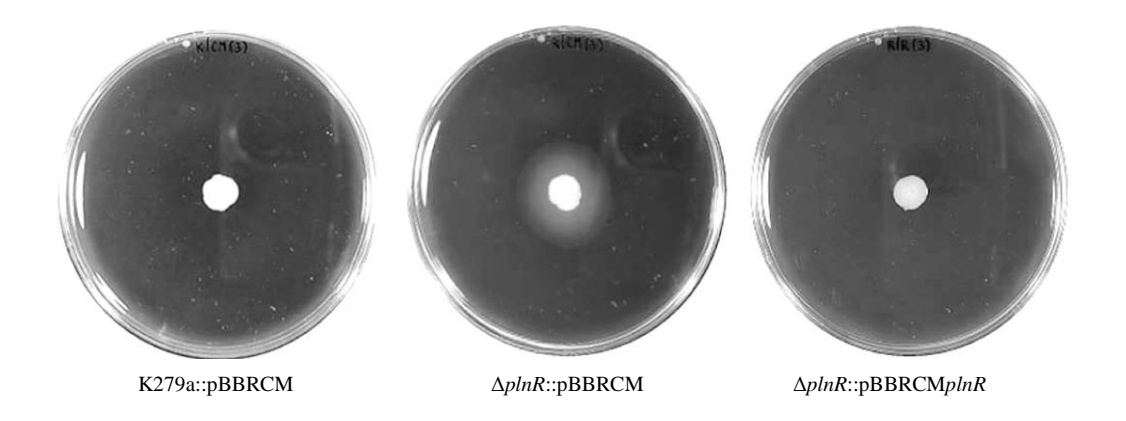


Figure 1: Twitching motility of the *S. maltophilia* strain K279a, $\Delta plnR$ mutant and complemented strain.

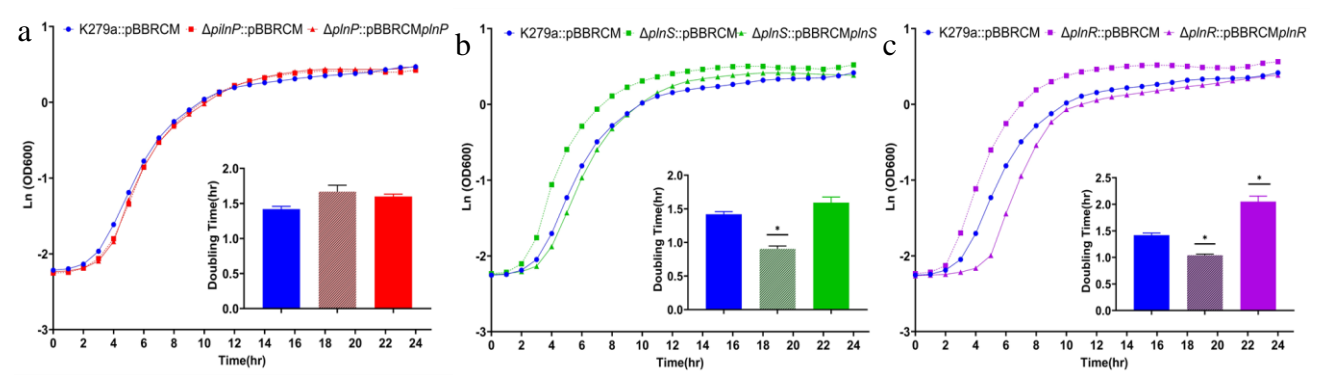


Figure 2: Growth curves and doubling times of *S. maltophilia* strain K279a, the mutant and complemented strain. (a) $\Delta plnP$ mutant, (b) $\Delta plnS$ mutant and (c) $\Delta plnR$ mutant.

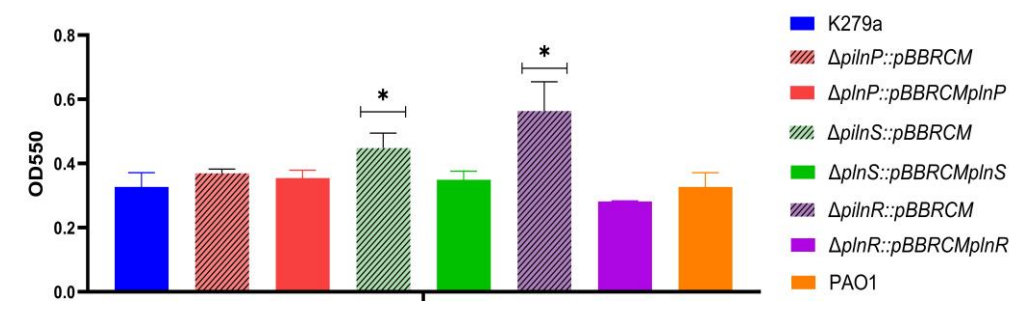


Figure 3: The biofilm formation of *S. maltophilia* strain K279a, the mutant and complemented strain. Significant differences were determined by t-test with p < 0.05.

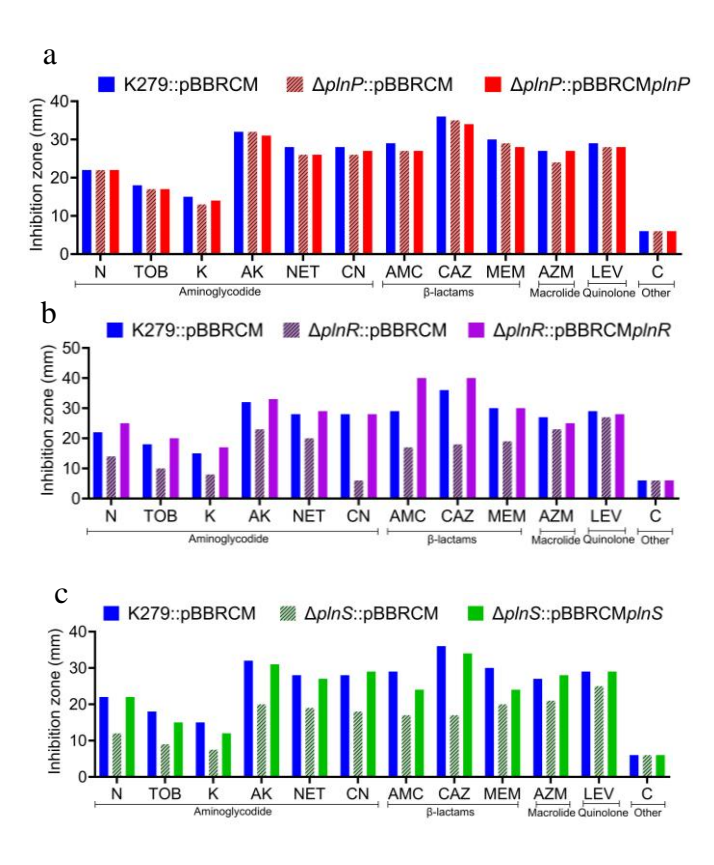


Figure 4: Antibiotic susceptibility of *S. maltophilia* strain K279a, the mutant and complemented strain. Antibiotics tested included nitrofurantoin (N), tobramycin (TOB), kanamycin (K), amikacin (AK), netilmicin (NET), gentamicin (CN), amoxicillin-clavulanic acid (AMC), ceftazidime (CAZ), meropenem (MEM), azithromycin (AZM), levofloxacin (LEV), and chloramphenicol (C). (a) $\Delta plnP$ mutant, (b) $\Delta plnS$ mutant and (c) $\Delta plnR$ mutant.

Acknowledgement:

This work received funding support from Chulabhorn Graduate Institute and Chulabhorn Research Institute. PL PV, NC, and SM received funding support from the CRI under grant number 4759806.

References:

- 1. Brooke, J. S. *Stenotrophomonas maltophilia*: an Emerging Global Opportunistic Pathogen. *Clin Microbiol Rev* **25**, 2–41 (2012).
- 2. Brooke, J. S. Advances in the Microbiology of *Stenotrophomonas maltophilia*. *Clin Microbiol Rev* **34**, (2021).
- 3. Vattanaviboon, P., Dulyayangkul, P., Mongkolsuk, S. & Charoenlap, N. Efflux pump systems as key contributors to multidrug resistance in *Stenotrophomonas maltophilia*: Physiological roles and gene regulation. *Acta Microbiol Immunol Hung* **72**, 81–92 (2025).
- 4. Looney, W. J., Narita, M. & Mühlemann, K. *Stenotrophomonas maltophilia*: an emerging opportunist human pathogen. *Lancet Infect Dis* **9**, 312–323 (2009).

- 5. Sharma, S. *et al.* Correction: Sharma et al. Microbial Biofilm: A Review on Formation, Infection, Antibiotic Resistance, Control Measures, and Innovative Treatment. Microorganisms 2023, 11, 1614. *Microorganisms* 12, 1961 (2024).
- 6. Kehl-Fie, T. E., Porsch, E. A., Miller, S. E. & StGeme, J. W. Expression of Kingella kingae Type IV Pili Is Regulated by σ 54, PilS, and PilR. *J Bacteriol* **191**, 4976–4986 (2009).
- 7. Kilmury, S. L. N. & Burrows, L. L. The *Pseudomonas aeruginosa* PilSR Two-Component System Regulates Both Twitching and Swimming Motilities. *mBio* **9**, (2018).
- 8. Yang, Y. *et al. Acidovorax citrulli* Type IV Pili PilR Interacts with PilS and Regulates the Expression of the pilA Gene. *Horticulturae* **9**, 1296 (2023).
- 9. Chatree, Y. *et al.* Induction of Antimicrobial Resistance of *Stenotrophomonas maltophilia* by Exposure to Nonlethal Levels of Antibiotics. *Microbial Drug Resistance* **29**, 115–126 (2023).
- 10. Hudzicki, J. Kirby-Bauer Disk Diffusion Susceptibility Test Protocol. *American Society for Microbiology [Online]* https://www.asm.org/Protocols/Kirby-Bauer-Disk-Diffusion-SusceptibilityTest-Pro. (2009).
- 11. Ronish, L. A., Lillehoj, E., Fields, J. K., Sundberg, E. J. & Piepenbrink, K. H. The structure of PilA from *Acinetobacter baumannii* AB5075 suggests a mechanism for functional specialization in Acinetobacter type IV pili. *Journal of Biological Chemistry* **294**, 218–230 (2019).
- 12. García, C. A., Alcaraz, E. S., Franco, M. A. & Passerini de Rossi, B. N. Iron is a signal for *Stenotrophomonas maltophilia* biofilm formation, oxidative stress response, OMPs expression, and virulence. *Front Microbiol* **6**, (2015).
- 13. Patil, P. P. et al. Global transcriptome analysis of *Stenotrophomonas maltophilia* in response to growth at human body temperature. *Microb Genom* 7, (2021).
- 14. Trifonova, A. & Strateva, T. *Stenotrophomonas maltophilia* a low-grade pathogen with numerous virulence factors. *Infect Dis* **51**, 168–178 (2019).
- 15. Gicharu, G. K. *et al.* The sigma 54 genes rpoN1 and rpoN2 of *Xanthomonas citri* subsp. citri play different roles in virulence, nutrient utilization and cell motility. *J Integr Agric* **15**, 2032–2039 (2016).
- 16. Burrows, L. L. *Pseudomonas aeruginosa* Twitching Motility: Type IV Pili in Action. *Annu Rev Microbiol* **66**, 493–520 (2012).
- 17. Geisinger, E. & Isberg, R. R. Interplay Between Antibiotic Resistance and Virulence During Disease Promoted by Multidrug-Resistant Bacteria. *J Infect Dis* **215**, S9–S17 (2017).

PRELIMINARY STUDY OF POLLEN AND PM_{2.5}: SEASONAL OVERLAP AND IMPLICATIONS FOR ALLERGY PREVENTION

Lilian Haidvogl^{1,2}, Yotin Juprasong^{2,3} and Wisuwat Songnuan^{2,4,5}

¹Graduate Program in Toxicology, Faculty of Science, Mahidol University, Bangkok

²Single-Cell Omics and Systems Biology of Diseases (scSyBiD) Research Unit,

Faculty of Science, Mahidol University, Bangkok

³Department of Biochemistry, Faculty of Medicine, Srinakharinwirot University, Bangkok

⁴Department of Plant Science, Faculty of Science, Mahidol University, Bangkok

⁵Center of Excellence on Environmental Health and Toxicology (EHT), Bangkok

Abstract:

Airborne pollen and particulate matter (PM_{2.5}, PM₁₀) provoke respiratory diseases such as rhinoconjunctivitis and asthma in susceptible individuals. Further, they may work synergistically to worsen respiratory symptoms and modulate the immune response. In Bangkok, seasonal peaks in pollen concentration and air pollution overlap. PM_{2.5} levels peak between January and March, while pollen concentrations, especially of the grass family (Poaceae), a major allergen in Thailand, are elevated year-round, highest in November and declining until July. To better understand their combined effect, this study explored the correlation between pollen load and particulate matter levels in central Bangkok.

Aeropollen sampling was conducted from late January until March 2025 using a RotoRod-Type Pollen Sampler at the Faculty of Science, Mahidol University. Samples were taken during the overlap of rush hour and the daily peak of pollen concentration (9:00–12:00). Pollen counts were compared to air pollutant data from the Air4Thai network.

No statistically significant correlation was observed between daily pollen concentrations and PM levels. Most collected pollen grains could not be taxonomically identified; however, among the known grains, Typhaceae and Poaceae were the most frequently observed.

The observed constant presence of either allergenic pollen or $PM_{2.5}$ peaks during this time of year presents a compounded risk for respiratory health and may severely impact the quality of life of affected individuals. No clear trend was observed across the selected time span, however, highlighting the need for a prolonged study period to uncover seasonal or meteorological patterns influencing both factors.

Keywords: Pollen allergy, pollen count, PM_{2.5}, PM₁₀

Introduction:

Exposure to airborne pollen may lead to respiratory disease such as allergic rhinoconjunctivitis, chronic obstructive pulmonary disease (COPD) and asthma in susceptible individuals¹. Air pollutants (PM_{2.5}, PM₁₀, and ozone)², similarly contribute to respiratory diseases such as rhinoconjunctivitis and asthma, as particulate matter can penetrate deep into the respiratory system and irritate eyes and throat³. Moreover, studies have shown a synergistic effect between pollen and particulate matter (PM_{2.5}), amplifying respiratory symptoms and allergic inflammation^{4–6}.

The so-called smog season in Bangkok typically lasts from October to May, with the highest pollution levels recorded between January and March and PM_{2.5} being the main pollutant throughout. The city experiences high particulate matter concentrations when temperatures drop and relative humidity and wind speed are low. The main source of smog in South-East Asia is, however, attributed to biomass burning ⁷.

Pollen season in Bangkok has its highest peak in November and then declines until July, but pollen concentrations remain abundant throughout the year ^{8,9}. Especially of grass pollen (Poaceae), which commonly elicits allergic reactions in Thai pollen allergy patients^{10,11}.

High pollen counts are promoted by warm, dry, and sunny weather, with moderate wind speeds, while an increase in relative humidity reduces them¹².

Though the link between high pollen exposure and air pollution leading to an increase in hay fever symptoms and allergy medication usage has been made⁴, no research has looked at the overlap of the two seasons in Bangkok. This study therefore aims to identify potential correlations between pollen concentration and particulate matter.

Methodology:

Sample collection

The modified Rotorod-Type Pollen Sampler (Scinnotech) was set up on the 5th floor (18 m) open-air walkway between two buildings, at least three meters away from any buildings or big obstructions that would hinder airflow. All samples were collected at the Faculty of Science, Phayathai Campus, Mahidol University from late January (28.01.2025) until March (30.03.2025). The sampler ran for 3 hours each sampling day from 9:00–12:00 — corresponding to the closest overlap between rush hour (07:00–09:30) and the time of day in which most pollen is released (10:00–13:00).

Pollen Count

The pollen count (grains/m³) was determined using the following equation¹³, whereby the average speed (s) of the motor was 2000 rpm. The samples were mounted in Calberla's dye (5 mL glycerol, 10 mL 95% ethanol, 15 mL distilled, saturated aqueous basic fuchsin) for staining and pollen grains were counted under a microscope.

$$pollen\; count\; (grains/m^3) = \frac{total\; number\; of\; pollen\; grains\; counted}{volume\; of\; air\; sampled\; (m^3) \; \cdot \; average\; motor\; speed\; (rpm) \; \cdot \; measuring\; time\; (min)}$$

Pollen identification

Pollen was identified based on its physical characteristics, such as size and apertures, and comparing it to known references. To increase chances of identification and reduce the number of counted unknown pollen, pollen samples were continuously collected from plants within the sampling vicinity and new references made.

Meteorological data

Data on air pollution and weather were taken from the closest available dataset to the collection site at Faculty of Science, Phayathai Campus, Mahidol University (13.765581, 100.525431). Meteorological data was collected from air4thai.pcd.go.th (location: Ratchathewi District Office, Bangkok Phayathai Roadside, Ratchathewi, Bangkok) located 1.16 km away from the sampling site.

Statistics

Pollen counts and meteorological data were analyzed and illustrated using GraphPad Prism version 9.0.0 (GraphPad Software Inc., CA, USA). The correlation was assessed using Spearman ρ. Statistical significance was determined at a level of 0.05.

Results and Discussion:

No significant correlation was observed between PM_{2.5} or PM₁₀ concentrations and airborne pollen count across the study period, suggesting that a longer surveillance period is needed to capture potential seasonal patterns. Though not significant, the higher recorded pollen counts coincided with the higher PM_{2.5} measurement, and vice versa, likely reflecting meteorological conditions attributed to both pollutant dispersion and enhanced pollen release (Fig.1). These factors should therefore be integrated more closely in future studies and monitoring of pollen counts.

Among the identified pollen, Typhaceae (22.1%) made up the largest portion, followed by Poaceae (13.9%) and Acanthaceae (7.2%). An additional 3.7% could be assigned to other families, while the majority (53.1%) could only be classified as pollen. Notably, at least one allergenic pollen type known to affect Thai patients (Typhaceae, Poaceae, Cyperaceae, and/or Amaranthaceae) was found on every sampling day.

Throughout the collection period, low $PM_{2.5}$ levels equivalent to Thai AQI "excellent" to "satisfactory" (0–25 $\mu g/m^3$) were recorded on 20 days and levels equivalent to "moderate" to "very unhealthy" (>25 $\mu g/m^3$) on 30 days (Fig.1 B.). $PM_{2.5}$ was consistently the dominant air pollutant determining AQI levels, followed by PM_{10} and ozone.

Pollen concentrations are strongly influenced by species-specific pollen seasons, which vary in timing and intensity according to plant genetics and meteorological conditions. Accurate prediction therefore requires additional monitoring of flowering wind-pollinated plants and weather forecasts. Similarly, air pollution levels are shaped by meteorological patterns and human emissions, leading to a relatively sudden rise rather than gradual change during a year. Still, within this defined overlap of the two seasons, weather patterns provide critical clues for anticipating exposure levels and thus should be the focus of future studies.

Further, the pollen captured depends largely on the immediate flowering plants in its vicinity. Consequently, pollen of primarily insect-pollinated plants, namely *Lagestroemia sp.*, was also counted. Thus, emphasizing the need of allergy patients to evade pollen exposure by removing or avoiding the pollen source from their surroundings whenever possible.

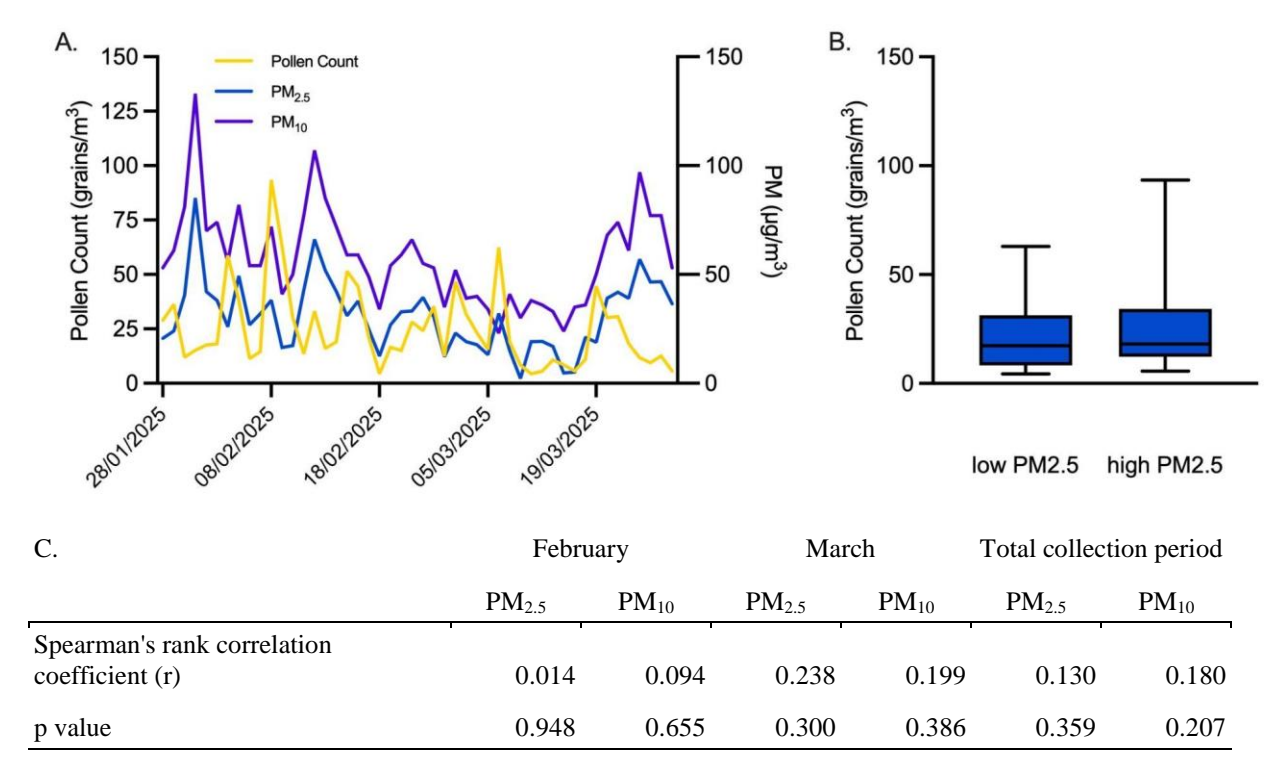


Figure 1 A. Average pollen count, PM_{2.5}, and PM₁₀ levels between 9:00–12:00 of Jan.28–Mar.30.2025 **B.** Distribution of pollen counts corresponding to low and high PM_{2.5} values **C.** Correlation analysis of atmospheric pollen concentrations (pollen count) and particulate matter using Spearman's rank correlation (r) at a significance level of 0.05.

Conclusion:

People who are susceptible to developing respiratory symptoms due to allergenic airborne pollen or particulate matter, especially PM_{2.5}, are constantly exposed to elevated levels of either during February and March, and likely the entire smog season, which severely affects their quality of life. It is therefore important to determine relevant weather patterns and improve co-monitoring of airborne pollen and pollutants. Doing so will improve public health forecasts, facilitating the implementation of prevention strategies so that the negative effects on patients can be minimized.

References:

- 1. Idrose NS, Lodge CJ, Erbas B, Douglass JA, Bui DS, Dharmage SC. A Review of the Respiratory Health Burden Attributable to Short-Term Exposure to Pollen. *Int J Environ Res Public Health*. 2022;19(12):7541. doi:10.3390/ijerph19127541
- 2. Izah SC, Ogwu MC, Etim NG, Shahsavani A, Namvar Z. Short-Term Health Effects of Air Pollution. In: Izah SC, Ogwu MC, Shahsavani A, eds. *Air Pollutants in the Context of One Health: Fundamentals, Sources, and Impacts*. Springer Nature Switzerland; 2024:249-278. doi:10.1007/698_2024_1132
- 3. Chen F, Zhang W, Mfarrej MFB, et al. Breathing in danger: Understanding the multifaceted impact of air pollution on health impacts. *Ecotoxicol Environ Saf.* 2024;280:116532. doi:10.1016/j.ecoenv.2024.116532

- 4. Carlsen HK, Haga SL, Olsson D, et al. Birch pollen, air pollution and their interactive effects on airway symptoms and peak expiratory flow in allergic asthma during pollen season a panel study in Northern and Southern Sweden. *Environ Health Glob Access Sci Source*. 2022;21(1). doi:10.1186/s12940-022-00871-x
- 5. Czarnobilska E, Bulanda M, Bulanda D, Mazur M. The Influence of Air Pollution on the Development of Allergic Inflammation in the Airways in Krakow's Atopic and Non-Atopic Residents. *J Clin Med*. 2021;10(11):2383. doi:10.3390/jcm10112383
- 6. Konishi S, Ng CFS, Stickley A, et al. Particulate matter modifies the association between airborne pollen and daily medical consultations for pollinosis in Tokyo. *Sci Total Environ*. 2014;499:125-132. doi:10.1016/j.scitotenv.2014.08.045
- 7. Tesfaldet YT, Chanpiwat P. The effects of meteorology and biomass burning on urban air quality: The case of Bangkok. *Urban Clim.* 2023;49:101441. doi:10.1016/j.uclim.2023.101441
- 8. Juprasong Y, Sirirakphaisarn S, Siriwattanakul U, Songnuan W. Exploring the effects of seasons, diurnal cycle, and heights on airborne pollen load in a Southeast Asian atmospheric condition. *Front Public Health*. 2022;10:1067034. doi:10.3389/fpubh.2022.1067034
- 9. Songnuan W, Bunnag C, Soontrapa K, Pacharn P, Siriwattanakul U, Malainual N. Airborne pollen survey in Bangkok, Thailand: A 35-year update. *Asian Pac J Allergy Immunol*. 2015;33(3):253-262.
- 10. Aud-in S, Juprasong Y, Pinkaew B, Talek K, Tantilipikorn P, Songnuan W. Incidence of grass and weed sensitization in Bangkok, Thailand: a clinical study. *Front Public Health*. 2024;12. doi:10.3389/fpubh.2024.1301095
- 11. Oncham S, Udomsubpayakul U, Laisuan W. Skin prick test reactivity to aeroallergens in adult allergy clinic in Thailand: a 12-year retrospective study. *Asia Pac Allergy*. 2018;8(2):e17. doi:10.5415/apallergy.2018.8.e17
- 12. Rojo J, Rapp A, Lara B, Fernández-González F, Pérez-Badia R. Effect of land uses and wind direction on the contribution of local sources to airborne pollen. *Sci Total Environ*. 2015;538:672-682. doi:10.1016/j.scitotenv.2015.08.074
- 13. Frenz DA, Boire AA. Pollen recovery in atmospheric samples collected with the Rotorod Sampler over multiple-day periods such as weekends. *Ann Allergy Asthma Immunol*. 1999;83(3):217-221. doi:10.1016/s1081-1206(10)62643-9
- 14. Bankhead P, Loughrey MB, Fernández JA, et al. QuPath: Open source software for digital pathology image analysis. *Sci Rep.* 2017;7(1):16878. doi:10.1038/s41598-017-17204-5

THE EFFECT OF ARSENIC EXPOSURE ON EXTRACELLULAR MATRIX REMODELING IN CHOLANGIOCARCINOMA MICROENVIRONMENT

Chilean Chheang¹, Chotirat Rattanasinchai ^{2,3}, and Panida Navasumrit ^{2,3}

¹Applied Biological Sciences Program, Chulabhorn Graduate Institute, Bangkok, Thailand, 10210 ²Laboratory of Environmental Toxicology, Chulabhorn Research Institute, Bangkok, Thailand, 10210 ³Center of Excellence on Environmental Health and Toxicology (EHT), OPS, MHESI, Thailand, 10210 Email: Chilean@cgi.ac.th

Abstract:

Cholangiocarcinoma (CCA) is an aggressive malignancy of the bile duct epithelium, often associated with poor prognosis. Increasing epidemiological evidence suggests that arsenic (As) exposure may contribute to CCA development and progression, yet the underlying mechanisms remain unclear. Herein, this study investigates the potential effects of As exposure on alteration of CCA microenvironment using an *in vitro* model comprising red fluorescent protein-expressing human intrahepatic CCA cells (HuCCA-A4) and hepatic stellate cells, HSC, (LX-2).

Method: The viability of cells treated with sodium arsenite (NaAsO₂) at concentrations of 0-10 μ M was assessed by using MTT assays. Expression levels of genes involved in fibrosis and ECM remodeling in HuCCA-A4 were evaluated by using qRT-PCR. Conditioned medium (CM) from NaAsO₂-treated HuCCA-A4 was applied to LX-2 cells to assess fibrotic and inflammatory responses evaluated at the mRNA levels using qRT-PCR and at the protein levels using ELISA. Collagen I deposition was evaluated in an HuCCA-A4/LX- 2 co-culture system via immunofluorescence staining.

Results: MTT analysis in NaAsO2- treated HuCCA-A4 cells showed reduced cell viability starting at 5-10 μ M (24 h), 2.5-10 μ M (48 h), and 2-10 μ M (72 h). NaAsO2 treatment in HuCCA-A4 induced dose-dependent upregulation of *CTGF*, a fibrotic marker, as well as both ECM remodeling enzymes, *LOX* and *MMP-1*. In LX-2 cells, CM from HuCCA-A4 alone significantly elevated *IL-6* and *IL-8* expressions at both mRNA and protein levels compared to a control condition. Notably, the levels of *IL-8*, but not *IL-6*, also further increased when LX-2 cells were exposed to CM from NaAsO2-treated HuCCA-A4 cells. In the co-culture system, deposition of extracellular collagen I could be visualized and the increase in its length and abundance was also observed when the co-culture was exposed NaAsO2 treatment. Taken together, these findings suggest that As may promotes CCA progression by directly inducing the expressions of ECM remodeling genes in CCA cells and by stimulating the secretion of pro-fibrotic and pro- inflammatory mediators, which activate surrounding stromal cells and contribute to a tumor- supportive microenvironment.

Keywords: Cholangiocarcinoma, arsenic, sodium arsenite, red fluorescent protein-expressing HuCCA-A4 cells, hepatic stellate cells, extracellular matrix remodeling.

Introduction:

Cholangiocarcinoma (CCA) is a heterogeneous and highly aggressive malignancy originating in the bile ducts, posing a significant health concern worldwide (1). CCA incidence in Thailand, especially in the northeastern region, is primarily attributed to liver fluke infestation (2). Although it is projected that the incidence of CCA in Thailand steadily declines (3), the incidence and mortality rates of intrahepatic CCA (iCCA) have been increasing in Western Europe, the United Kingdom, the United States, and Australia, affecting both genders (4). Arsenic (As) exposure is a significant global public health issue in both developed and developing countries; approximately 200 million people are unintentionally exposed to arsenic primarily through drinking water (5). Chronic As exposure has been epidemiologically linked to various adverse health effects, including non-carcinogenic and carcinogenic effects (6). Growing evidence suggests a strong association between a prolonged exposure to sodium arsenite (NaAsO2)-contaminated drinking water and the development of CCA (7).

Aberrant ECM remodeling plays a critical role in fibrosis and cancer (8). Alteration of the TME caused by atypical expressions of ECM remodeling enzymes, *e.g.* matrix metalloproteinase 1 (MMP-1) and lysyl oxidase (LOX), and pro-fibrogenic mediators, *e.g.* connective tissue growth factor (CTGF), may orchestrate ECM remodeling within the tumor mass forming a favorable microenvironment for CCA progression (9). Although there is no direct *in vitro* and *in vivo* data to demonstrate the association between As exposure and CCA progression (7), several studies have already reported that As exposure can lead to liver fibrosis, which can eventually progress to cancer (10). Therefore, this research aims to explore the potential mechanisms of how the environmental toxicant such as As affects the TME of CCA, particularly its role in ECM remodeling and the influence on surrounding cells such as HSC.

Objective:

- 1. Investigating the direct effect of NaAsO₂ exposure on alteration of genes involved in fibrosis and ECM remodeling in CCA cells.
- 2. Assessing the effect of conditioned media (CM) from NaAsO₂-exposed CCA cells on alteration of genes involved in inflammatory responses and ECM remodeling in HSC cells.

Methodology:

1. Cell culture

HuCCA-A4 cells expressing RFP were cultured in Ham's F-12 medium supplemented with FBS, L-GlutaMax, penicillin/streptomycin and puromycin. Human hepatic stellate LX2 cells were maintained in DMEM supplemented with FBS, L-GlutaMax, sodium pyruvate without antibiotic.

2. Dose response and cell viability

An MTT assay was used to assess cell viability of HuCCA-A4 and LX-2 cells treated with NaAsO $_2$ (0-10 μ M) for 24, 48, and 72 h. The absorbance of purple formazan which corresponds to cell viability was read by using Spectra Imax ID3 spectrophotometer (Molecular devices). Cell morphology was also examined at each time point using the BioTek Lionheart FX microscope (Agilent).

3. Gene expression analysis

Gene expression analysis was performed on HuCCA-A4 cells treated directly with NaAsO2 (0-5 μ M for 48 h), and on LX-2 cells exposed to conditioned media (CM) collected from HuCCA-A4 cells treated with 0, 1 and 2.5 μ M NaAsO2 for 48h, compared to the media pretreated with the corresponding NaAsO2 concentrations for 48 h. Total RNA was extracted using the RNeasy Mini Kit (Qiagen), and cDNA was synthesized with the qScript cDNA Synthesis Kit (Quantabio). qRT-PCR was performed using CFX96 thermocycler (Bio-rad) with Thunderbird Tm Next SYBR qPCR Mix (Toyobo). PPIA served as a housekeeping control gene. Target genes for HuCCA-A4 included: *CTGF*, *MMP1*, *LOX*, *TGFB1*, *TGFB1R*, and *COL1A1*. For LX-2 cells, target genes included: *CTGF*, *MMP1*, *LOX*, *COL1A1*, *FN1*, *IL6*, *IL8*.

4. Enzyme Linked immunosorbent assay (Elisa)

Conditioned media from LX-2 cells treated with supernatants of HuCCA-A4 cells exposed to NaAsO₂ were collected and analyzed using IL-6 (R&D Systems) and IL-8 (BioLegend) ELISA kit, following the manufacturers' protocols. The absorbance was read using a SpectraMax iD3 spectrophotometer. Cytokine concentrations were calculated from the mean of duplicate wells based on standard curves.

5. Immunofluorescent (IF) staining assay

Immunofluorescence staining was performed to assess the presence of extracellular collagen I fibers in a HuCCA-A4/LX-2 co-culture model treated with NaAsO $_2$ (0-5 μ M for 48 h). No permeabilization step was performed prior to blocking. Samples were incubated with anti-collagen I antibody and counterstained with DAPI. Fluorescence images were captured using the BioTek Lionheart FX microscope.

Result and Dicussion:

1. The effect of NaAsO2 exposure of cell viability and morphology

NaAsO₂ treatment reduced cell viability in a dose- and time-dependent manner in both HuCCA-A4 and LX-2 cells. Higher concentrations ($\geq 2.5-5~\mu M$) significantly decreased viability, especially at 48–72 h, while lower doses had minimal effects. Morphological changes, including reduced density and cell elongation in IX-2, were observed at cytotoxic concentrations of 2.5–5 μM .

2. Gene expression analysis in NaAsO₂-treated HuCCA-A4 and CM-treated LX-2 Cells

NaAsO₂ treatment upregulated *CTGF*, *MMP1*, and *LOX* gene expressions in HuCCA- A4 cells in a dose-dependent manner, with significant increases at 5 μ M. *TGF-\beta1* and *TGF-\betaR1* showed modest changes, while *COL1A1* was undetectable. In LX-2 cells, CM from NaAsO₂-treated HuCCA-A4 cells significantly elevated *IL-6*, *IL-8*, *MMP-1*, and *LOX* expression, especially at CM with 2.5 μ M NaAsO₂ treatment. Additionally, *CTGF* in LX-2 decreased at CM from lower NaAsO₂ doses but slightly increased when LX-2 cells were treated with CM with 2.5 μ M NaAsO₂ treatment. *COL1A1*, *FN1*, and *VIM* exhibited fluctuating or reduced expression across treatments.

3. Cytokine Secretion in LX-2 exposed to CM from NaAsO₂-treated HuCCA-A4 cells

CM from NaAsO₂-treated HuCCA-A4 cells significantly increased secretion of *IL*-6 and *IL*-8 in LX-2 cells, compared to arsenite treatment alone. *IL*-6 levels peaked in CM 0 and 1 μ M groups (~18 ng/mL, p < 0.0001), with a slight decrease at 2.5 μ M. *IL*-8 levels showed a dose-dependent increase, reaching ~30 ng/mL at CM 2.5 μ M (p < 0.0001). However, direct As treatment had minimal effect on cytokine production.

4. Collagen I fibers in HuCCA-A4/LX-2 Co-Cultures

Immunofluorescence staining of co-cultured cells revealed enhanced extracellular collagen I fibers in a treatment with 1 and 2.5 μ M NaAsO₂, compared to the control group. Additionally, the collagen I fibers at 5 μ M NaAsO₂ treatment appears to be fluctuated as it dropped in some experiment while slightly increase in the others.

Conclusion:

Collectively, our observations indicate that NaAsO₂ exposure may be linked to alterations in ECM remodeling within iCCA tumors, alongside enhanced secretion of proinflammatory factors. These changes could potentially influence surrounding stromal cell activity and support the development of a microenvironment favorable to tumor progression.

Reference:

- 1. Vij M, Puri Y, Rammohan A, G G, Rajalingam R, Kaliamoorthy I, et al. Pathological, molecular, and clinical characteristics of cholangiocarcinoma: A comprehensive review. World J Gastrointest Oncol. 2022;14(3):607-27.
- 2. Kamsa-ard S, Luvira V, Suwanrungruang K, Kamsa-ard S, Luvira V, Santong C, et al. Cholangiocarcinoma Trends, Incidence, and Relative Survival in Khon Kaen, Thailand From 1989 Through 2013: A Population-Based Cancer Registry Study. Journal of Epidemiology. 2018;29.
- 3. Kamsa-Ard S, Santong C, Kamsa-Ard S, Luvira V, Luvira V, Suwanrungruang K, et al. Decreasing trends in cholangiocarcinoma incidence and relative survival in Khon Kaen, Thailand: An updated, inclusive, population-based cancer registry analysis for 1989-2018. PLoS One. 2021;16(2):e0246490.
- 4. Pascale A, Rosmorduc O, Duclos-Vallée J-C. New epidemiologic trends in cholangiocarcinoma. Clinics and Research in Hepatology and Gastroenterology. 2023;47(9):102223.
- 5. Muzaffar S, Khan J, Srivastava R, Gorbatyuk MS, Athar M. Mechanistic understanding of the toxic effects of arsenic and warfare arsenicals on human health and environment. Cell Biology and Toxicology. 2023;39(1):85-110.
- 6. Hong YS, Song KH, Chung JY. Health effects of chronic arsenic exposure. J Prev Med Public Health. 2014;47(5):245-52.
- 7. Reyes D, Ganesan N, Boffetta P, Labgaa I. Arsenic-contaminated drinking water and cholangiocarcinoma. Eur J Cancer Prev. 2023;32(1):10-7.
- 8. Cox TR, Erler JT. Remodeling and homeostasis of the extracellular matrix: implications for fibrotic diseases and cancer. Dis Model Mech. 2011;4(2):165-78.
- 9. Closset L, Gultekin O, Salehi S, Sarhan D, Lehti K, Gonzalez-Molina J. The extracellular matrix immune microenvironment crosstalk in cancer therapy: Challenges and opportunities. Matrix Biology. 2023;121:217-28.
- 10. Liu J, Waalkes MP. Liver is a target of arsenic carcinogenesis. Toxicological Sciences. 2008;105(1):24-32.

THE EVALUATION OF GREENHOUSE GAS EMISSIONS IN PRIMARY COFFEE CULTIVATION AND PRIMARY PROCESSING

<u>Nutrada Wichanuchit</u>¹, Thanakrit Neamhom^{2,3}, Withida Patthanaissaranukool^{2,3} and Chate Jaikanlaya^{2,3}

¹Master of Science Program in Environmental, Faculti of Public Health,
Mahidol University, Rajvithi Road, Bangkok, 10400, Thailand

²Department of Environmental Health Science, Faculty of Public Health,
Mahidol University, Rajvithi Road, Bangkok, 10400, Thailand

³Center of Excellence on Environmental Health and Toxicology (EHT), OPS, MHESI, Thailand

Abstract:

Coffee cultivation and primary processing contribute significantly to greenhouse gas emissions (GHGs), Particularly using fertilizers, fossil fuels, and energy consumption during processing. This study aimed to evaluate greenhouse gas emissions from coffee production in Nan Province, Thailand, focusing on two phases 1. Coffee cultivation and coffee processing. Cultivation processes were divided into mono-cultivation and poly-cultivation. Results showed that monoculture cultivation emitted 0.13 kgCO₂/kg-coffee, whereas polyculture cultivation released a higher amount at 3.74 kgCO₂/kg-coffee, primarily due to greater fertilizer input during the planting phase. For coffee processing, the total emissions were relatively low, averaging 0.042 ± 0.020 kgCO₂/kg-coffee, with the main contributions arising from the milling and transportation by using diesel-fueled pickup trucks. A study found that polyculture systems demonstrated relatively lower greenhouse gas (GHG) emissions per unit of yield compared to monoculture practices, suggesting their potential as a more sustainable cultivation model. The findings highlight two key emission hotspots: fertilizer application during cultivation and water use during the coffee milling process. The results emphasize that adopting intercropping and optimized water management practices are potential solutions to significantly reduce GHG emissions. This study provides scientific evidence and practical recommendations to support Thailand's national strategies toward carbon neutrality by 2050 and net-zero emissions by 2065.(1)

Keywords: Greenhouse gas emissions, coffee cultivation, coffee processing, carbon footprint

Introduction:

Climate change has become one of the most pressing global challenges, with Thailand ranked among the countries most vulnerable to its impacts. In response, the Thai government has committed to the Paris Agreement (COP21) and COP26, aiming to achieve carbon neutrality by 2050 and net-zero greenhouse gas (GHG) emissions by 2065. Agriculture, which occupies nearly half of the nation's land area, is a significant contributor to GHG emissions due to heavy reliance on fertilizers, energy consumption, and land-use change. Therefore, understanding and quantifying emissions from specific agricultural systems is crucial for guiding mitigation strategies.

Coffee is an important economic crop in Thailand, particularly in Nan Province, a major production area for Arabica coffee. In 2022(2), the total cultivation area in Nan Province reached 12,572 rai, producing 682 tons of coffee. Despite its economic value, limited research has been conducted on GHG emissions from coffee production in Thailand, especially concerning the cultivation and primary processing stages. Previous studies (e.g., Ratchawat et al., 2017(3); Trinh et al., 2020(4),:Iglesias et al., 2025(5),:Nab et al., (6))

have shown that fertilizer application and intensive farming practices are the dominant sources of emissions, whereas intercropping systems and improved resource management can substantially lower the carbon footprint Cibelli et al, 2021(7).

Although coffee contributes substantially to regional economies, research on its environmental impacts in Thailand is limited. Existing studies, such as Ratchawat et al. (2017)(3), reported that fertilizer use during cultivation was responsible for up to 75% of emissions in roasted coffee production. International studies (de Souza et al., 2010(8); Van et al., 2014; Trinh et al., 2020(4),(9)) also confirm that intensive mono-cultivation systems release higher emissions, while intercropping systems and sustainable farming practices reduce the carbon footprint(10-12).

There is still limited research on greenhouse gas emissions from coffee cultivation and primary processing in Thailand, as previously mentioned. Therefore, this research project aims to study greenhouse gas emissions from the coffee cultivation and primary processing chain by examining different cultivation methods (mono-cultivation and poly-cultivation with other crops) in Arabica varieties, The findings of this study could serve as a guideline for reducing greenhouse gas emissions from related activities and provide valuable information for agricultural land-use planning to mitigate greenhouse gas emissions, contributing to tangible sustainable development solutions in the future.

Material and Methods:

This research was designed as an analytical survey to assess greenhouse gas (GHG) emissions from coffee cultivation and primary processing in Nan Province, Thailand. Data collection was conducted through field surveys with coffee farmers and processors in the main cultivation areas. The sample size was determined using Cochran's formula at a 90% confidence level, resulting in 80 farmer samples, separated into mono-cultivation and polycultivation systems, and 26 processing samples. Information gathered included fertilizer use, fuel and electricity consumption, water use, transportation distance, yield, and by-products. The assessment of GHG emissions followed the Thailand Greenhouse Gas Management Organization (TGO) guidelines(13), in which activity data were multiplied by standard emission factors to estimate emissions in kilograms of carbon dioxide equivalent. After calculating emissions for both cultivation and processing, the data were analyzed to identify significant emission hotspots. Finally, scenarios for emission reduction were developed and interpreted, with an emphasis on fertilizer management, cultivation practices, and resource efficiency as potential strategies to mitigate the carbon footprint of coffee production in the study area.

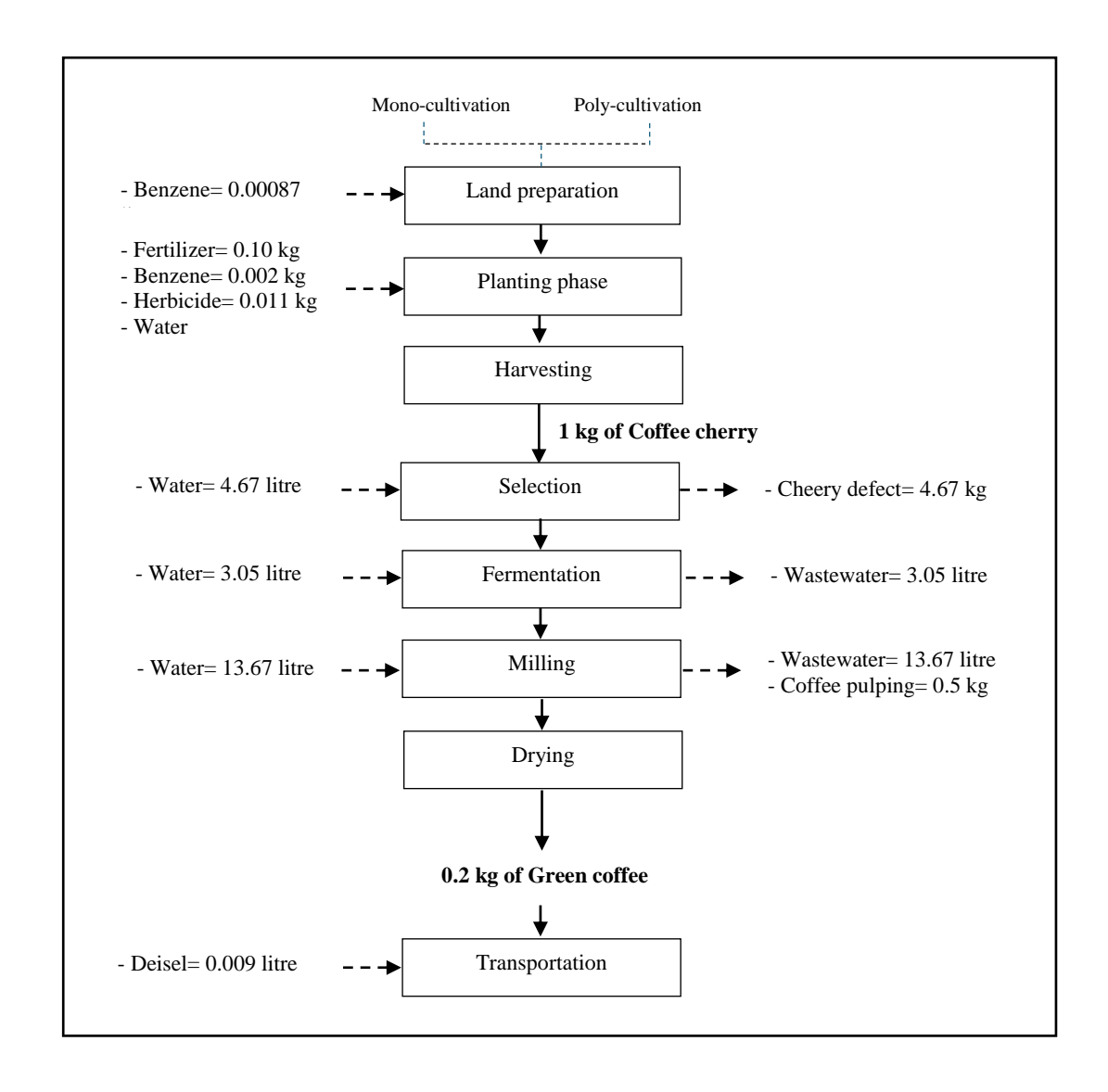


Figure 1 Mass flow of coffee cultivation and primary processing

Results and discussion:

From the data collection and interviews with 80 coffee farmers in Nan Province, 62 samples represented mono-cultivation, and 18 samples represented poly-cultivation. The results indicated that coffee farmers utilized various resources, including gasoline for water pumps and grass cutters, chemical fertilizers, and pesticides for pest control. The quantities of these inputs used in the cultivation process are shown in table 1 Resource consumption of Mono-cultivation and Poly-cultivation

Table 1 Resource consumption of Mono-cultivation and Poly-cultivation

Activity	Unit	Resource consumption (unit per kg-coffee)		
Activity	Omt	Mono-cultivation	Poly-cultivation	
Land preparation				
- Benzene fuel	litre	0.00087 ± 0.00142	0.00142 ± 0.00046	
Cultivation				
- 1 st Fertilizer	kg	0.06 ± 0.06	0.95 ± 0.69	
- 2 nd Fertilizer	kg	0.04 ± 0.04	0.94 ± 0.70	
- 1 st Herbicide	kg	0.002 ± 0.002	0.005 ± 0.005	
- 2 nd Herbicide	kg	0.009 ± 0.007	-	
- Benzene fuel	litre	0.002 ± 0.001	0.001 ± 0.001	

From the data collection of 26 coffee processors, the greenhouse gas (GHG) emissions were estimated at 0.042 ± 0.028 kgCO₂ per kg-coffee. The main resources contributing to these emissions included water and gasoline used for water pumps, as well as fuel consumption for transporting green coffee beans to roasting facilities. Although the emission values from processing were relatively low compared to cultivation, they represent an important stage in the value chain, particularly due to high water demand and transportation-related fuel use. The details of resource consumption in the processing stage are presented in Table 2 Resource Consumption of Coffee Processing.

Table 2 Resource consumption of Coffee processing

Activity	Unit _	Resource consumption (unit per kg-coffee)		Carbon emission (kg-CO2 per kg-coffee)	
,		Average	SD	Average	SD
Selection process					
- Water	litre	4.67	1.44	-	-
- Benzene	litre	7	0	0.0134	1.44
Fermentation process					
- Water	litre	3.05	2.03	-	-
Milling process					
- Water	litre	13.67	6.42	-	-
Drying process	-	-	-	-	-
Transportation	litre	0.009	0.003	0.028	0.010

The assessment of greenhouse gas (GHG) emissions from coffee cultivation revealed clear differences between mono-cultivation and poly-cultivation systems. Polyculture showed significantly higher emissions, with an average of 3.74 kgCO_{2eq} per kg-coffee, compared to 0.13 kgCO_{2eq} per kg-coffee in monoculture. In both systems, fertilizer application was the dominant source of emissions. For polyculture, fertilizer use accounted for 3.724 kgCO₂eq, representing nearly 99% of the total emissions, while in monoculture it contributed 0.115 kgCO₂eq, or approximately 88%. The variation is strongly related to the types of fertilizers applied. Farmers practicing polyculture tended to use larger amounts of urea fertilizer (46-0-0), whereas those in monoculture mainly applied compound fertilizer (15-15-15) combined with organic chicken manure. These findings highlight fertilizer management as the critical hotspot influencing the overall carbon footprint of coffee cultivation.

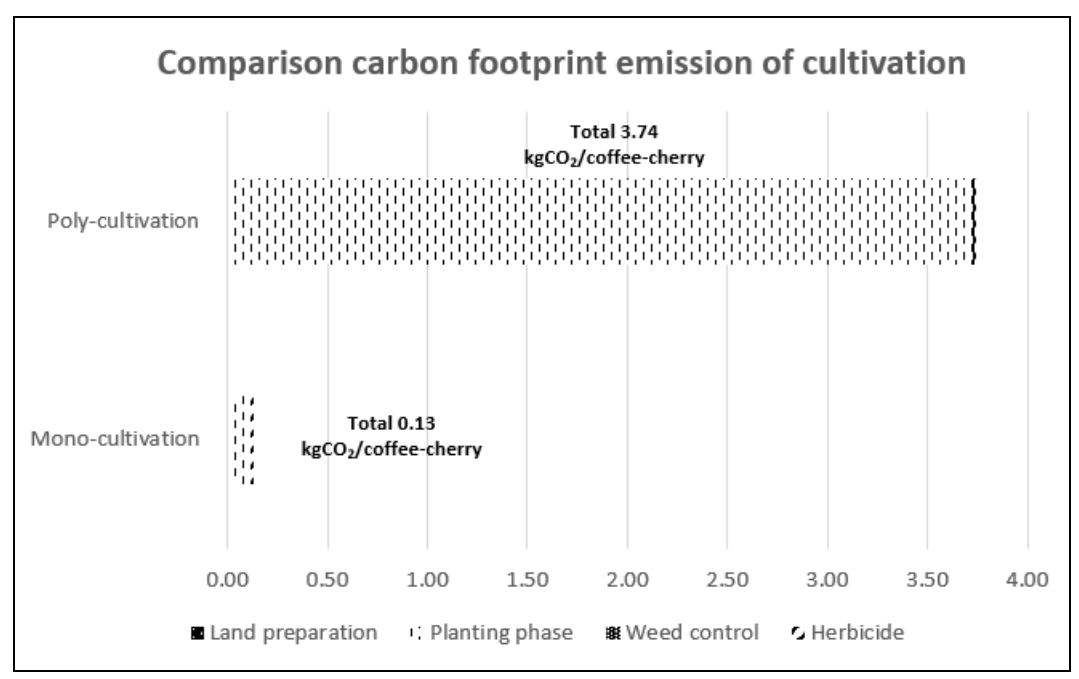


Figure 2 Comparison carbon footprint emission of cultivation

Conclusion:

This study assessed greenhouse gas (GHG) emissions from coffee cultivation and processing in Nan Province, Thailand. Overall emissions were relatively low, largely because farmers rely on rainfall for irrigation rather than energy-intensive pumping. However, fertilizer application was identified as the major hotspot, contributing 88–99% of total emissions. Urea fertilizer, due to its high nitrogen content, produced significantly higher GHG emissions compared to other inputs. Replacing urea with alternatives such as chicken manure or compound fertilizer (15-15-15) could substantially reduce emissions, lower production costs, and improve soil quality in the long term.

In the processing stage, GHG emissions were minor, with transportation identified as the main contributor. Collective transport and load optimization could reduce fuel use, thereby lower costs while improving logistical efficiency. Importantly, adopting these low-carbon practices offers farmers additional benefits, including opportunities to market their products as sustainable or climate-friendly coffee. This not only enhances their bargaining power in trade but also creates higher value in niche markets.

In conclusion, strategies focused on fertilizer management and transport efficiency can both mitigate GHG emissions and deliver economic and competitive benefits to farmers, aligning agricultural practices with Thailand's climate goals of carbon neutrality by 2050 and net-zero emissions by 2065.

Reference:

- 1. (MNRE). TOoNRaEPaPiaautMoNRaE. Mission is to develop and present a plan and policy to support and conserve the environment https://www.onep.go.th/en/2024 [
- 2. (OAE) OoAE. Agricultural statistics of thailand 2015 [
- 3. Ratchawat T. Greenhouse Gas Emissions from Roasted and Ground Coffee Productions in Thailand. 2017.
- 4. Trinh LTK. Comparative life cycle assessment for conventional and organic coffee cultivation in Vietnam. 2019.
- 5. Iglesias SP. Carbon footprint of coffee production: the case study of Indian Robusta coffee. 2025.
- 6. Nab C. Life cycle assessment synthesis of the carbon footprint of Arabica coffee: Case study of Brazil and Vietnam conventional and sustainable coffee production and export to the United Kingdom. 2020.
- 7. Cibelli M. Carbon footprint of different methods of coffee preparation. 2021.
- 8. Souza SPd. Greenhouse gas emissions and energy balance of palm oil biofuel. 2010.
- 9. Salinas B. Life Cycle Assessment of Coffee Production. 2008.
- 10. Rikxoort H. Carbon footprints and carbon stocks reveal climate-friendly coffee production. 2015.
- 11. Usva K. Carbon and water footprint of coffee consumed in Finland—life cycle assessment. 2020.
- 12. Soto-Pinto L. Carbon sequestration through agroforestry in indigenous communities of Chiapas, Mexico. 2009.
- 13. TGO TGGMOPO. Guidelines for the Calculation and Reporting of Organizational Carbon Footprint 2022 [Available from: https://thaicarbonlabel.tgo.or.th/index.php?lang=EN&mod=YjNKbllXNXBlbUYwYVc5 dVgyRndjSEp2ZG1Gcw.

TRANSCRIPTOMIC INSIGHTS INTO PA2806 DISRUPTION REVEAL ALTERED STRESS AND VIRULENCE BALANCE

IN Pseudomonas aeruginosa PAO1

<u>Duong Do Van¹</u>, Chonthicha Khotchakasorn¹, Skorn Mongkolsuk^{1,2,3}, and Mayuree Fuangthong^{1,2,3}

¹Program in Applied Biological Sciences, Chulabhorn Graduate Institute, Bangkok, Thailand ²Laboratory of Biotechnology, Chulabhorn Research Institute, Bangkok, Thailand ³Center of Excellence on Environmental Health and Toxicology (EHT), Vajira Operation and Support Program (VOPS), Ministry of Higher Education, Science, Research and Innovation (MHESI), Bangkok, Thailand

Abstract:

Copper is an essential micronutrient but becomes toxic at elevated concentrations. To explore how genetic factors contribute to copper stress adaptation, we examined a *Pseudomonas aeruginosa* PAO1 mutant lacking *PA2806*, a gene involved in tRNA modification. Comparative transcriptomic analysis between wild type and mutant strains revealed distinct transcriptional responses. Notably, loss of *PA2806* led to induction of oxidative stress defense genes and the repression of secretion-associated genes, suggesting a trade-off between stress tolerance and virulence. These findings highlight a previously unrecognized role of *PA2806* in shaping the bacterial response to copper.

Keywords: Pseudomonas aeruginosa PAO1, copper stress, transcriptomics, PA2806

Introduction:

Pseudomonas aeruginosa PAO1 is an opportunistic pathogen capable of thriving in diverse environments, including clinical settings where it contributes to chronic and acute infections. Its adaptability stems from versatile metabolic networks and complex regulatory systems that balance growth, stress resistance, and virulence (1). Copper is an essential micronutrient but becomes toxic at higher concentrations due to its redox activity, which can drive oxidative stress and damage macromolecules. Bacteria counteract copper toxicity through efflux systems, sequestration, and metabolic adaptations (2). Notably, copper stress can also influence virulence gene expression, although the underlying mechanisms remain incompletely understood (3).

The PA2806 gene encodes a key enzyme in queuosine biosynthesis, a tRNA modification implicated in translation fidelity and stress response. Disruption of PA2806 has been linked to altered cellular physiology (4), but its role in mediating the response to copper in P. aeruginosa remains unexplored. Here, we performed transcriptomic analysis comparing the PAO1 wild type and a $\Delta PA2806$ mutant to investigate the broader impact of PA2806 loss on bacterial gene expression.

Methodology:

Bacterial strains and conditions

Pseudomonas aeruginosa wild type PAO1 and Δ*PA2806* strains were cultured in M9 media (5 X M 9 m e d i a s a l t, 1 M MgSO₄.7H₂O, 20% glucose, 1M CaCl₂, and 1% casaminocacid) at 37 °C overnight. Cultures were subcultured to mid-logarithmic phase (OD₆₀₀ \approx 0.5) before harvesting. Cells were collected by centrifugation, washed with phosphate-buffered saline (PBS, pH 7.4), snap-frozen in liquid nitrogen, and stored at -80 °C for subsequent transcriptomic analyses.

RNA extraction and sequencing

Cell pellets were treated sequentially with Solution I (0.3 M sucrose, 10 mM sodium acetate, pH 4.8) and Solution II (2% SDS, 10 mM sodium acetate). Total RNA was extracted from biological triplicates using an acid-phenol: chloroform protocol optimized for *P. aeruginosa*. RNA integrity and concentration were assessed using an Agilent Bioanalyzer. Sequencing libraries were prepared and subjected to high-throughput sequencing by Novogene (Illumina platform). Raw reads were quality-checked, mapped to the *P. aeruginosa* PAO1 reference genome, and normalized to fragments per kilobase of transcript per million mapped reads (FPKM).

Differential expression analysis

Differentially expressed genes (DEGs) were identified using appropriate statistical thresholds (adjusted p-value < 0.05, |log2| fold-change|>1), with comparison included Q vs W. Venn diagrams were used to visualize overlaps. Gene ontology (GO) enrichment was performed to identify significantly overrepresented biological processes.

Principal component analysis (PCA)

FPKM-normalized gene expression values were subjected to PCA to assess clustering by condition. Three-dimensional visualization was performed to evaluate the contribution of *PA2806* deletion to overall transcriptional variance.

Results and Discussion:

Sequencing quality and mapping

RNA-seq of Q and W samples generated 25.1 - 32.3 million clean reads per sample, corresponding to 3.8–4.8 Gb of clean bases, with a consistently low base-calling error rate of 0.01%. High sequencing quality was confirmed by Q20 > 98.6% and Q30 > 94%, and GC content ranged from 62.19% to 63.1% for Q and 62.19% - 62.92% for W samples, consistent with the *Pseudomonas aeruginosa* PAO1 genome. These metrics indicate robust sequencing performance and sufficient coverage for downstream transcriptomic analyses.

Table 1 Summary of RNA-seq read quality and mapping metrics for Q and W samples

Sample	Raw reads	Clean reads	Raw bases	Clean	Error rate (%)	Q20 (%)	Q30 (%)	GC content (%)
Q1	33311806	32320608	5.0G	4.8G	0.01	98.73	94.9	63.1
Q2	28671570	27840514	4.3G	4.2G	0.01	98.79	94.97	63.1
Q3	25912048	25141800	3.9G	3.8G	0.01	98.74	94.88	62.99
W1	27346622	26531124	4.1G	4.0G	0.01	98.81	95.16	62.19
W2	25849542	25043126	3.9G	3.8G	0.01	98.76	94.95	62.48
W3	26534942	25742924	4.0G	3.9G	0.01	98.62	94.22	62.92

Gene-level quality control

Figure 1 shows the distribution of gene expression values across Q and W samples. Raw read counts follow the expected long-tailed RNA-seq pattern, with most genes expressed at low levels and a few highly expressed (Figure 1A). Replicate curves are similar, indicating consistent sequencing depth and no technical outliers. After normalization

(Figure 1B), FPKM values are comparable across samples, confirming effective library size correction. Overall, most genes exhibit low to moderate expression, consistent with the *P. aeruginosa* transcriptome.

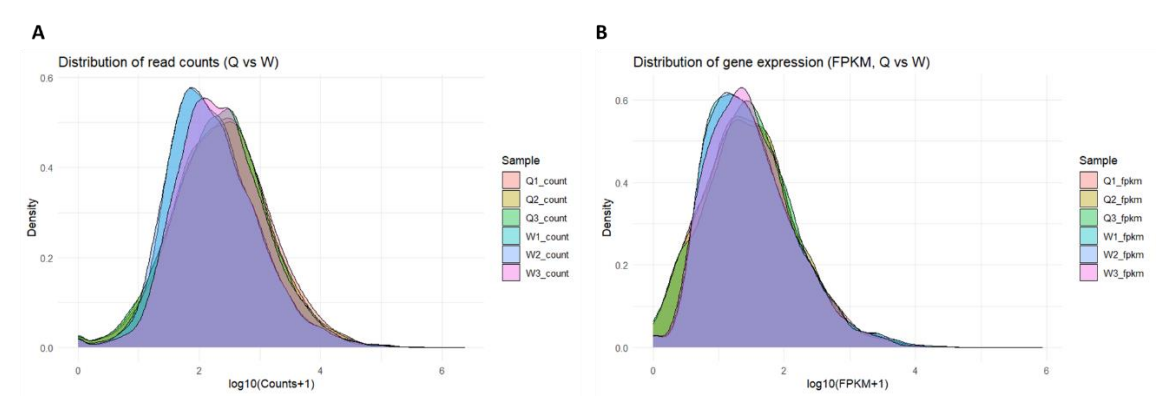


Figure 1 Distribution of gene expression values in Q and W samples. (A) Density plots of raw read counts showing that most genes were expressed at low levels, with a smaller fraction highly expressed. (B) Density plots of normalized FPKM values demonstrating comparable expression distributions across samples after normalization.

Sequencing depth and detected genes

Sequencing of the $\triangle PA2806$ mutant (Q1-Q3) and wild-type (W1-W3) transcriptomes produced 10.2 - 13.1 million reads per sample (Table 2), providing sufficient depth for bacterial transcriptomic profiling. Across all replicates, ~6,020-6,042 genes were detected, covering the majority of the PAO1 genome. Gene detection was highly consistent within each group, indicating comparable sequencing quality and coverage, and confirming the dataset is suitable for downstream differential expression analyses.

Table 2 Summary of sequencing depth and detected genes in *P. aeruginosa* PAO1 wild type (W) and $\Delta PA2806$ mutant (Q) samples

Sample	Total read	Detected genes
Q1	13122963	6031
Q2	11477384	6030
Q3	10247265	6026
W1	10798556	6039
W2	10438730	6042
W3	10383288	6042

Global transcriptional variation is driven by copper and PA2806

Three-dimensional PCA (Figure 2) revealed distinct separation between wild type and $\Delta PA2806$. This demonstrates that PA2806 deletion independently shape transcriptional states. These findings indicate that PA2806 contributes significantly to basal transcriptome architecture.

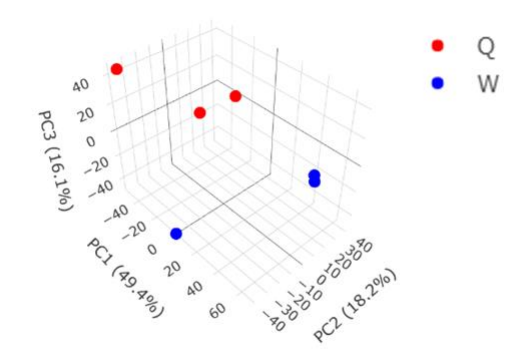


Figure 2 Principal component analysis (PCA) of transcriptome profiles of *P. aeruginosa* PAO1 wild type (W) and $\Delta PA2806$ mutant (Q) strains. Three-dimensional clustering illustrates distinct separation based on PA2806 deletion, highlighting their contributions to transcriptional variation.

Constitutive effects of PA2806 deletion under basal conditions

In the basal condition (Q vs W), $\Delta PA2806$ up-regulated oxidative stress defense genes including peroxiredoxin (ahpC), glutathione peroxidase, and several reductases, together with a metal-transporting P-type ATPase. These changes suggest that PA2806 contributes to redox stability, and its loss triggers compensatory activation of antioxidant and metal-handling systems. Conversely, genes encoding adhesion pili, Type VI secretion components (hcpC), and translational elements (tRNAs and tRNAs) were down-regulated. This indicates reduced investment in virulence-related secretion and translational machinery, pointing to a physiological shift toward stress management.

Conclusion:

This study demonstrates that *PA2806* plays a critical role in maintaining transcriptional balance in *Pseudomonas aeruginosa* POA1. Its loss enhances oxidative stress responses while suppressing secretion-related functions, pointing to a trade-off between stress survival and virulence.

References:

- 1. Rossi E, La Rosa R, Bartell JA, Marvig RL, Haagensen JAJ, Sommer LM, et al. *Pseudomonas aeruginosa* adaptation and evolution in patients with cystic fibrosis. Nature Reviews: Microbiology. 2021;19(5):331-42.
- 2. Teitzel, G. M., Geddie, A., De Long, S. K., Kirisits, M. J., Whiteley, M., & Parsek, M. R. (2006). Survival and growth in the presence of elevated copper: transcriptional profiling of copper-stressed *Pseudomonas aeruginosa*. Journal of Bacteriology, *188*(20), 7242-7256.
- 3. Young, C. A., Gordon, L. D., Fang, Z., Holder, R. C., & Reid, S. D. (2015). Copper tolerance and characterization of a copper-responsive operon, copYAZ, in an M1T1 clinical strain of *Streptococcus pyogenes*. Journal of Bacteriology, *197*(15), 2580-2592.
- 4. Pollo-Oliveira, L., Davis, N. K., Hossain, I., Ho, P., Yuan, Y., Salguero García, P., ... & de Crécy-Lagard, V. (2022). The absence of the queuosine tRNA modification leads to pleiotropic phenotypes revealing perturbations of metal and oxidative stress homeostasis in *Escherichia coli* K12. Metallomics, 14(9), mfac065.

Development of biologically active compounds for control, prevention and treatment of environmental health problems /diseases



GREEN BANANA FLOUR AND PROBIOTIC SYNERGIES: UNLOCKING THE FUNCTIONAL FOOD POTENTIAL OF THAI BANANAS

Natchaya Chatsaengsupawong¹, Wannaphorn Kookeaw¹, Jamorn Somana³, Surang Chankhamhaengdecha¹ and Thitinun Sumranwanich^{1,2}*

¹Department of Biology, Faculty of Science, Mahidol University, Bangkok, Thailand ²Center of Excellence on Environmental Health and Toxicology (EHT), OPS, MHESI, Bangkok, Thailand

³Department of Biochemistry, Faculty of Science, Mahidol University, Bangkok, Thailand *Email: thitinun.sum@mahidol.ac.th

Abstract:

Bananas (Musa spp.) are among the most important tropical fruits in Thailand, serving as both a staple food and cultural symbol, and as a promising source of bioactive compounds and resistant starch for functional food development. Thai banana cultivars, derived from Musa acuminata (A genome) and Musa balbisiana (B genome), exhibit genomic diversity that contributes to their nutritional and health-promoting properties. In this study, five cultivars: Teep (ABB), Hin (BBB), Tanee Pa (BB), Hakmuk (ABB), and Theppharot (ABB) were selected for evaluation of total phenolic content (TPC), total flavonoid content (TFC), antioxidant activity, and their potential as prebiotic substrates. Additionally, the encapsulation of Pediococcus pentosaceus with green banana flour from Theppharot cultivar was investigated as a freeze-drying strategy to enhance probiotic viability and shelf life. The results revealed that Tanee Pa exhibited the highest phenolic and flavonoid levels with strong antioxidant activity, while Theppharot cultivar demonstrated superior potential for probiotic encapsulation. Collectively, these findings highlight the nutritional diversity of Thai banana cultivars and their dual role as sources of bioactive compounds and encapsulating matrices, supporting their development into novel functional foods that promote gut health and overall well-being.

Keywords: Green banana flour, phenolic compounds, flavonoid content, antioxidant, *Pediococcus pentosaceus*

Introduction:

The human gut harbors trillions of microorganisms that significantly influence overall health, playing pivotal roles in metabolic processes, immune system regulation, and pathogen defense (1). Maintaining a balanced and diverse gut microbiota is crucial for human wellbeing, and disruptions in this delicate ecosystem are frequently associated with various chronic diseases (2, 3). One promising strategy to support a healthy gut microbiome and mitigate these disorders is through the consumption of prebiotics (4). Prebiotics are defined as non-digestible food components that selectively stimulate the growth and/or activity of beneficial bacteria in the colon, thereby improving host health. They are resistant to digestion by stomach acid and mammalian enzymes in the upper gastrointestinal tract, arriving intact in the colon where they are fermented by the resident microbiota.

Among the most important types of prebiotics is resistant starch (RS), which is characterized as starch and its degradation products that are not absorbed in the small intestine of healthy individuals (5). RS, particularly type II (RS2) found in uncooked foods like green bananas, is fermented by colonic bacteria to produce beneficial metabolites,

notably short-chain fatty acids (SCFAs) such as acetate, propionate, and butyrate (6). These SCFAs are critical for host health, serving as the primary energy source for colonocytes, maintaining the integrity of epithelial cells, regulating cell proliferation and apoptosis, and improving the intestinal barrier. SCFAs also play roles in regulating energy metabolism, immunological function, and gut cell proliferation, while also decreasing potentially harmful substances like secondary bile acids, ammonia, and phenols (6).

Given these profound benefits, there is growing interest in exploring natural sources of resistant starch for dietary intervention. Thai green banana flour, derived from unripe banana cultivars, emerges as a highly promising candidate due to its exceptional resistant starch content. Cultivars like Kluai Hin and Kluai Hakmuk, belonging to the BB genome group, are particularly rich in RS, with flour containing 52.2-68.1% RS and isolated starch reaching 70.1-79.2% RS (7). This high RS content, primarily as Type II resistant starch (RS2), makes it an excellent natural prebiotic. This study aims to investigate the prebiotic potential of five Thai green banana cultivars and to assess their ability to support the growth of the beneficial gut bacterium *Pediococcus pentosaceus* using *in vitro* fermentation models. The findings provide important insights into the functional properties of these cultivars and highlight their potential as a sustainable and accessible source of prebiotics for improving gut health.

Methodology:

Green bananas flour preparation

Five banana cultivars: Tanee Pa, Tanee Dam, Hin, Teep and Theppharot were selected at stage 1 according to the Vol Loesecke ripening scales. The bananas were first washed with tap water, then peeled or intact then sliced into 1 mm thick. To prevent browning, banana slices were soaked in a 0.3% (w/v) citric acid solution for 10 minutes. Banana slices were dried in a hot air oven at 50°C for 8 hours. After drying, banana slices were ground and sieved through a 100-mesh screen to obtain fine banana flour, then stored at 4°C until further use.

Moisture and ash content

Approximately 5 g of green banana flour were placed in a porcelain crucible and heated 105°C for 3 hours for measuring moisture content, where 550°C at 2 hours were used for ash content.

Total phenolic compounds (TPC)

The total phenolic content was determined using the Folin-Ciocalteu method, with gallic acid as the standard across a concentration range of 0 to 1000~mg/L

Antioxidant activity by 2,2'-Diphenyl-2-picryl-hydrazyl (DPPH)

In a 96-well plate, 40 μ L of the sample or Trolox standard (0–200 μ g/mL) was mixed with 260 μ L of 0.1 mM DPPH solution and incubated at 25°C for 30 minutes. Absorbance was measured at 517 nm, and the results were reported as the mean Trolox equivalent (TE) in milligrams per gram of dry mass.

Cultivation of *Pediococcus pentosaceus* with green banana flour

One gram of green banana flour was added to 10 mL of BHIY (Brain Heart Infusion with Yeast extract) medium containing 100 μ L of *P. pentosaceus*. The mixtures were incubated under anaerobic condition for 3, 5 and 7 days. Bacterial growth was monitored by measuring optical density (OD) at 600 nm.

Encapsulation of *Pediococcus pentosaceus* with Freeze-drying process

Bacteria was inoculated in 200 mL of BHIY and cultured at 37°C for 12 hours. The culture was centrifuged at 5,000 rpm for 20 minutes, washed and resuspended with 0.1M phosphate-buffered saline (PBS), pH 7.4. Bacterial solution was mixed with 20g of green banana flour dissolved in 150 mL water containing 1% (w/v) Tween 80 and stirred at 60°C. Sucrose 2% (w/v) was added as a cryoprotectant and the mixture was gently stirred for 1 hour. The emulsion was frozen at -20°C for 12 hours before subjecting to freeze drying for 24 hrs.

Results and Discussion:

Properties in Thai green banana flour (GBF)

GBF from five cultivars—Teep, Hin, Tanee Pa, Theppharot, and Hakmuk—was analyzed for pH, moisture content, and ash content (**Table 1**). Both peeled and unpeeled samples were examined to evaluate the influence of peel inclusion on these properties. The results revealed slight variations in moisture and ash content, largely attributable to the presence or absence of peel. All cultivars exhibited pH values within the acidic range, consistent with typical characteristics of banana-based products. Among the cultivars, Tanee Pa (both peeled and unpeeled) displayed the highest ash content.

	рН	Moisture (%)	Ash (%)
unpeel			
banana:			
Hakmuk	5.64	4.22	8.48
Hin	6.90	6.93	12.17
Teep	5.77	6.01	10.05
Taneepa	6.35	6.70	20.16
1	5.90	5.41	12.42
Theppharot			
peeled			
banana:			
Hakmuk	5.57	5.87	9.56
Hin	6.85	4.21	7.56
Teep	5.78	5.66	12.12
Taneepa	6.00	7.54	20.89
1	6.02	2.40	12.98
Theppharot			

Table 1 pH, moisture content (%), and ash content (%) of green banana flour (GBF) from five Thai cultivars, analyzed separately for peeled and unpeeled samples. Values are expressed as mean \pm standard deviation (SD) from three independent replicates (n = 3). Different superscript letters within the same column indicate significant differences (p < 0.05).

Total Phenolic Content (TPC) and Antioxidant Activity

As shown in **Figure 1**, the GBF from Tanee Pa cultivar exhibited the highest total phenolic content (TPC) in both peeled and unpeeled forms, which corresponded with its strong antioxidant activity observed in **Figure 2**. GBF from the Teep and Theppharot cultivars also demonstrated high DPPH radical scavenging activity. The inclusion of peel significantly influenced both TPC and antioxidant activity, with peeled samples generally exhibiting higher levels than unpeeled ones.

Prebiotic Potential and Probiotic Encapsulation

GBF from the Taneedam and Theppharot cultivars demonstrated superior prebiotic effects, exhibiting the highest colony-forming units (CFU) of *P. pentosaceus* after three days of incubation (**Figure 3**). Although bacterial growth declined after day three, significant survival was observed in GBF from both Theppharot and Taneedam. Based on these results, Theppharot GBF was selected for probiotic encapsulation. As shown in **Figure 4**, the freezedrying approach effectively enhanced the viability of the encapsulated bacteria. The encapsulated probiotics maintained high viability, with no significant decrease observed from one week to one month post-encapsulation, highlighting the potential of Theppharot green banana flour as a protective matrix for live probiotic cultures.

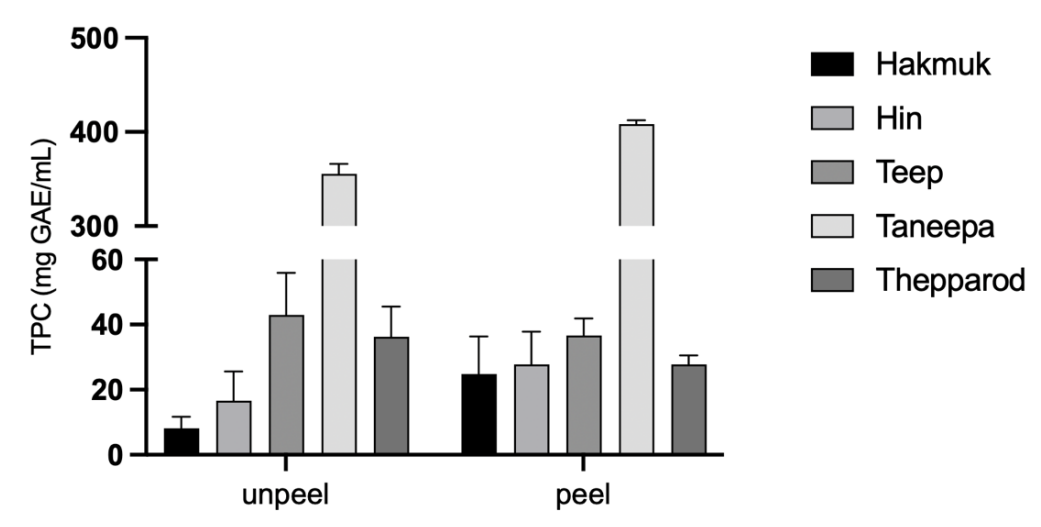


Figure 1 Total phenolic content of peeled and unpeeled samples from different banana cultivars. Values are presented as mean \pm standard deviation (SD) of three independent replicates (n = 3). Different superscript letters indicate significant differences between samples (p < 0.05).

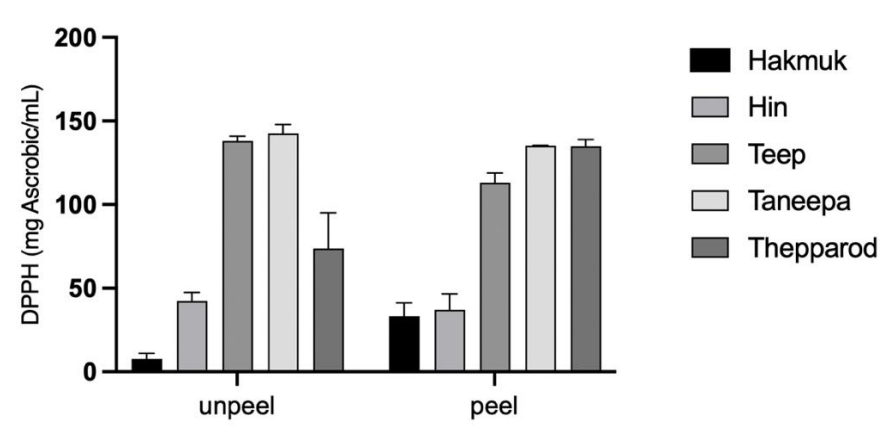


Figure 2 DPPH radical scavenging activity of peeled and unpeeled samples from different banana cultivars.

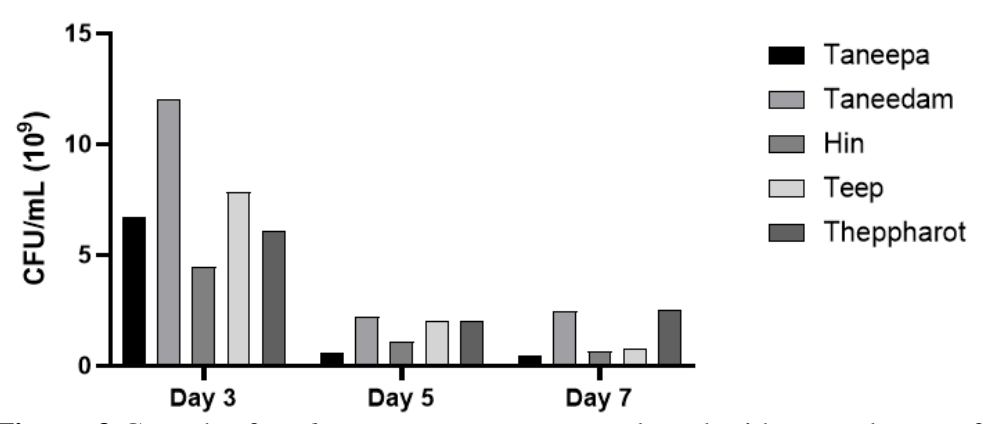


Figure 3 Growth of *Pediococcus pentosaceus* cultured with green banana flour (GBF) from different cultivars.

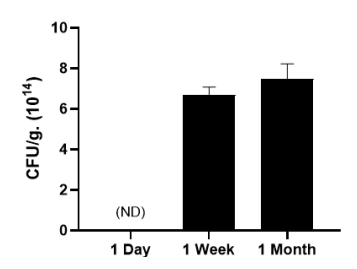


Figure 4 Viability of encapsulated probiotic *Pediococcus pentosaceus* after 1 day, 1 week, and 1 month of storage.

Conclusion:

Thai green banana flours exhibit cultivar-dependent functional properties. Tanee Pa showed the highest phenolic content and antioxidant activity, while Taneedam and Theppharot promoted the growth and survival of *Pediococcus pentosaceus*. Theppharot GBF effectively preserved probiotic viability after freeze-drying, highlighting its potential as a functional ingredient for gut health.

References:

- 1. Xu J, Knight R. Unlocking the secrets of the human gut microbiota. World J Gastroenterol, 2025; 31(5):99913.
- 2. Li P, Li M, Song Y, Huang X, Wu T, Xu ZZ, Lu H. Green banana flour contributes to gut microbiota recovery and improves colonic barrier integrity in mice following antibiotic perturbation. Front Nutr. 2022 Mar 13;9:860049.
- 3. Sharma A, Singh P. Gut microbiota and its impact on chronic diseases: A comprehensive review. J Pharm Bioallied Sci. 2025 Jun;17(Suppl 2):S1080-2.
- 4. Fang Q, Yu L, Tian F, Chen W, Zhai Q. Understanding of the efficacy of gut microbiota-directed foods on human health. Trends Food Sci Technol. 2023;136:92-99.
- 5. Zhang X, Yi X, Yu W, Chen T, Gao B, Gilbert RG, Li C. Targeting gut microbiota by starch molecular size and chain-length distribution to produce various short-chain fatty acids. Carbohydr Polym. 2024;329:121779.
- 6. Wang J, Li Y, Chen Y, Zhang X. The mechanisms in the gut microbiota regulation and type 2 diabetes therapeutic activity of resistant starches. Trends Food Sci Technol. 2024;142:113-125.
- 7. Pailumpa N, Thongngam M, Naivikul O. Resistant starch content, *in vitro* starch digestibility and physico-chemical properties of flour and starch from Thai bananas. Maejo Int J Sci Technol. 2012;6(2):283-292.

MELATONIN-MEDIATED MODULATION OF HYPOXIA-INDUCED NEUROINFLAMMATION IN SH-SY5Y HUMAN NEUROBLASTOMA CELLS

<u>Kultasnim Kado¹</u>, Chutikorn Nopparat² and Piyarat Govitrapong^{1,*}

¹Applied Biological Sciences: Environmental Health Program, Chulabhorn Graduate Institute, Bangkok 10210, Thailand ²Innovative Learning Center, Srinakharinwirot University, Bangkok 10110, Thailand *Corresponding author. Email: Piyarat@cgi.ac.th

Abstract:

Neuroinflammation plays a significant role in the progression of neurodegenerative diseases, such as Alzheimer's disease (AD), Parkinson's disease (PD), and Amyotrophic Lateral Sclerosis (ALS). Neuroinflammation is a response that serves both protective and pathological roles in the central nervous system (CNS). However, the prolonged and dysregulated neuroinflammation promotes a plethora of adverse effects on the CNS. Apart from infection, the neuronal damage caused by hypoxia can stimulate the neuroinflammatory response, which is a contributing cause of subsequent neurodegenerative disease. Melatonin is an endogenous molecule primarily synthesized in the pineal gland. The physiological role of melatonin is to regulate sleep cycles and serve as a potent antioxidant. Recently, melatonin has also affected the inflammatory response. Several mechanisms were elucidated to investigate the anti-inflammatory role of melatonin. In this study, we studied the antiinflammatory effect of melatonin in different concentrations after hypoxia induction in the SH-SY5Y cell line. After inducing an oxygen-glucose deprivation/ reperfusion (OGDR) condition in the SH-SY5Y cell line, the protein expression related to neuroinflammation, the NLRP3 inflammasome, was markedly increased. Different concentration of melatonin was added to the reperfusion medium. The results demonstrated that the protein expression of the NLRP3 inflammasome was significantly reduced in a concentration-dependent manner. This finding led to a further study of the mechanism of melatonin as a potential therapeutic agent for neurodegenerative diseases.

Keywords: Melatonin, neuroinflammation, hypoxia, NLRP3 inflammasome

Introduction:

Neuroinflammation is defined as an immune response occurring in the CNS. When neuroinflammation is activated, immune cells infiltrate the CNS. Additionally, the activation of primary resident immune cells, including microglia, is promoted. These activations provide protective and detrimental roles to the CNS. Pathogen-associated molecular patterns (PAMPs) and Damage-associated molecular patterns (DAMPs) are activators for the innate immune system. Especially, DAMPs are endogenous molecules released from damaged or dying cells to act as danger signals and initiate an inflammatory response (1). In the context of hypoxia, there are several types of DAMPs released from cells, such as heat shock proteins (HSPs), mitochondrial DNA (mtDNA), high mobility group box 1 (HMGB1), S100 proteins, and extracellular adenosine triphosphate (eATP). These DAMPs could activate innate immunity and subsequently promote assembly of the Nod-Like Receptors family Pyrin domain containing 3 (NLRP3) inflammasome. The assembly of the NLRP3 complex promotes the upregulation of proinflammatory cytokines IL-1 β and IL-18, which ultimately leads to neuroinflammation (2).

Melatonin is an endogenous molecule primarily secreted by the pineal gland. It is a potent free radical scavenger that could eliminate the toxicity of reactive oxygen species (ROS). In addition to its antioxidant role, melatonin provides a plethora of protective effects, such as anti-inflammation (3). Even though the inhibitory effect of melatonin on Nuclear Factor Kappa-light-chain-enhancer of activated B cells (NF-kB) is prominent for suppressing inflammatory response (4). However, its protective role on neuroinflammation related to the NLRP3 inflammasome under hypoxic conditions is still unclear. The SH-SY5Y cell line is widely used in *In vitro* model for investigating neuroinflammation. Moreover, the SH-SY5Y cell line demonstrates the human-specific protein expression, which is suitable for studying human neurological disorders.

Therefore, this study aims to investigate the effect of melatonin treatment on NLRP3 expression after inducing hypoxia in SH-SY5Y cells.

Methodology:

Cell culture: SH-SY5Y human neuroblastoma cell line (ATCC, CRL-2266) was cultured in Minimum Essential Medium (41500-067, Gibco, USA) with Ham's Nutrient Mixture F-12 (21700-026, Gibco, USA) (MEM/F12) supplemented with 10% fetal bovine serum (A5256701, Gibco, USA), 100 mmol/L of L-glutamine, and 1% of penicillin and streptomycin antibiotics. The SH-SY5Y cells were maintained in a humidified atmosphere of 5% CO₂ at 37°C.

Hypoxia induction and melatonin treatment of SH-SY5Y cells: The experiment of the OGDR was performed according to our previous study (5) as shown in Figure 1. After 80% confluency, the SH-SY5Y cell line was cultured in a 60 mm dish at 1.5 x 10⁶ cells/dish in complete medium for 24 hours, maintained in a humidified atmosphere of 5% CO₂ and 95% at 37°C. After that, the cultured medium was removed and washed with phosphate-buffered saline (PBS) three times. Subsequently, the FBS and glucose-free MEM/F12 medium were added, accompanied by 1% O₂ and 5% CO₂ at 37°C for 4 hours. After 4 hours, 10% FBS and 25 mM of glucose were added to the cultured medium together with an adjustment of O₂ up to the normal level (20%) for the OGDR group for 24 hours. While the melatonin-treated group, 10% FBS, 25 mM of glucose, and 10 μM of melatonin were added to the cultured medium together with an adjustment of O₂ up to the normal level (20%) for 24 hours.

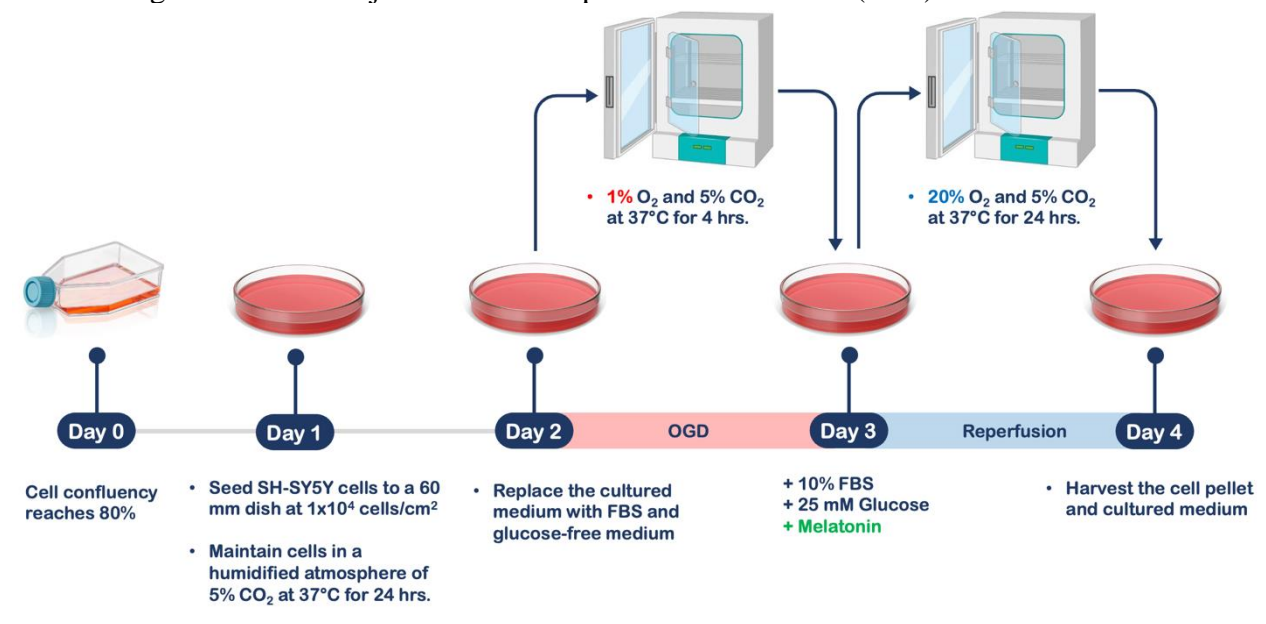


Figure 1 Experimental design for OGDR induced in the SH-SY5Y cell line, and representing the period of melatonin treatment

Western Blot analysis: The cell pellet was harvested using cold lysis buffer with cold PBS. The cell suspension was sonicated to break the cell membrane and extract protein. The concentration of total protein was measured using the Bradford assay. An equal amount of total protein was separated through 8% Sodium Dodecyl Sulfate—Polyacrylamide Gel Electrophoresis (SDS-PAGE). The separated proteins were transferred to PVDF membranes. The PVDF membranes were blocked with TBST containing 5% bovine serum albumin (BSA) before incubation with anti-NLRP3 primary antibody (PA1665, Boster Biological Technology, USA) in a dilution of 1:1,000 overnight at 4°C. They were extensively washed in TBST and incubated with anti-rabbit IgG HRP-linked antibody (AP132F, Merck, USA) as a secondary antibody for 1.5 hours. The signal was detected by an enhanced chemiluminescence method (ECL kit, Biorad)

Statistical analysis: Data are expressed as means \pm SEM from at least three independent experiments. Statistical significance (p < 0.05) was determined by a paired sample t-test using Graph Pad Prism version 10.6.0 (890) for Windows (GraphPad Software, Boston, Massachusetts, USA, www.graphpad.com)

Results:

OGDR-induced neuroinflammation in the SH-SY5Y cell line

Following the OGDR induction, the NLRP3 protein expression was significantly increased when compared to the control. However, when melatonin was administered in the OGDR induction group, the NLRP3 protein expression was significantly decreased in a concentration-dependent manner (Figure 2).

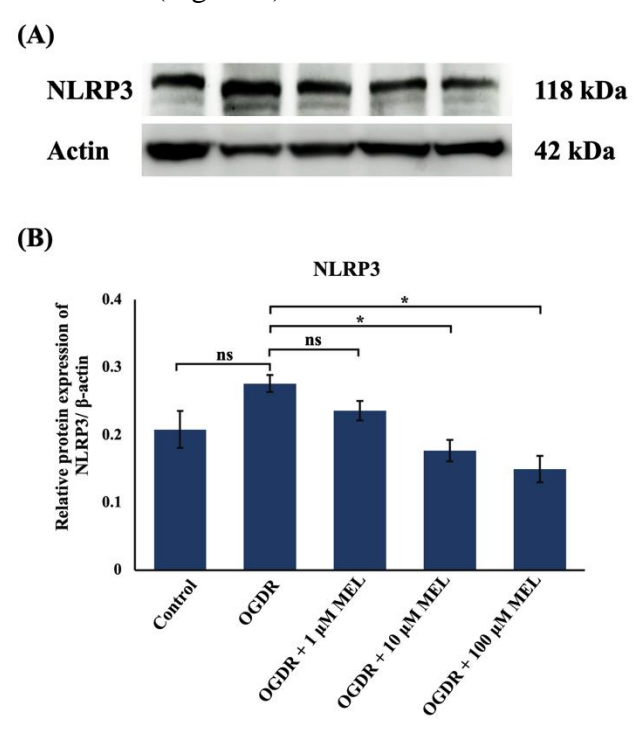


Figure 2 Relative expression of the NLRP3 protein. (A) Western blot of NLRP3 protein extracted from SH-SY5Y cells from different OGDR groups. (B) The protein expression was normalized with β-actin. (C) Percent inhibition of melatonin on NLRP3 inflammasome expression. The data were presented as a mean \pm SEM (n=3). *p<0.05 compared to OGDR.

Discussion and Conclusion:

NLRP3 protein is a component of the inflammasome, which can be activated by OGDR. NLRP3 inflammasome is an important mediator of neuroinflammation. In addition, neuroinflammation is a pathological hallmark of neurodegenerative disease. Therefore, it has been used as a potential target for developing therapeutic tools for several diseases, including ischemic stroke and neurodegenerative disorders.

In this study, the melatonin treatment after OGDR induction demonstrated the reduction of neuroinflammation response by detecting NLRP3 protein expression. Moreover, the reduction of NLRP3 protein expression was significantly lower than the OGDR group (without melatonin treatment) in a concentration-dependent manner. Therefore, further study might need to identify the mechanism of action of melatonin for diminishing the neuroinflammation response to promote the development of new potential therapeutic for neurodegenerative disease.

Acknowlegdement:

This research project is supported by Chulabhorn Graduate Institute (Fundamental Fund by National Science Research and Innovation Fund (NSRF): fiscal year 2025) (FRB680079/0518 Project code 209041), Chulabhorn Graduate Institute Research Grant (651-AB01). Furthermore, this research work was partially supported by the grant from the Chulabhorn Graduate Institute Scholarship Scheme Commemorating Princess Chulabhorn's 60th Birthday Anniversary Commemoration Scholarship whose goal is to develop those with science and technology (CGS2022/01).

References:

- 1. Shi F-D, Yong VW. Neuroinflammation across neurological diseases. Science. 2025;388(6753):eadx0043.
- 2. Thankam FG, Ayoub JG, Ahmed MMR, Siddique A, Sanchez TC, Peralta RA, et al. Association of hypoxia and mitochondrial damage associated molecular patterns in the pathogenesis of vein graft failure: a pilot study. Translational Research. 2021;229:38-52.
- 3. Reiter RJ, Mayo JC, Tan DX, Sainz RM, Alatorre-Jimenez M, Qin L. Melatonin as an antioxidant: under promises but over delivers. J Pineal Res. 2016;61(3):253-78.
- Li SJ, Cheng WL, Kao YH, Chung CC, Trang NN, Chen YJ. Melatonin Inhibits NFκB/CREB/Runx2 Signaling and Alleviates Aortic Valve Calcification. Front Cardiovasc Med. 2022;9:885293.
- 5. Singrang N, Nopparat C, Panmanee J, Govitrapong P. Melatonin Inhibits Hypoxia-Induced Alzheimer's Disease Pathogenesis by Regulating the Amyloidogenic Pathway in Human Neuroblastoma Cells. Int J Mol Sci. 2024;25(10).

MODULATION OF GLYCOSYLATION PROFILE IN CHO-DERIVED MONOCLONAL ANTIBODY PRODUCTION USING MONOSACCHARIDE ANALOGUE

<u>Diana Atsieno</u>¹, Charlermchai Artpradit², Tharakarn Srisuporn², Amnart Khongmanee², Kamolchanok Tianpanich², Bhawat Wongkhamprai², and Mayuree Fuangthong^{1,2,3,4}

¹Program in Applied Biological Sciences, Chulabhorn Graduate Institute, Bangkok, Thailand

² Translational Research Unit. Chulabhorm Research Institute, Bangkok, Thailand

³ Center for Biologics Research and Development, Chulabhorn Research Institute, Bangkok. Thailand.

⁴ Center of Excellence on Environmental Health and Toxicology (EHT), OPS, MHESI, Bangkok, Thailand.

E-mail: diana@cgi.ac.th

Abstract:

HER2-positive breast cancer remains a major cause of cancer-related mortality globally and in Thailand, where trastuzumab access is restricted by high costs and lack of local biosimilar production. Trastuzumab acts by blocking HER2 signaling and inducing antibody-dependent cellular cytotoxicity (ADCC), a function strongly influenced by Fc glycosylation. The presence of core α1,6-fucose at Asn297 reduces FcγRIIIa binding, whereas partial afucosylation, consistently observed in reference trastuzumab, is essential for biosimilarity. However, Chinese hamster ovary (CHO) cells predominantly produce fucosylated IgG, limiting equivalence. To combat this, multiple glycoengineering strategies like genetic approaches have been employed to enhance afucosylation but raise biosafety, intellectual property, and regulatory barriers. As a non-genetic alternative, 2F-Peracetyl Fucose (2F-PAF) has been reported to competitively inhibit Fucosyltransferase 8 (FUT8), enabling reversible and dose-dependent modulation of core fucosylation. In this study, stable CHO expressing trastuzumab biosimilar fed-batch cultures were supplemented with different 2F-PAF concentrations and assessed for growth, productivity, and product quality by Octet, LC-MS, and CEX-HPLC. Supplementation at 10-13 µM reproducibly increased afucosylation into the Herceptin® benchmark range while maintaining viability, yield, and charge heterogeneity comparing with no treatment control group. These findings demonstrate 2F-PAF as a scalable strategy for tuning glycosylation, strengthening biosimilarity, and supporting affordable trastuzumab production least affordable comparing with genetic modification methods.

Keywords: Trastuzumab, 2F-Peracetyl Fucose, afucosylation, CHO cells, ADCC, biosimilarity.

Introduction:

Breast cancer is the leading malignancy among women in Thailand, with 20–30% of cases exhibiting overexpression of human epidermal growth factor receptor 2 (HER2), a transmembrane tyrosine kinase associated with aggressive disease and poor prognosis. Trastuzumab (Herceptin®), a humanized IgG1 monoclonal antibody, has reshaped HER2-positive therapy by combining direct inhibition of HER2 signaling with immune-mediated clearance via antibody-dependent cellular cytotoxicity. The potency of ADCC depends on Fc–FcγRIIIa binding, which is markedly reduced by core α1,6-fucose on the conserved Fc N-glycan at Asn297. In contrast, afucosylated variants demonstrate up to 50-fold stronger

Fc γ RIIIa binding and enhanced effector function (1). A key challenge for biosimilar development is that reference Herceptin® consistently displays partial fractional afucosylation (~3-9%) (2), whereas Chinese hamster ovary (CHO) cells, the standard host for antibody production, typically generate highly fucosylated IgG (>80%) (3) . To address this, multiple glycoengineering strategies have been investigated such as gene-editing strategies such as Fucosyltransferase 8 (FUT8) knockout that can shift the glycan profile but pose regulatory, biosafety, and intellectual property challenges that complicate application.

An alternative approach is chemical modulation using metabolic analogs. 2F-peracetyl fucose (2F-PAF) is a cell-permeable fucose monosaccharide analog that competitively inhibits fucosyltransferase 8 in a reversible and dose-dependent manner. This strategy offers flexibility, avoids permanent genetic modification, and is compatible with large-scale bioprocessing (4). Although 2F-PAF has been shown to reduce fucosylation, its performance in fed-batch CHO cultures producing trastuzumab has not been fully defined, especially at concentrations that balance afucosylation with yield and product integrity. This study addresses this gap by evaluating 2F-PAF in CHO cells producing trastuzumab cultures, examining growth, productivity, glycan profile, and charge heterogeneity to establish its potential as a scalable strategy for biosimilar trastuzumab production, a least intervention for production cell line.

Methodology:

Cell culture, 2F-PAF treatment, and monitoring of culture performance.

CHO 1043-6.7 cells producing trastuzumab were cultured in fed-batch mode (37 °C, 8% CO₂, 130 rpm). Cultures were inoculated at 0.3×10^6 cells/mL and supplemented with 2F-PAF concentrations at 0, 5, 10, 11, 12, 13, 14, 15, 20, 50, 100, and 1,000 μ M. Growth kinetics and viability were monitored daily over 11 days using trypan blue exclusion technique.

Harvest, Protein A purification, and IgG Quantitation

Supernatants were harvested by centrifugation and filtration, and antibodies were purified by protein A affinity chromatography. Eluted fractions were buffer-exchanged into PBS (pH 7.4) and concentrated to 5–6 mg/mL. IgG titers in crude fractions were quantified by biolayer interferometry (Octet®).

Analytical characterization (CEX-HPLC and LC-MS)

Fc glycosylation was assessed using LC-MS following IdeS digestion, DTT reduction, and determination of fractional abundances of afucosylated and galactosylated species. Charge heterogeneity was profiled using CEX-HPLC with a linear NaCl gradient, quantifying acidic, main, and basic isoforms at 215 nm. All data were compared with different Herceptin® lots (EU and US) as reference products.

Results, Discussion and Conclusion:

Cell culture performance and productivity

Untreated CHO cultures reached $14.73 \pm 0.27 \times 10^6$ cells/mL VCD with IgG titers >2,000 µg/mL. Supplementation with 2F-PAF (5-50 µM) maintained similar performance (VCD $14.1\text{-}15.6 \times 10^6$ cells/mL; titers 2,000-2,400 µg/mL), with 10-15 µM 2F-PAF showing the most consistent results (VCD $14.1\text{-}14.7 \times 10^6$ cells/mL; titers ~2,000-2,400 µg/mL). Higher dose of 2F-PAF (100 µM) reduced VCD to 11.1×10^6 cells/mL and titers to ~2,007 µg/mL, while 1,000 µM 2F-PAF caused rapid viability loss (<30% by day 7) and culture collapse

 $(0.31 \times 10^6 \text{ cells/mL}; 52 \,\mu\text{g/mL})$. These results indicate that 5-50 μ M 2F-PAF addition to the culture represents the optimal range for trastuzumab production based on the highest combination of consistent growth, sustained productivity, and minimal detrimental effects throughout the culture period (Figure 1).

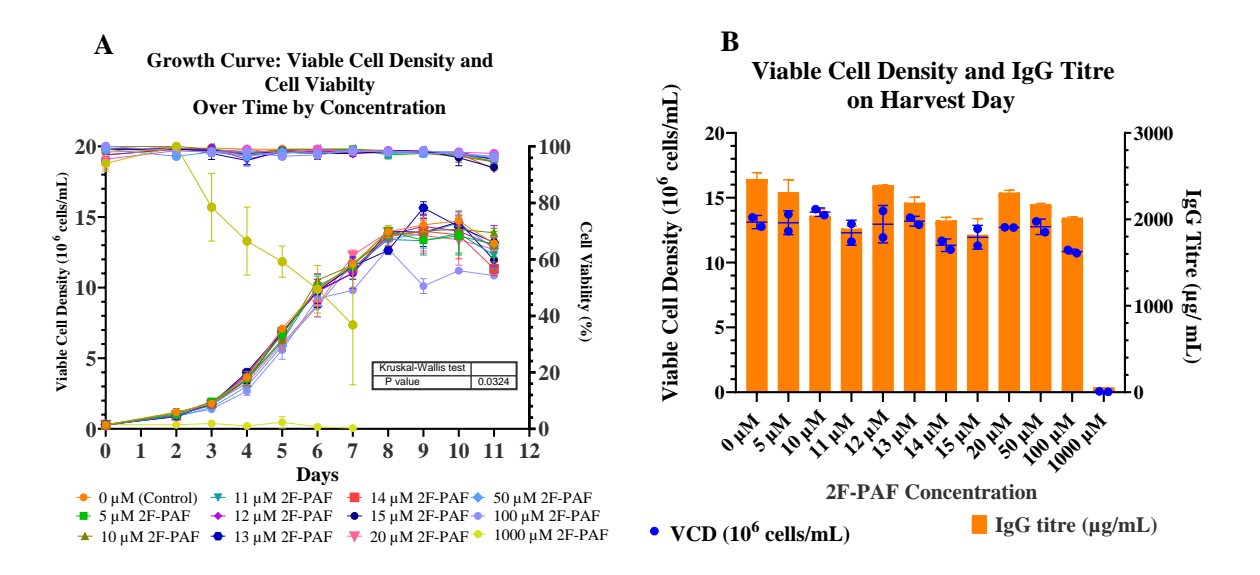


Figure 1 Effect of 2F-PAF on CHO 1043-6.7 cell growth and IgG production. (A) Viable cell density (VCD) and cell viability over 11 days at different 2F-PAF concentrations (0–1000 μ M). (B) Maximum VCD (left y-axis) and IgG titer (right y-axis) on day 11 harvest. Data are mean \pm SD (n = 2).

Analytical Characterization

LC–MS analysis demonstrated dose-dependent inhibition of fucosyltransferase 8 (FUT 8) with fractional afucosylation rising from $\sim 3\%$ in controls to 6% at 12 μ M 2F-PAF addition in culture, which are within the ranges of both Herceptin reference product from the US and Europe. Fractional galactosylation of trastuzumab produced with the addition of 10-15 μ M 2F-PAF in the culture were well within the ranges of Herceptin reference products (Figure 2).

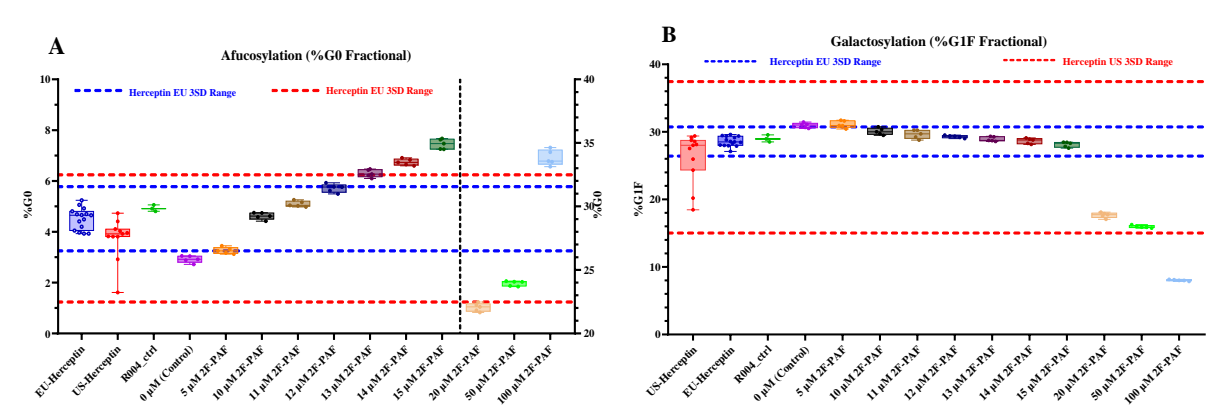
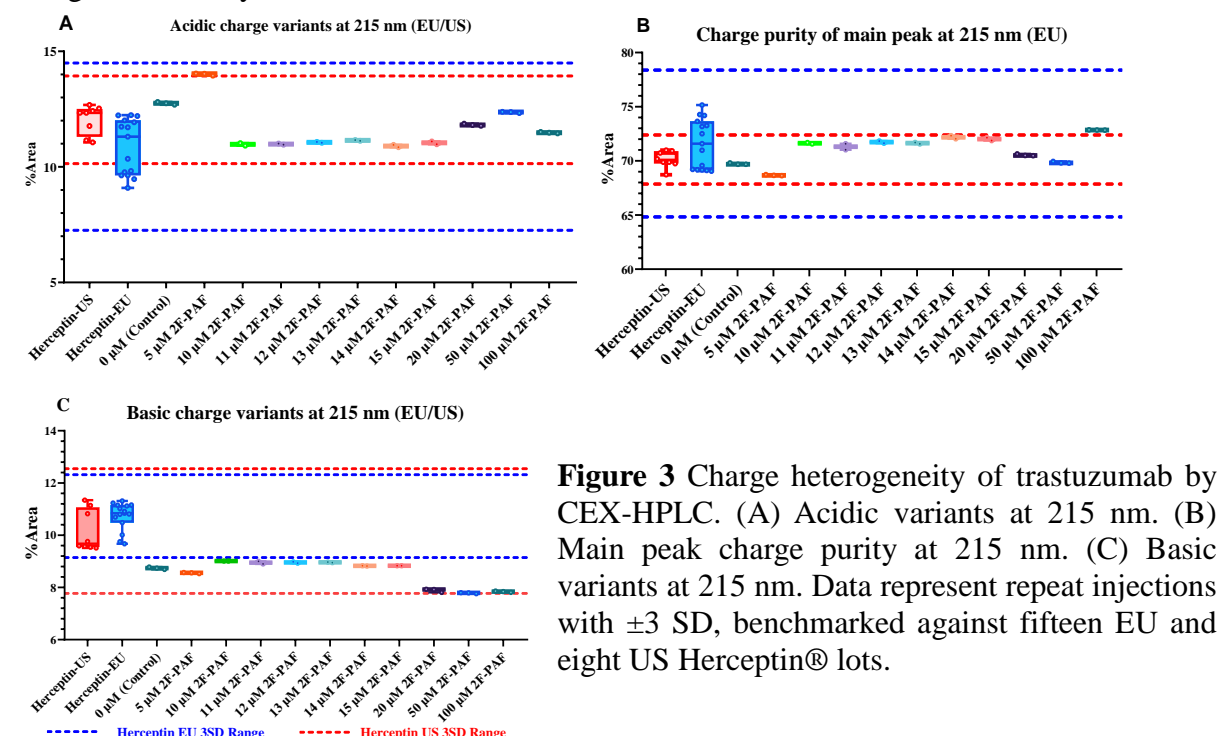


Figure 2 Fc glycan profiling by LC–MS. (A) Afucosylation (% G0 fractional) across PAF concentrations. (B) Galactosylation (% G1F fractional) across PAF concentrations. Data expressed as repeat injections with ± 3 SD, benchmarked against fifteen EU and eleven US Herceptin® lots.

CEX-HPLC analysis showed that both treated and control growth conditions produced antibodies that exhibited a dominant main peak with acidic and basic variants, all within EU and US Herceptin® reference ranges (Figure 3). No unexpected charge species were detected. Minor and marginal shifts appeared at 20, 50, and 100 μ M, while other concentrations stayed within reference batch variability, indicating that 2F-PAF does not markedly alter trastuzumab charge species, with concentrations 10-15 μ M best maintaining charge consistency.



Conclusion:

Based on our results, 2F-PAF supplementation provides a controllable and selective approach to modulate Fc afucosylation in CHO-derived trastuzumab biosimilars. Within the $10{\text -}12~\mu\text{M}$ range, it achieves afucosylation levels within the biosimilar-acceptable range while maintaining culture integrity, IgG titers, and overall glycosylation profiles. This demonstrates that chemical intervention can modulate Fc glycosylation effectively without compromising product quality.

- 1. Shields RL, Lai J, Keck R, O'Connell LY, Hong K, Meng YG, et al. Lack of fucose on human IgG1 N-linked oligosaccharide improves binding to human FcγRIII and antibody-dependent cellular toxicity. Journal of Biological Chemistry. 2002;277(30):26733-40.
- 2. Kim S, Song J, Park S, Ham S, Paek K, Kang M, et al. Drifts in ADCC-related quality attributes of Herceptin®: Impact on development of a trastuzumab biosimilar. MAbs. 2017;9(4):704-14.
- 3. Upton R, Bell L, Guy C, Caldwell P, Estdale S, Barran PE, et al. Orthogonal assessment of biotherapeutic glycosylation: A case study correlating N-glycan core afucosylation of Herceptin with mechanism of action. Analytical Chemistry. 2016;88(20):10259-65.
- 4. Mishra N, Spearman M, Donald L, Perreault H, Butler M. Comparison of two glycoengineering strategies to control the fucosylation of a monoclonal antibody. Journal of Biotechnology. 2020;324:100015.

PRODUCTION OF AN ANTIBODY AGAINST Burkholderia pseudomallei

Adiati Bintari Ayuningtias¹, Karnpob Kanhasut², Tharakarn Srisuporn³, Charlermchai Artpradit³, Narisara Chantratita⁴, Mayuree Fuangthong^{1,2,3,5}

¹Program in Applied Biological Sciences, Chulabhorn Graduate Institute, Bangkok 10210, Thailand
 ²Center for Biologics Research and Development, Bangkok 10210, Thailand
 ³Translational Research Unit, Chulabhorn Research Institute, Bangkok 10210, Thailand
 ⁴Mahidol-Oxford Tropical Medicine Research Unit, Faculty of Tropical Medicine,
 Mahidol University, Bangkok 10210, Thailand
 ⁵Center of Excellence on Environmental Health and Toxicology (EHT), OPS, MHESI,
 Bangkok 10400, Thailand

Abstract:

Burkholderia pseudomallei is the causative agent of melioidosis, a tropical disease common in northern Australia and Southeast Asia. Thailand has the highest incidence and mortality rates. Due to its difficulty in diagnosis, melioidosis remains a major health risk. The bacterium was also resistant to many drugs, and the infection frequently recurred. Research into novel treatment is essential. Although monoclonal antibodies (mAbs) targeting capsular polysaccharide (CPS) of B. pseudomallei have emerged as a promising strategy for melioidosis treatment, the development of anti-melioidosis mAbs for potential therapeutic use remains challenging. In this study, we produce an anti-melioidosis monoclonal antibody that binds specifically to the capsular polysaccharide (CPS) of the B. pseudomallei strain from 4B11 hybridoma cells and test its functionality for binding to CPS. Results showed that the 4B11 hybridoma clone maintained stable viability and cell density over 8 passages, with its production curve peaking within five days. Growth curves showed cell viability above 50% during the 5-day production period. Protein A affinity chromatography was used to purify the antibody, which demonstrated a purity of 84% based on SDS-PAGE results. Western blot also proved the structural identity and functionality of this antibody. Finally, an indirect ELISA showed a high affinity binding to the CPS antigen. Taken together, we present the production and characterization of anti-melioidosis (4B11) monoclonal antibody. In the future, humanization of this antibody for human use can be explored as a potential therapeutic candidate.

Keywords: Monoclonal antibody, melioidosis, *Burkholderia pseudomallei*, hybridoma cell

Introduction:

Melioidosis is an opportunistic infection caused by the Gram-negative bacterium *Burkholderia pseudomallei* (1). Melioidosis is widespread in Southeast Asia and Northern Australia. Thailand has the highest incidences and deaths, especially in the northeast, at a high rate of 4-21 cases per 100,000 people per year (2). Melioidosis is also a common cause of community-acquired bacteraemia associated with a 30-day death rate of up to 39% despite antibiotic therapy (3). Emergence of antibiotic resistance, diverse clinical symptoms, and the likelihood of relapse have posed a challenge for clinical management, emphasizing the urgent need for alternative therapeutic and diagnostic methods.

In recent years, immunotherapy with monoclonal antibodies (mAbs) has shown great promise for combating infectious diseases. Monoclonal antibodies can bind specifically to the target antigens and elicit different functions, such as neutralizing virulence factors or enhancing the clearance of pathogens by activating macrophages. Epitopes of *Burkholderia pseudomallei*, such as capsular polysaccharides (CPS), have been identified as important

targets for antibody-based interventions due to their immunogenicity and surface accessibility (4). However, the development of monoclonal antibodies targeting the CPS can be challenged due to the complexity of the CPS structure. Despite its time-consuming nature, hybridoma technology remains a reliable and robust platform for the identification of highly stable and specific antibodies. Given the need for novel treatment for melioidosis, we aim to produce and characterize an anti-melioidosis monoclonal antibody produced from 4B11 hybridoma cells that binds specifically to the capsular polysaccharide (CPS) of *B. pseudomallei* strain. The antibody can be used for detection of K96243 capsular polysaccharide (CPS) antigen by Western blot and indirect ELISA. In the future, it is worth exploring the humanization of this antibody for human use as a potential therapy alternative.

Methodology:

Culture of hybridoma cells for monoclonal antibody production

Iscove's Modified Dulbecco's Medium supplemented with 10% fetal bovine serum (FBS) was used to cultivate the 4B11 hybridoma cells at 37 °C, 8% CO₂. The cells were maintained at a density of 1.2×10^6 cells/mL. A hemocytometer coupled with trypan blue dye exclusion assay was used to measure the cell density and viability before subculture every two days. For growth and production testing, cells at passage 15 were seeded at 0.5×10^6 cells/mL and allowed to grow continuously until their viability reduced to 50% as a harvesting criterion. Cell density and viability were monitored, and supernatant was sampled every 24 hours. IgG concentration on each production day was measured using Octet biolayer interferometry (Octet®) coupled with protein A biomass based on the principle of real-time binding kinetics between antibody molecules and immobilized ligands. 4B11 hybridoma cells were kindly gifted from Dr. Narisara Chantratita.

Purification of antibodies

Culture was centrifuged at 5,000 rpm at 4 °C for 10 minutes to collect supernatant. Antimelioidosis mAb in supernatant was purified using a Fast Protein Liquid Chromatography (FPLC) instrument equipped with a protein A-based column (Cytiva) that was preequilibrated with a binding buffer (20 mM sodium phosphate, 0.15 M NaCl, pH 7.2), followed by washing with binding buffer. The bound anti-melioidosis antibody was eluted with elution buffer (0.1 M sodium citrate, pH 3.0). Next, eluted samples were subjected to sodium dodecyl sulfate-polyacrylamide gel electrophoresis (SDS-PAGE) before Coomassie staining (InstantBlue®). ImageQuant was utilized to visualize the gel and determine the percentage purity of the eluted fractions.

Indirect ELISA and Western blot for antibody characterization

Crude *B. pseudomallei* K96243 antigen (kindly gifted by Narisara Chantratita) was coated onto 96-well plates (2 μ g/mL) and incubated at 4 °C overnight. After washing with PBST, the plate was incubated with 1% BSA for 1 hour at 25 °C, followed by incubation with two-fold serially diluted anti-melioidosis antibody. Plates were washed again with PBST, and then goat anti-human IgG H&L conjugated with HRP (Abcam) was added and incubated for 1 hour at 25 °C. After washing with PBST, the plate was incubated with TMB substrate (KPL) for 3 minutes at 25 °C, and quenched with 1 N H₂SO₄. The absorbance was measured at 450 nm using a Spectramax S5 plate reader (Molecular Devices). For Western blot, crude K96243 antigen was separated on an 8% SDS-polyacrylamide gel (Bio-Rad), then transferred to nitrocellulose membrane and followed by immunoblotting. 2.6 μ g/ μ L of purified antimelioidosis mAb (1:10,000) was used as the primary antibody. 1 μ g/ μ L of goat anti-mouse IgG antibody linked with horseradish peroxidase (HRP) (1:10,000, Bio-Rad) was used as a secondary antibody. Blots were detected by enhanced chemiluminescence (ECL Prime Western Blotting Detection Reagent, GE Healthcare).

Results, Discussion, and Conclusion:

Hybridoma characterization: Cell stability test, growth curve, and productivity

4B11 hybridoma cells were subcultured every 2 days for 8 passages. In each subculture, we measured cell density and percentage viability. Results showed that the 4B11 hybridoma cells consistently grew as a suspension culture in the desired condition for 8 passages (**Figure 1**). For growth and production studies, cells sustained a good percent viability for 2 days and reduced to 50% between Days 4 and 5 (**Figure 2**). Protein concentrations gradually increased every day, with the maximum IgG concentration approximately 600 μg/mL at day 5 (**Figure 3**).

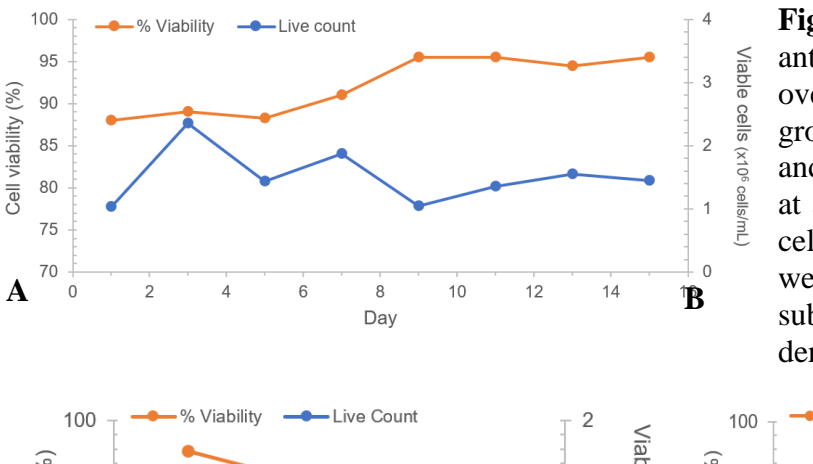
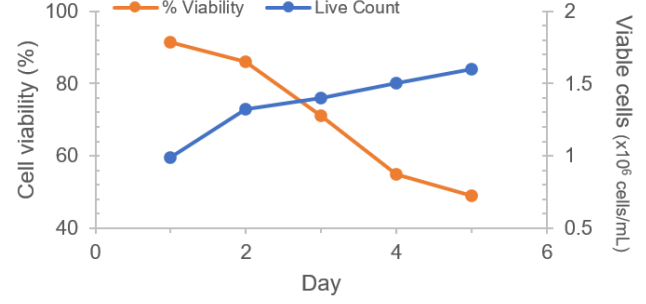


Figure 1 The stability of 4B11 anti-melioidosis hybridoma cells over 8 passages. Cells were grown as a suspension culture and maintained by subculturing at an initial seeding of 0.3 x 10⁶ cells/mL every 2 days. Cells were counted before being subcultured to calculate cell density and percent viability



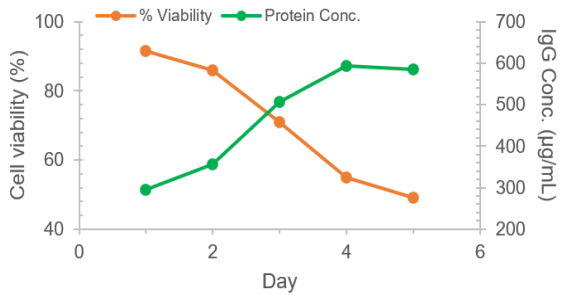


Figure 2 The growth and production curve of 4B11 hybridoma cells. (**A**) Cells at passage 15 were allowed to grow continuously until viability dropped to 50%. Viable cell density and percentage viability showed a stable growth curve with a gradual decline in viability after Day 3. (**B**) IgG titer (green) by Octet continuously increased every day.

Purification and characterization of mouse anti-melioidosis mAbs

Protein A column was equilibrated with PBS, pH 7.4 before loaded with supernatant. The mAbs were eluted using 50 mM Citrate, pH 3.5. The eluted fractions containing purified mAbs were collected before exchanged with PBS, pH 7.4 using centrifugal filters. The FPLC chromatogram showed a peak at fraction#3 (Figure 3). SDS-PAGE analysis with reducing condition of the PBS-exchanged anti-melioidosis mAb was performed. The observed bands were at roughly 50 kDa and 25 kDa, validating the expected molecular weight of heavy and light chains of the IgG molecule, respectively. The percentage yield of IgG recovery after Protein A column FPLC was determined as 84% based on Octet analysis.

Detection of K96243 capsular polysaccharide (CPS) antigen using Western blot and indirect ELISA

Anti-melioidosis mAbs were also evaluated for their function in antigen recognition by Western blot analysis. Figure 4 shows the specific binding of the purified anti-melioidosis mAb to K96243 capsular polysaccharide (CPS) in the crude extract, indicating the functionality in binding to the denatured form of CPS as previously reported (5). While ELISA requires antibodies that recognize the nature form of desired antigen. Here, indirect ELISA was performed to test the binding activity of the produced anti-melioidosis mAb. K96243 antigen was coated on the plate, and anti-melioidosis mAb was serially diluted and tested for binding to the antigen. Results showed that anti-melioidosis mAb can bind to CPS with a high affinity (EC $_{50} = 12.9$ nM), suggesting a valid functionality of purified anti-melioidosis mAb for both Western blot and ELISA applications.

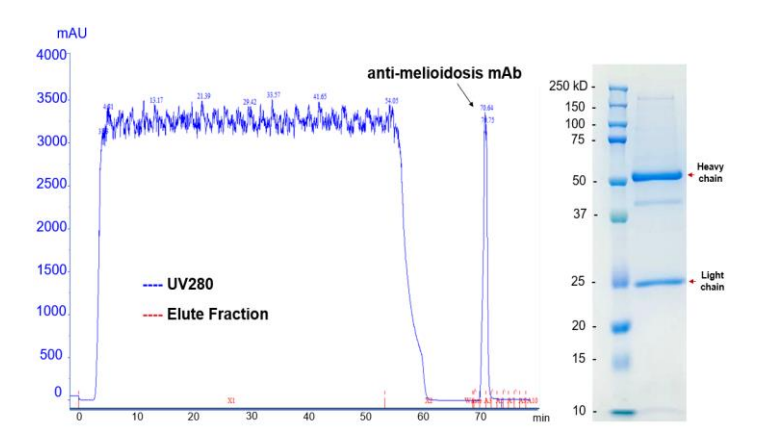


Figure 3 FPLC chromatogram and purity of anti-melioidosis mAb. Protein A column was used to purify the supernatant. The chromatogram showed a single peak elution of 4B11 mAb. SDS-PAGE indicated the expected bands of 25 and 50 kDa for light and heavy chains, respectively. Percentage purity was determined as 84%.

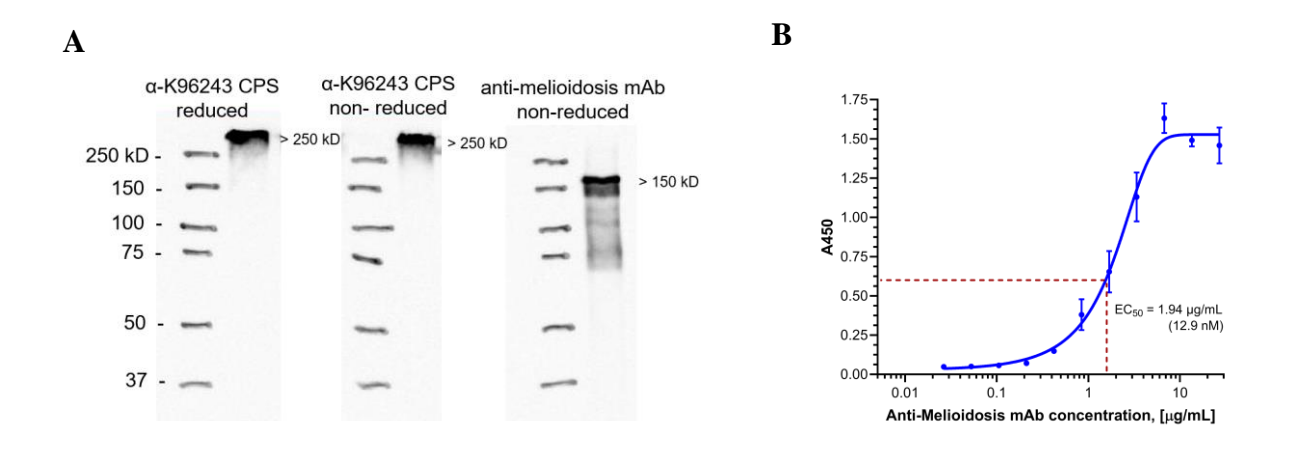


Figure 4 Western blot analysis and indirect ELISA for detection of K96243 CPS. (**A**) Western blot result shows that the mAb specifically bound to the K96243 CPS in both reduced and non-reduced conditions at the molecular weight > 250 kDa, and a target band at 150 kDa of anti-melioidosis mAb. (**B**) Indirect ELISA showed a binding activity with EC₅₀ of 12.9 nM.

- 1. Birnie E, Savelkoel J, Reubsaet F, Roelofs J, Soetekouw R, Kolkman S, et al. Melioidosis in travelers: An analysis of Dutch melioidosis registry data 1985-2018. Travel Medicine and Infectious Disease. 2019;32:101461.
- 2. Limmathurotsakul D, Wongratanacheewin S, Teerawattanasook N, Wongsuvan G, Chaisuksant S, Chetchotisakd P, et al. Increasing incidence of human melioidosis in Northeast Thailand. American Society of Tropical Medicine and Hygiene. 2010;82(6):1113-7.
- 3. Chantratita N, Phunpang R, Yarasai A, Dulsuk A, Yimthin T, Onofrey LA, et al. Characteristics and one year outcomes of melioidosis patients in Northeastern Thailand: a prospective, multicenter cohort study. The Lancet Regional Health Southeast Asia. 2023;9.
- 4. Peacock SJ, Limmathurotsakul D, Lubell Y, Koh GC, White LJ, Day NP, et al. Melioidosis vaccines: a systematic review and appraisal of the potential to exploit biodefense vaccines for public health purposes. PLoS Neglected Tropical Disease. 2012;6(1):e1488.
- 5. Anuntagool N, Sirisinha S. Antigenic relatedness between *Burkholderia pseudomallei* and *Burkholderia mallei*. Medical Microbiology and Immunology. 2002;46(3):143-50.

PROTECTIVE EFFECTS OF MELATONIN ON ERASTIN-INDUCED FERROPTOSIS NEUROTOXICITY IN MURINE HIPPOCAMPAL HT-22 CELLS

<u>Anuttree Boontor</u>¹, Suwakon Wongjaikam¹, Parichart Boontem¹, Soraya Boonmag², and Piyarat Govitrapong^{1,*}

¹Applied Biological Sciences: Environmental Health Program, Chulabhorn Graduate
Institute, Lak Si, Bangkok 10210, Thailand,

²Research Center for Neuroscience, Institute of Molecular Biosciences, Mahidol University,
Nakhon Pathom 7317, Thailand

*Corresponding author. Email: piyarat@cgi.ac.th

Abstract:

Ferroptosis is an iron-dependent and membrane lipid peroxidation-mediated form of programmed or regulated cell death. A number of recent studies have demonstrated that ferroptosis contributes to neurodegeneration-mediated nerve cell death. The pathology of neurodegenerative disease has been investigated to identify underlying mechanisms and determine efficient therapeutic strategies. Melatonin, a functionally versatile natural indoleamine, has shown promise in deferring neurodegenerative processes. Recent studies on melatonin also have identified its efficacy in mitigating key events of ferroptosis, introducing it as an anti-ferroptosis agent. In this study, we studied the effects of melatonin on HT-22 cells-induced ferroptosis using erastin. To confirm the occurrence of ferroptosis, we conducted measurements of cell cytotoxicity. The result showed that elastin decreased the cell viability and disrupted the regulation of glutathione peroxidase 4 (GPX4), proteins involved in ferroptosis. Following melatonin treatment, cell viability and the expression of GPX4 were increased. This study demonstrated that melatonin could effectively inhibit the pathological effects caused by erastin in HT-22 cells and further research is needed to confirm melatonin's efficacy in these pathological conditions, both in animal models and clinical trials.

Keywords: Melatonin, neurotoxicity, ferroptosis, glutathione peroxidase 4

Introduction:

Ferroptosis is a form of programmed cell death driven by iron-dependent lipid peroxidation. It can be triggered through either the extrinsic or the intrinsic pathway. The extrinsic pathway is initiated through the regulation of transporters (e.g., inhibition of the amino acid antiporter system xc- or activation of the iron transporters transferrin and lactotransferrin), whereas the intrinsic pathway is mainly induced by blocking the expression or activity of intracellular antioxidant enzymes, such as glutathione peroxidase 4 (GPX4) (1). Erastin, a well-known ferroptosis inducer, triggers cell death by inhibiting system Xc-, a cystine/ glutamate antiporter, leading to glutathione (GSH) depletion and subsequent inactivation of glutathione peroxidase 4 (GPX4) (2). Since GPX4 plays a crucial role in protecting cells from lipid peroxidation, its suppression leads to oxidative stress and ferroptotic cell death (3).

Melatonin is a potent antioxidant that exerts neuroprotective effects through direct free radical scavenging and by enhancing the activity of endogenous antioxidant enzymes (4). However, its role in ferroptosis regulation, particularly in erastin-induced ferroptosis, remains unclear. HT-22 cells, a mouse hippocampal neuronal cell line, are commonly used to study ferroptosis due to their susceptibility to oxidative stress and glutathione depletion. Therefore, this study aims to investigate the effect of melatonin on the expression of GPX4 in erastin-induced ferroptosis in HT-22 cells.

Materials and Methods:

Cells culture

Murine hippocampal neuroblastoma HT-22 cells (ATCC, Manassas, VA, USA) were cultured in a 75 cm² flask, with 10 mL of high-glucose DMEM (Dulbecco's Modified Eagle Medium; Gibco, Thermo Fisher Scientific, Inc., Massachusetts, USA), 10% heat-inactivated fetal bovine serum (FBS), 100 mmol/L L-glutamine, and 1% antibiotics (penicillin and streptomycin) supplemented with 10% fetal bovine serum (FBS; Gibco, Gaithersburg, MD, USA), and 1mM Na-pyruvate at 37°C in a humidified atmosphere containing 5% CO₂.

Cell viability MTT (tetrazolium) assay

The MTT (3-(4,5-dimethylthiazol-2-yl)-2,5-diphenyl tetrazolium bromide; PanReac AppliChem, Darmstadt, Germany) reduction assay was used to determine cell viability. HT-22 cells were seeded in 96-well plates at a density of 8,000 cells/well 18 h prior to receiving various experimental treatments. Cells were treated with erastin at various concentration (0, 0.5, 1, 1.5, 2, and 2.5 μM) for 24 h. Afterwards, MTT at a final concentration of 0.5 mg/mL was added to each well and incubated for 4 h at 37°C under 5% CO2. After incubation, the MTT-containing medium was removed, and 100 μL of DMSO was added to each well to dissolve the MTT formazan. The absorbance of the MTT formazan was measured at 590 nm with a reference wavelength of 650 nm using a microplate reader. The final absorbance was calculated by subtracting the value at 650 nm from the value at 590 nm, and the background absorbance from blank wells (containing medium and MTT without cells) was further subtracted from all wells.

Treatment of HT-22 cells

HT-22 cells were seeded in a 24-well plate containing a poly-L-lysine-precoated coverslip and cultured for 24 h under standard conditions. Cells were pretreated with 100 μ M melatonin (Mel) for 2 h before co-treatment with 0.5 μ M Erastin (5) for another 18 h in DMEM supplemented with 1% fetal bovine serum, and 1mM Na-Pyruvate and incubate at 37°C in a humidified atmosphere containing 5% CO₂ for 18 h (Figure 1).

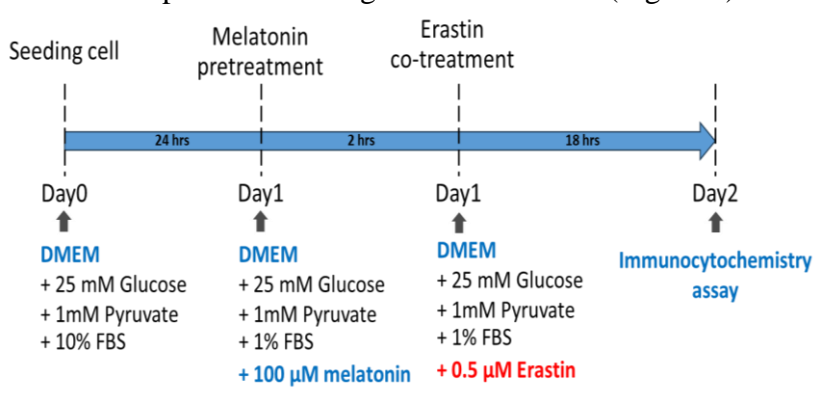


Figure 1 Time line of the experiment.

Immunofluorescence staining of HT-22 cells

HT-22 cells were fixed with 4% paraformaldehyde in PBS for 20 minutes and then washed three times with PBS. The cells were permeabilized using PBS containing 0.1% Triton X-100 for 15 minutes at room temperature (RT), followed by three washes with PBS. Blocking was performed using 10% normal goat serum (NGS) in PBS for 1 h at RT. The cells were then incubated with primary antibodies (anti-GPX4 1:200) overnight at 4°C. After

primary antibody incubation, cells were washed and incubated with Alexa Fluor 568-conjugated goat anti-rabbit secondary antibody at a 1:500 dilution in PBS containing 10% NGS for 1 h at RT. Following additional washes with PBS, the cells were mounted using an antifade reagent and nuclei were counterstained with 10 μ g/mL DAPI. Fluorescent signals were visualized using the FV3000 confocal laser scanning microscope (Olympus, Tokyo, Japan).

Statistical analysis

The data were expressed as the mean and standard error of the mean (Mean \pm SEM). Statistical analyses were performed by one-way ANOVA followed by Tukey's multiple comparisons test using Graph Pad Prism version 10.6.0 (890) for Windows (GraphPad Software, Boston, Massachusetts USA, www.graphpad.com). The p values < 0.05 were considered statistically significant

Results:

Erastin-induced neurotoxicity in HT-22 cells

Dose-response tests evaluated the effect of treatment of HT-22 neurons with and showed decreased survival of neurons over time (MTT assay). Erastin decreased significantly the viability of hippocampal HT-22 neurons at 0.5-2.5 μ M erastin (Figure 2). For further study, we selected the 0.5 μ M erastin.

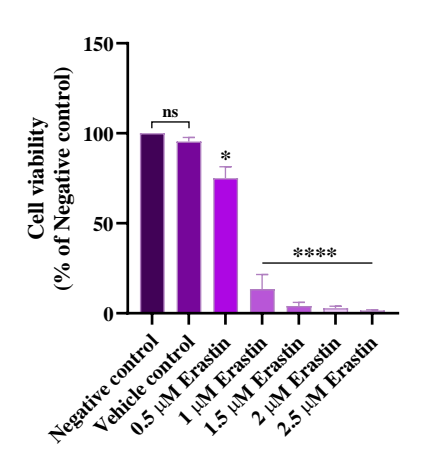


Figure 2 Cell viability of HT-22 cells under various concentrations of erastin treatment. The effect of erastin induced neurotoxicity in HT-22 cells was assessed using MTT assay. Cell viability of HT-22 cells after treatment with different (0.5, 1, 1.5, 2, 2.5 μ M) concentrations of erastin for 24 h. The data were presented as mean \pm SEM (n=3). * p<0.05, ****p<0.0001 compared to the vehicle control.

Melatonin protected erastin-induced neurotoxicity

Following treatment with melatonin at concentrations of 1, 10 and 100 μM , cell viability significantly increased compared to erastin treatment alone as shown in Figure 3. Moreover, none of the doses of melatonin was cytotoxic to the HT-22 cells compared to their vehicle control as shown in Figure 3. Moreover, the % cell viability remained unchanged when cells were treated with either the vehicle control (EtOH, DMSO). The results suggest that erastin induces neurotoxicity, while melatonin alleviates this effect, significantly enhancing the viability of HT-22 cells.

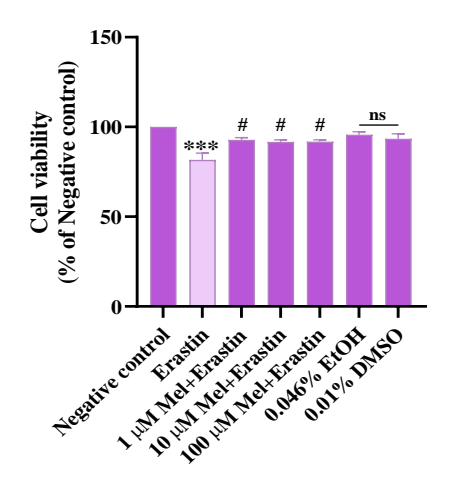


Figure 3 Melatonin increases cell viability in erastin-induced neurotoxicity. The effect of melatonin (Mel), on erastin induced neurotoxicity in HT-22 cells was assessed using MTT assay. DMSO served as the vehicle control for erastin treatments, while EtOH was used as the vehicle control for melatonin treatment. The final concentrations of DMSO and EtOH were 0.01% and 0.046%, respectively. Cell viability of HT-22 cells after treatment with either Mel or 0.01% DMSO or 0.046% ethanol for 24 h. Cell viability of HT-22 cells after Mel treatment for 1 h, followed by erastin treatment for 24 h. The data were presented as mean \pm SEM (n=3). ***p<0.001 compared to the vehicle control and *p<0.05 compared to erastin treatment alone.

Melatonin attenuated erastin-suppressed expression of GPX4 in HT-22 cells

Immunocytochemistry analysis was performed to visualize GPX4 (glutathione peroxidase 4) expression under different experimental conditions using DAPI for nuclear staining (cyan) and an antibody against GPX4 (red) (Figure 4). In the control group, GPX4 expression was prominently detected in the cytoplasm, indicating normal antioxidant enzyme activity. In the 0.1 μ M erastin-treated group, GPX4 fluorescence intensity was visibly reduced, indicating that erastin downregulates GPX4 expression, consistent with its role in inducing ferroptosis. However, in the 0.5 μ M erastin + 100 μ M melatonin group, GPX4 expression was partially restored compared to the erastin-only group, suggesting that melatonin helps restore GPX4 levels and may protect against ferroptosis. In the melatonin-only group, GPX4 expression remained similar to the control group, suggesting that melatonin alone does not alter GPX4 expression under normal conditions. These findings suggest that erastin suppresses GPX4 expression, contributing to ferroptosis, while melatonin may counteract this effect by preserving GPX4 levels.

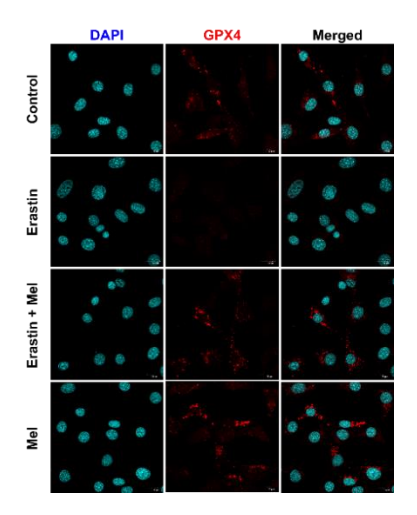


Figure 4 Immunostaining of Glutathione Peroxidase 4 (GPX4) in HT-22 Cells. HT-22 cells were pretreated with Mel for 2 hours before co-treatment with erastin for an addition 18 hours. Cells were stained with a GPX4-specific antibody (red), while nuclei were counterstained with DAPI (cyan). Fluorescence images were captured using the confocal laser scanning microscope (Olympus, Tokyo, Japan). Scale bar = $20 \, \mu m$.

Discussion and Conclusion:

The major findings of the present study are as follows: 1) erastin, a well-known ferroptosis inducer, decreased cell viability in HT-22 cells; 2) melatonin increased cell viability of elastin-induced neurotoxicity; 3) elastin caused the reduction of ferroptotic protein, GPX4, while melatonin increased the expression of GPX4 in elastin- treated cells. Melatonin could reduce neuronal cell death caused by ferroptosis. Additionally, the findings reinforce that melatonin may be used as an innovative medicine for prevention or treatment in ferroptosis-mediated neurodegeneration.

Acknowledgement:

This research project is supported by Chulabhorn Graduate Institute (Fundamental Fund by National Science Research and Innovation Fund (NSRF): fiscal year 2025) (FRB680079/0518 Project code 209037 and Chulabhorn Graduate Institute (631-AB03)

- 1. Tang D, Kroemer G. Ferroptosis. Current Biology. 2020;30(21):R1292-R1297.
- 2. Zhao J, Xu B, Xiong Q, Feng Y, Du H. Erastin-induced ferroptosis causes physiological and pathological changes in healthy tissues of mice. Mol. Med. Rep. 2021;24(4):713.
- 3. Gan B. . How erastin assassinates cells by ferroptosis revealed. Protein & Cell. 2023;14(2):84-86.
- 4. Reiter RJ., Mayo JC, Tan DX, Sainz RM, Alatorre-Jimenez M, Qin L. Melatonin as an antioxidant: under promises but over delivers. J. Pineal Res. 2016;61(3):253-278.
- 5. Xuan W, Lu X, Yang Z, Li J, Jin W, Li Y. Propofol Protects Against Erastin-Induced Ferroptosis in HT-22 Cells. Journal of Molecular Neuroscience. 2022;72(9):1797-1808.

RUTIN: AN ANTI- INFLAMMATORY AGENT FOR MANGANESE INDUCED INFLAMMATION IN RAW 264.7 CELLS

Oneshi De Silva³, Suthipong Chujan^{1,2} and Jutamaad Satayavivad^{1,2,3}

¹Environmental Toxicology Program, Chulabhorn Graduated Institute ² Laboratory of Pharmacology, Chulabhorn Research Institute, Bangkok, Thailand. ³ Center of Excellence on Environmental Health and Toxicology (EHT), OPS, MHESI, Bangkok, Thailand.

Abstract:

Manganese is a naturally occurring trace metal that is also introduced into the environment through anthropogenic activities. While it is essential for numerous physiological functions, prolonged exposure to elevated levels of manganese has been associated with adverse health outcomes, including neurotoxicity and inflammation. In silico studies have suggested a potential pro-inflammatory role of manganese; however, the precise molecular mechanisms underlying manganese-induced inflammation remain poorly understood. Rutin, a well-characterized flavonoid, exhibits diverse therapeutic properties, including notable anti-inflammatory activity. Despite this, its role in modulating manganeseinduced inflammation has not been comprehensively investigated. In this study, RAW 264.7 macrophage cells were exposed to various concentrations of manganese chloride for 24 hours to simulate acute exposure conditions. Differentially expressed genes (DEGs) were identified and analyzed using Gene Ontology (GO), Kyoto Encyclopedia of Genes and Genomes (KEGG) pathway enrichment, protein-protein interaction (PPI) networks, and molecular clustering. Further analyses included transcription factor profiling, disease association mapping, and tissue specificity using the Metascape platform. Publicly available manganese exposure datasets from the Gene Expression Omnibus (GEO) were utilized to validate hub genes. Experimental validation was conducted through ELISA and immunoblotting to assess key inflammatory markers. The findings from this study provide novel insights into the molecular mechanisms of manganese-induced inflammation and support the potential of rutin as a therapeutic agent for mitigating these effects.

Keywords: Manganese, inflammation, bioinformatics, rutin, macrophage

Introduction:

Manganese is an essential trace element necessary for normal physiological functions. Manganese is a naturally abundant element, widely distributed in the environment through both natural processes and human activities. Natural sources of manganese include the earth's crust, water, soil, air, and various food items. Anthropogenic activities contributing to environmental manganese contamination encompass the discharge of municipal wastewater, sewage sludge application, mineral processing and mining operations, emissions from iron, steel, and alloy production, as well as fossil fuel combustion.

Previous studies have demonstrated that manganese toxicity is associated with a range of adverse health outcomes, including inflammation, Parkinson's disease, cognitive and behavioral impairments, hepatic damage, and detrimental effects on the respiratory and reproductive systems. Specifically, manganese-induced inflammation significantly affects the brain and other tissues by promoting oxidative stress and disrupting cellular and immune responses. Rutin, a flavonoid compound, has been recognized for its diverse therapeutic properties, notably its anti-inflammatory activity, there is currently no evidence regarding its

efficacy in mitigating manganese-induced inflammation in immune cells. Although several studies have documented the effects of manganese toxicity on immune responses, the underlying molecular mechanisms by which manganese affects immune cell function remain insufficiently characterized.

Environmentally relevant concentrations of manganese have been shown to modulate immune responses by altering the expression of key regulatory genes. The objective of this study was to elucidate the underlying molecular mechanisms by which manganese influences inflammation in the RAW 264.7 macrophage cell line. Additionally, this study analyzed the resulting dataset to predict potential links between manganese-induced immunomodulation and the development of immune-related disorders, including autoimmune and inflammatory diseases, as well as impaired immune function. Furthermore, the study assessed the anti-inflammatory effects of rutin on inflammation triggered by manganese toxicity.

Methodology:

For *in silico* analysis a microarray dataset was obtained from publicly available resources in the PubMed database based on a predefined selection criterion using the keyword "manganese exposure." Specifically, the Gene Expression Omnibus (GEO) dataset GSE214181 was selected for analysis. This dataset comprises gene expression profiling conducted via microarray technology in human subjects. The GSE214181 dataset, consisting of six samples divided into two groups—manganese-exposed and control—was downloaded for further investigation. Differentially expressed genes (DEGs) were identified using the GEO2R web tool.

The Database for Annotation, Visualization, and Integrated Discovery (DAVID) bioinformatics tool was employed to identify significantly enriched genes associated with functional categories. Gene ontology (GO) analysis, encompassing biological processes, molecular functions, and cellular components, was conducted using DAVID. Ten differentially expressed genes (DEGs) were selected for further investigation of their associated biological processes and signaling pathways using the graphical tool ShinyGO version 0.77. To elucidate the functional roles of the DEGs, Kyoto Encyclopedia of Genes and Genomes (KEGG) pathway analysis was performed. KEGG serves as an integrated data mining resource for the interpretation of biological pathways from genomic sequences. Pathway analyses focused on significantly enriched pathways, applying a significance threshold of p < 0.05. To explore the protein–protein interaction (PPI) networks of the differentially expressed genes (DEGs), a protein interaction network was constructed using Metascape. Modular clustering technique was used to groups genes, proteins, and other biological entities based on their similarities, allowing for the identification of natural clusters within the dataset.

For *in-vitro* experiment, RAW 264.7 macrophage cells were cultured in Dulbecco's Modified Eagle's Medium (DMEM) supplemented with 10% fetal bovine serum (FBS), 1% penicillin-streptomycin, and 1% L-glutamine. Cells were maintained in a humidified incubator at 37 °C with 5% CO₂ and 95% air. To validate the findings derived from the *in-silico* analysis, additional experiments including MTT assay for cell viability, immunoblotting analysis, and ELISA were performed on the cell line.

Results, Discussion and Conclusion:

Differential gene expression analysis between untreated and manganese chloride-treated samples revealed that 26,573 genes were upregulated, while 27,045 genes were downregulated. The top ten differentially expressed genes (DEGs) were selected for further investigation. Gene Ontology (GO) enrichment analysis indicated that the predominant biological processes (BP) involved were the carboxylic acid metabolic process, oxoacid metabolic process, and response to cytokine. Enrichment analysis of cellular components (CC) highlighted significant representation of the cytoplasmic vesicle lumen, lytic vacuole, and lysosome. For molecular functions (MF), notable enrichment was observed in lipoprotein particle activity, monosaccharide binding, and magnesium ion binding. Kyoto Encyclopedia of Genes and Genomes (KEGG) pathway analysis revealed significant enrichment in the NF-κB signaling pathway, tumor necrosis factor (TNF) signaling pathway, and C-type lectin receptor signaling pathway. These pathways are well-documented for their roles in immune regulation and inflammation.

Specifically, the NF-κB pathway is critical for modulating gene expression in immune and inflammatory responses, TNF-α functions as a key pro-inflammatory cytokine, and the C-type lectin receptor signaling pathway contributes to immune system modulation and inflammation. In vitro experiments corroborated these findings, showing that exposure of RAW 264.7 cells to manganese chloride induced the release of pro-inflammatory cytokines TNF-α and NF-κB proteins. A network-based analysis of enriched terms, organized by p-values, demonstrated that terms with higher numbers of DEGs tended to exhibit greater statistical significance. For visualization, the most significantly enriched term (i.e., with the lowest p-value) was selected from each of 20 clusters, with no more than 15 terms per cluster and a maximum total of 250 terms. Network analysis further revealed that carboxylic acid metabolism, immune signaling, adaptive immune response, and inflammatory response were closely interconnected, suggesting that alterations in one pathway may influence others.

Disease enrichment analysis identified associations with conditions such as malignant glioma, myocardial ischemia, and juvenile arthritis. Tissue-specific expression analysis indicated that DEGs were predominantly enriched in blood, smooth muscle tissue, and CD33+ myeloid cells. Finally, transcription factor analysis using the TRUST database identified NFKB1, SP1, RELA, ATM, and JUN as the most significantly enriched transcription factors regulating the DEGs.

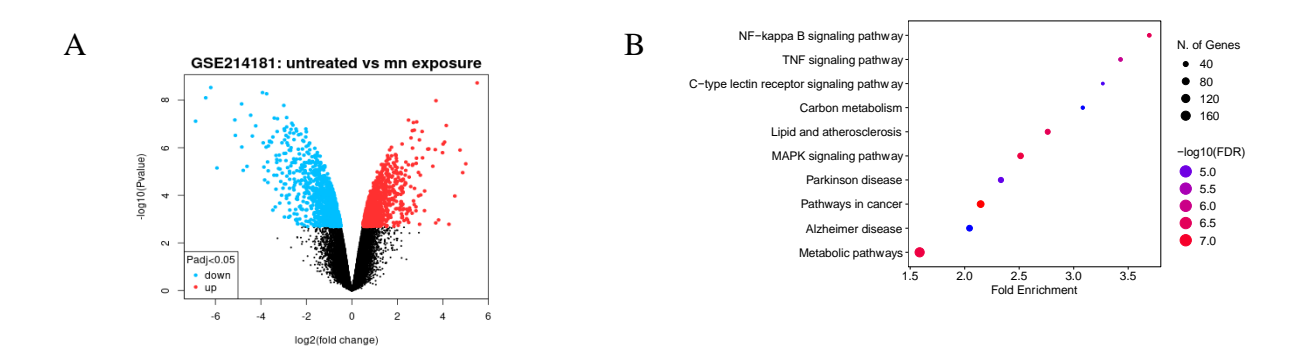


Figure 1 (**A**) Identification of differentially expressed genes (DEGs) between untreated and manganese chloride treated. (**B**) The KEGG (Kyoto Encyclopedia of Genes and Genomes) pathway analysis showed NF-kappa B signaling pathway was the most enriched pathway.

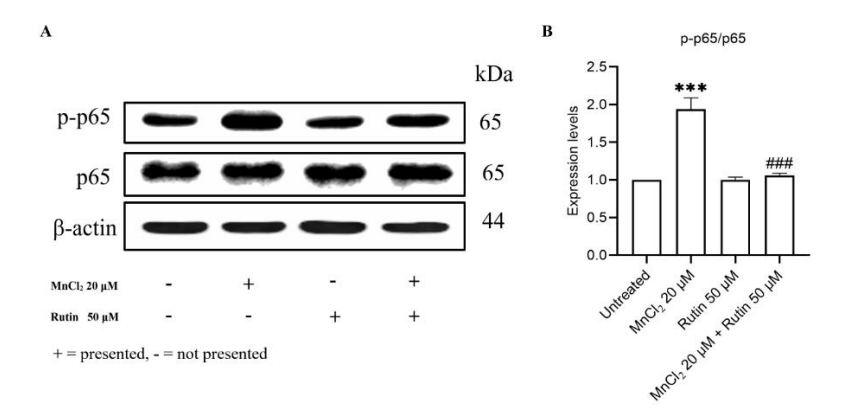


Figure 2 (**A**) Protein expression of p65. (**B**) Relative expression of p65. The data are represented as means \pm SEMs (n=3) and each protein was normalized to the levels of β-actin, ***P <0.001 compared with untreated group, and *##P <0.001 compared with MnCl₂ exposed group, were considered as significant.

This study employed both *in silico* and *in vitro* approaches to investigate the effects of manganese exposure on inflammation and its potential link to related diseases. *In silico* analysis was performed using *Homo sapiens* datasets, while the *in vitro* experiments were conducted on the RAW 264.7 macrophage cell line derived from mice. Findings from both approaches consistently demonstrated that exposure to toxic levels of manganese induces inflammatory responses.

Pathway enrichment analysis identified the NF- κB signaling pathway, TNF- α signaling, and cytokine-mediated immune signaling as the most significantly activated pathways upon manganese exposure—pathways that are strongly associated with the inflammatory response. Following this, the anti-inflammatory potential of rutin was evaluated in RAW 264.7 cells pre-exposed to manganese. The results indicated that rutin effectively reduced NF- κB protein levels in the cell lysate, suggesting that it attenuates manganese-induced inflammation.

In conclusion, the study confirms that manganese toxicity can trigger inflammatory signaling pathways, and rutin possesses anti-inflammatory properties capable of mitigating these effects. These findings suggest a potential therapeutic application of rutin in conditions involving manganese-induced inflammation.

- 1. Crossgrove J, Zheng W. Manganese toxicity upon overexposure. NMR Biomed. 2004;17(8):544-53.
- 2. National Institute of Health. Manganese data sheet [Internet]. 2021 [cited 2025 Jan 10]. Available from: https://ods.od.nih.gov/factsheets/Manganese-HealthProfessional/.
- 3. Finley JW, Penland JG, Davis CD, Pettit RE. Dietary Manganese Intake and Type of Lipid Do Not Affect Clinical or Neuropsychological Measures in Healthy Young Women. The Journal of Nutrition. 2003;133(9):2849-56.

- 4. Rondanelli M, Faliva MA, Peroni G, Infantino V, Gasparri C, Iannello G, et al. Essentiality of Manganese for Bone Health: An Overview and Update. Natural Product Communications. 2021;16(5):1934578X211016649.
- 5. Chen P, Bornhorst J, Aschner M. Manganese metabolism in humans. Front Biosci (Landmark Ed). 2018;23(9):1655-79.
- 6. Goyal J, Verma PK. An Overview of Biosynthetic Pathway and Therapeutic Potential of Rutin. Mini Rev Med Chem. 2023;23(14):1451-60.
- 7. Erikson KM, Aschner M. Manganese: Its Role in Disease and Health. Met Ions Life Sci. 2019;19.
- 8. Wang X, Jones MR, Pan Z, Lu X, Deng Y, Zhu M, et al. Trivalent manganese in dissolved forms: Occurrence, speciation, reactivity and environmental geochemical impact. Water Res. 2024;263:122198.
- 9. Jia L, Zhou Q, Li Y, Wu W. Application of manganese oxides in wastewater treatment: Biogeochemical Mn cycling driven by bacteria. Chemosphere. 2023;336:139219.
- 10. Bowler RM, Beseler CL, Gocheva VV, Colledge M, Kornblith ES, Julian JR, et al. Environmental exposure to manganese in air: Associations with tremor and motor function. Sci Total Environ. 2016;541:646-54.
- 11. Kermani M, Jonidi Jafari A, Gholami M, Arfaeinia H, Shahsavani A, Fanaei F. Characterization, possible sources and health risk assessment of PM2.5-bound Heavy Metals in the most industrial city of Iran. J Environ Health Sci Eng. 2021;19(1):151-63.
- 12. Lorieri D, Elsenbeer H. Aluminium, iron and manganese in near-surface waters of a tropical rainforest ecosystem. Sci Total Environ. 1997;205(1):13-23.

Safety and toxicity of food, drugs and other chemicals including biofuels



ECOLOGICAL RISK ASSESSMENT OF MICROPLASTICS POLLUTION IN THAILAND

Bongkotrat Suyamud¹

¹Department of Sanitary Engineering, Faculty of Public Health, Mahidol University, Bangkok, 10400, Thailand

Abstract:

This study synthesized data on microplastic abundance and characteristics within Thailand from 118 peer-reviewed publications (2017–2024). Predominant microplastic presence in crustaceans ranged of 1.69–160.15 items/g, followed by Mollusca (0.03–9.5 items/g) and fishes (0.01–28.17 items/g), with higher abundances in wastewater (4× 10² to 6.09 × 10⁵ items/m³) compared to that in freshwater (1.44–2.92× 10⁶ items/m³) and seawater (2.70× 10⁻¹ to 6.25× 10⁴ items/m³). Marine sediments (48.3–2.13×10⁴ items/kg) also showed significantly higher microplastic concentrations than terrestrial sediments (3 –2 .9 2 ×1 0³ items/kg). Predominant microplastics were identified as fibers (59.36% and 35.05% for biological and environmental samples, respectively) and fragments (24.14%, 30.68%) in blue (25.95%, 18.64%), and colorless/transparent (20.01%, 14.47%), primarily composed of polyethylene terephthalate (19.46%, 9.19%), nylon (3.23%, 9.99%), polypropylene (19.78%, 24.23%), and polyethylene (14.81%, 11.66%). The potential ecological risk was low in all ecosystems except for wastewater. This study has compiled up-to-date insights into the prevalence, distribution, and risks associated with microplastics, which is instrumental in formulating effective strategies for contaminant control and ultimately reducing plastic pollution.

Keywords: Microplastics, Thailand, ecological risk

Introduction:

Thailand is the sixth largest contributor of marine debris globally and ranks fourth in Asia (Jualaong et al., 2023; Marks et al., 2020). Microplastic research in Thailand began in 2004, suggesting that the widespread use of plastics began in the 1960s (Matsuguma et al., 2017). This inference is supported by the notable increase in microplastics found in sediment cores, with a significant increase observed from the 6-12 cm layer (1990s) to the surface layer (2000s) (Matsuguma et al., 2017). The effects of microplastics on human health have received considerable attention. Microplastics are found to compromise tissues and organs in the digestive, nervous, respiratory, reproductive, and cardiovascular systems, leading to various diseases and human health disturbances (Liu and You, 2023). Several review papers have been published on microplastic pollution in Southeast Asia (SEA). For instance, the pollution levels of microplastics in water, sediment, and aquatic organisms from Southeast Asian Nations have been summarized (Gabisa and Gheewala, 2022; Sin et al., 2023). Although these reviews have enriched our understanding of microplastic pollution in Southeast Asia, an evident gap exists owing to the absence of comprehensive meta-analyses and discussions on the ecological risks posed by microplastics in Thailand. This study aims to (1) synthesise available evidence regarding microplastic pollution across water, sediment, and biota in Thailand and (2) assess the potential risks linked to microplastics from terrestrial and marine environments via a national meta-analysis. Understanding the environmental risks and exposure consumption of plastic pollution will help create a more comprehensive understanding of the ecological implications and human health risks.

Methodology:

Literature search and data processing

The collected studies were rigorously reviewed from two databases, Scopus and Google Scholar, using the following keywords: ("Microplastic pollution in Thailand"), and ("microplastic AND pollution AND in AND Thailand"). The information was categorized based on the following criteria: (1) the sampling site should be in Thailand; (2) abundance and occurrence in the environment (water, sediment, and biota (e.g., various aquatic species and products)); and (3) the studies must have data on one of the following microplastic characteristics (abundance, shape, size, colour, and polymer types). For comparative analysis, the units for microplastic abundance were recorded or recalculated in items/m3 for the water samples. For the sediment samples, items/kg dry weight units were used or recalculated from published data. For biota samples, items/g wet weight units and items/ individuals were obtained from published data.

Pollution load index

The integrated pollution load index (PLI) method developed by Tomlinson et al. (1980) employs concentration factors (CFi) to assess microplastic pollution levels in aquatic environments, including water and sediment (Nyaga et al., 2024). The contamination factor (CFi) is the ratio of the microplastic concentration (Ci) at each site to the background value (Coi) (Gurumoorthi and Luis, 2023). The CFi and PLI were estimated using:

$$CFi = \frac{Ci}{Coi}$$
 Eq. (1)

$$PLI = \sqrt{CFi}$$
 Eq. (2)

The *PLI* was categorized into four pollution risk levels: <10 (low level), 10-20 (medium 119 level), 20-30 (high level), and >30 (extremely high level).

Polymer hazard index

The polymer hazard index (*PHI*) was derived from the concentrations and chemical compositions of various types of MPs, incorporating a hazard score for each (Xu et al., 2018). Hazard scores sourced from Lithner et al. (2011). *PHI* was calculated as follows:

$$PHI = \sum_{n=1}^{n} Pn \times Sn$$
 Eq. (3)

where Pn is the percentage abundance of each polymer in each sample and Sn is the corresponding hazard score of the polymer type. The PHI is also classified into four risk levels: values < 10 represent risk level I, 10–100 represent risk level II, 100–1000 risk level III, and >1000 represent risk level IV.

Potential ecological risk index

The potential ecological risk index (*PERI*) was calculated to assess the ecological, environmental, and hazardous effects of microplastics, following the methodology outlined by Ranjani et al. (2021) with the following equations:

$$CF_i = \frac{Ci}{Coi}$$
 Eq. (1)

$$T_i = \sum_{n=1}^n \frac{P_n}{C_i} \times S_n$$
 Eq. (4)

$$PERI = CF_i \times T_i$$
 Eq. (5)

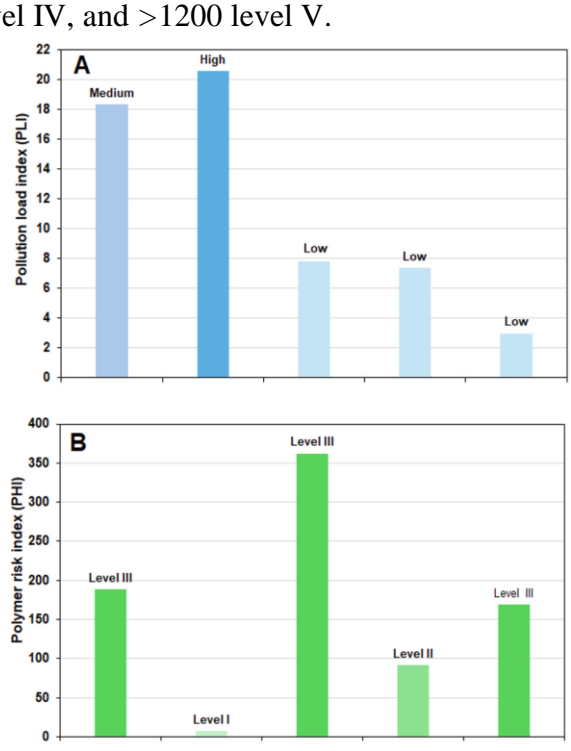
Ti is the toxicity coefficient, expressed as the sum of the polymer proportion (Pn) as a fraction of the concentration of microplastics at the sampling site (Ci), multiplied by the hazard score of the respective polymers. PERI values were categorized as: <150 level I, 150–300 level II, 300–600 level III, 600–1200 level IV, and >1200 level V.

Results, Discussion and Conclusion:

Ecological risk assessment of microplastics

The pollution loads for the water and sediment were estimated based on PLI (Fig. 1A). A high pollution load (category III) was detected in the seawater at an average of 20.58. The PLI for freshwater was 18.32 and classified as Category II or medium. Overall, wastewater (7.79), terrestrial sediment (7.36), and marine sediment (2.97) were classified as Category I or low-level risk.

The hazard level was in the range of I-III based on the PHI values (Fig. 1B). The overall PHI of the water and sediment were polymer calculated from the average composition of microplastics and their respective hazard scores. The highest reported hazard level was found in wastewater (326.28) owing to the abundance of microplastics with high hazard scores, such as polyurethane (PUR) with a high hazard score of 13,844 and a percentage of 16%. The second highest PHI was found in freshwater (188.23) because of the presence of polyvinyl chloride (PVC: 5001) and polymethyl methacrylate (PMMA:1021), followed by marine (169.33) and terrestrial sediments (91.9). The lowest PHI was observed in seawater (7.62), which was classified as risk The abundance of microplastics in seawater is composed of low-hazard polymers, that is, PE and PP, as the dominant types, reflecting a minor risk.



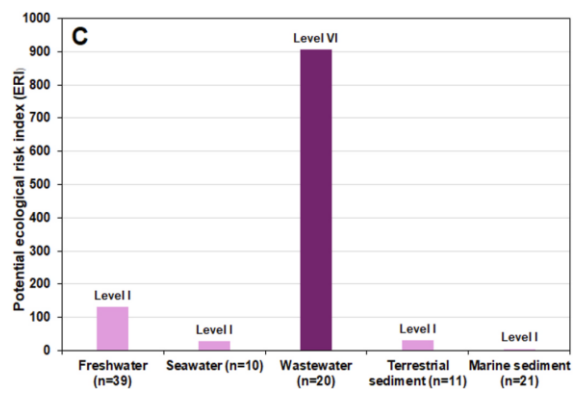


Figure 1 Risk of microplastic pollution in Thailand. The pollution load index (PLI) in water and sediment (A), polymer risk assessment index (H Index) in water and sediment (B), and potential ecological risk index (PERI) in waters and sediment (C).

The PERI index of microplastics considers the effects of the abundance and polymer type on the ecological risk of microplastics (Gurumoorthi and Luis, 2023). In Thailand, average PERI values were reported as 130.71 for freshwater, 28.21 for seawater, 905.71 for wastewater, 30.63 for terrestrial sediments, and 5.49 for marine sediment, respectively (Fig. 1C). Most PERI values calculated in this review fell below 150 (Level I), except for wastewater, which was classified as level IV. The highest PERI value was attributed to the dominance of polyurethane (PUR) microplastics, which constituted 16% with a hazard score of 13.844.

Conclusion:

This information provides the basis for regulations as well as the design, prioritization, and timing of solutions. Microplastics may be transmitted to humans through the consumption of plastic-tainted aquatic organisms. This raises concerns about the potential health impacts, as research on the direct effects of microplastic ingestion by humans is limited. Understanding the extent of microplastic pollution, environmental risks, and exposure to plastic pollution is crucial for developing informed strategies to mitigate plastic pollution and safeguard human well-being.

- 1. Gabisa, E.W., Gheewala, S.H., 2022. Microplastics in ASEAN region countries: a review on current status and perspectives. Mar. Pollut. Bull. 184, 114118.
- 2. Gurumoorthi, K., Luis, A.J., 2023. Recent trends on microplastics abundance and risk assessment in coastal Antarctica: regional meta-analysis. Environ Pollut 324, 121385.
- 3. Jualaong, S., Towatana, P., Pradit, S., Puttapreecha, R., 2023. Type and distribution of microplastic contamination in beach sediment along the coast of the lower Gulf of Thailand. Appl. Ecol. Environ. Res. 21 (3), 2671–2682.
- 4. Liu, Z., You, X.Y., 2023. Recent progress of microplastic toxicity on human exposure base on in vitro and in vivo studies. Sci. Total Environ. 903, 166766.
- 5. Marks, D., Miller, M.A., Vassanadumrongdee, S., 2020. The geopolitical economy of Thailand's marine plastic pollution crisis. Asia Pac. Viewp. 61 (2), 266–282.
- 6. Y., Boonyatumanond, R., Zakaria, M.P., Weerts, S., Newman, B., 2017. Microplastics in sediment cores from Asia and Africa as indicators of temporal trends in plastic pollution. Arch. Environ. Contam. Toxicol. 73 (2), 230–239.
- 7. Nyaga, M.P., Shabaka, S., Oh, S., Osman, D.M., Yuan, W., Zhang, W., Yang, Y., 2024. Microplastics in aquatic ecosystems of Africa: a comprehensive review and metaanalysis. Environ. Res. 248, 118307.
- 8. Ranjani, M., Veerasingam, S., Venkatachalapathy, R., Mugilarasan, M., Bagaev, A., Mukhanov, V., Vethamony, P., 2021. Assessment of potential ecological risk of microplastics in the coastal sediments of India: a meta-analysis. Mar. Pollut. Bull. 163, 111969.
- 9. Sin, L.T., Balakrishnan, V., Bee, S.T., Bee, S.L., 2023. A review of the current state of microplastic pollution in south Asian countries. Sustainability 15 (8), 6813.
- 10. Tomlinson, D.L., Wilson, J.G., Harris, C.R., Jeffrey, D.W., 1980. Problems in the assessment of heavy-metal levels in estuaries and the formation of a pollution index. Helgol. Meeresunters. 33, 566–575.
- 11. Xu, P., Peng, G., Su, L., Gao, Y., Gao, L., Li, D., 2018. Microplastic risk assessment in surface waters: a case study in the Changjiang Estuary, China. Mar. Pollut. Bull. 133, 647–654.

Environment/health impact assessment and management



ASSESSING RECYCLING OF BEVERAGE CARTONS IN THAILAND: A PASSIVE COLLECTION SYSTEM

<u>Sudthinee Wichenwan^{1,2}</u>, Suphaphat Kwonpongsagoon ^{1,2*}, Manaporn Wongsoonthornchai³, and Kanokwan Kingphadung⁴

Department of Sanitary Engineering, Faculty of Public Health, Mahidol University, Thailand
 Center of Excellence on Environmental Health and Toxicology (EHT), OPS, MHESI, Thailand
 Faculty of Public Health, Thammasat University, Pathumthani, Thailand
 Department of Food Technology, Faculty of Engineering and Industrial Technology, Silpakorn University, Thailand
 *Corresponding author: suphaphat.kwo@mahidol.ac.th

Abstract:

This study aimed to evaluate the recycling of used beverage cartons (UBCs) through a passive collection system in Thailand. The specific objectives are: (1) to determine the proportion of UBCs present in waste paper supplied to paper mills, and (2) to estimate the total quantity of UBCs in waste paper streams, including the expected recyclable materials (paper pulp) and residual wastes (polyethylene and aluminium foil). The study employed both primary and secondary data. The physical waste sampling of both old corrugated containers (OCC) and mixed paper (MP) were conducted at six paper mills and four large-scale baling facilities. The findings indicated that used beverage cartons (UBCs) were present only in the mixed paper (MP) grade. The study found that the average UBC content in MP was $0.029\% \pm 0.040\%$. The annual quantity of UBCs embedded in MP domestic collection was estimated from 157 to 162 tonnes between 2020 and 2023. Of these, approximately 153 tonnes of used beverage cartons (UBCs) were processed annually at domestic paper recycling mills, yielding about 84 tonnes of recyclable pulp converted into Kraft paper and 46 tonnes of Poly-Alu residue, which was utilized as an alternative fuel either internally in boilers or externally in cement and power plants.

Keywords: Used beverage cartons (UBCs), waste paper, mixed paper (MP), recycling

Introduction:

Beverage cartons (BCs), including both ultra-high temperature (UHT) and pasteurized are multilayer packaging materials typically composed of approximately 75% paperboard, 20% polyethylene, and 5% aluminum foil [1]. Recycling used beverage cartons (UBCs) is significantly more complex than it appears. Their multilayered composition makes material separation during recycling technically challenging. Standard paper mills are unable to process UBCs without specialized equipment [2]. In terms of sorting and collection, UBCs are often disposed of through co-mingled waste streams alongside other recyclables, which complicates identification and recovery. Contamination from residual liquids or food further reduces their efficient sorting and collection for recycling. Additional barriers include the low market value of recovered materials, particularly the plastic and aluminum fractions, and the lack of enforcement of extended producer responsibility (EPR) in certain regions. Moreover, limited public awareness regarding proper disposal and recycling options for UBCs continues to hinder effective recovery. An efficient collection process is key for successful recycling; therefore, many countries have established UBC collection systems to achieve UBCs recycling. These systems vary significantly across regions, with European countries typically adopting two main approaches. The first and most common method involves co-collecting UBCs with lightweight packaging, a system implemented in the Netherlands, Germany and Belgium. The second approach is co-collecting UBCs with paper-based packaging, which operate in Norway, Sweden and Finland. Some countries mixed collection with both lightweight and paper packaging (e.g., Italy) and some countries (e.g., Switzerland), have established separation of UBC collection systems [3]. High recycling rates of up to 70–90% have been reported in certain countries, such as Germany and Belgium.

In Thailand, less than 100 thousand tonnes of beverage cartons (BCs) are consumed annually, all of which are disposed of as waste within the same year [4]. The annual collection for recycling has been reported at a very low quantity, primarily driven by active campaigns initiated by private sector stakeholders [4,5] — a pattern that contrasts with practices in European countries. However, beyond these targeted efforts, UBCs are often co-disposed with waste paper stream due to their paper-based composition and similar external appearance—a practice hereinafter referred to as "passive collection for recycling". Internationally, the proportion of beverage cartons (BCs) present in waste paper streams varies considerably: approximately 0.5% in the European Union [6], between 0.01% and 1.7% in India [7,8], 0.6% in Italy, and as high as 15–16% in Denmark and Sweden [9,10]. In Thailand, the flow pathway of used beverage cartons (UBCs) co-disposed with waste paper typically passes through informal channels—such as waste pickers, saleng, and waste dealers—and ultimately leads to recycling at paper recovery facilities.

In addition to formal (active) collection efforts aimed at pure recycling, Thailand has not yet documented any data on passive UBC collection practices. Therefore, this study aims to assess passive collection of UBCs for recycling at paper recovery facilities. The objectives of this study are: (1) to determine the proportion of used beverage cartons (UBCs) present in waste paper supplied to paper mills, and (2) to estimate the total quantity of UBCs in waste paper streams, including the expected recyclable fraction (paper pulp) and residual components (polyethylene and aluminium foil).

Methodology:

Scope and system boundary: The study focuses on the passive collection of UBCs, referring to cartons embedded within waste paper streams. Due to their similarity to other waste paper, UBCs enter the recycling chain alongside old corrugated containers (OCC) and mixed paper (MP). They typically move from households and commercial sources to small and medium-sized waste dealers, then to large-scale waste buying and baling facilities, where they are compacted into bales. From there, UBCs are transported to paper mills, where the fiber content can be partially recovered, while non-fiber residues such as Poly-Alu are rejected or managed through alternative disposal and recycling options.

Data collection: The study used both primary and secondary data. Primary data were obtained from UBCs in waste paper streams at paper recycling mills and large-scale baling facilities through physical waste sampling, conducted inside paper mills and at the exit points of baling plants using a manual sampling technique described in steps 1–5 below. Secondary data were obtained from government reports, industry associations, international organizations, and previous research.

- 1. Randomly select at least five representative compressed bales per facility.
- 2. Cut the wires and break apart each bale for sampling
- 3. Randomly select two samples of 50 kg each per bale or a minimum of 100 kg per bale
- 4. Sort UBCs out from each sample and weight it
- 5. Record the results

All samples of waste paper and UBCs were weighed on a wet weight basis.

Analysis of waste composition:

The results are calculated as the percentage of UBC found per bale using the following equation.

Where:
$$\begin{aligned} & \textit{Percent by weight}(\%) = \frac{w_c}{w_t} \times 100\% \\ & W_c = \text{weight of used beverage cartons (UBCs) found} \\ & W_t = \text{weight of waste paper sample} \end{aligned} \tag{1}$$

Data analysis: The collected data were analyzed using several techniques. The mass balance principle was applied to track the movement of UBCs within the system, ensuring consistency between inputs, outputs, and losses across the system boundary [8]. Descriptive statistics were also used, including the mean to determine the average percentage of UBCs from physical sampling across paper mills, and the standard deviation (SD) to measure the variation in UBC content within the waste paper stream. In addition, other measures of central tendency such as the mode and median were also analyzed to describe the distribution of UBC content.

Results and Discussion:

This study involved the sampling of two waste paper grades—old corrugated containers (OCC) and mixed paper (MP)—to assess the quantity of used beverage cartons (UBCs). For OCC bales, a total of 7 tonnes were sampled across two paper recycling mills, and no UBCs were found in these samples. In contrast, MP bale sampling was conducted at four paper recycling mills and four large-scale waste purchasing and baling facilities, with a total sampled weight of 14.955 tonnes. A total of 40 bale samples were analyzed, comprising 20 from paper mills and 20 from large-scale waste buying and baling facilities. The analysis revealed differences in UBC content between two facility types. Based on the original samples, the average UBC percentage at paper mills was 0.132%, with the highest recorded value reaching 1.084%. In contrast, large-scale waste purchasing and baling facilities exhibited a much lower average of 0.033%, with the highest value recorded at only 0.024%. These results are presented in Table 1.

Table 1 UBC percentage statistics (pre- and post-outlier removal)

	Original sample			Sample after outlier removal		
UBC percentage statistics	Paper mills (n=20)	LWPB plant* (n=20)	Total (n=40)	Paper mills (n=17)	LWPB plant* (n=20)	Total (n=37)
Min	0.000	0.000	0.000	0.000	0.000	0.000
Max	1.084	0.204	1.084	0.124	0.204	0.204
Mean $(ar{X})$	0.132	0.033	0.082	0.024	0.033	0.029
Median	0.014	0.016	0.014	0.008	0.016	0.011
Mode	0.000	0.000	0.000	0.000	0.000	0.000
Standard Deviation (SD)	0.283	0.046	0.206	0.033	0.046	0.040

Note: *Large-scale waste purchasing & baling plant

Upon analysis of all 40 original samples, the overall mean percentage of UBCs in mixed paper (MP) was 0.082%, with a median of 0.014% and a standard deviation (SD) of 0.206%. The statistical analysis of all samples identified three data points from paper mills that exceeded 0.495 (a threshold representing the mean plus two standard deviations), indicating abnormally high UBC percentage values. After removing these outliers, the dataset was reduced to 37 samples. This adjustment decreased the SD to 0.040% and lowered the mean UBC percentage to 0.029%, indicating reduced variability and a more consistent dataset. All statistical measures before and after outlier removal is presented in Table 1.

In Thailand between 2020 and 2023, the amount of UBCs embedded in MP was calculated, ranging between 157 and 162 tonnes per year. These passively collected UBCs were managed through both domestic recycling at paper mills and export.

In addition to the estimated total passive collection of UBCs in the country, the majority were processed annually at local paper recycling plants. Figure 1 presents the average quantity of UBCs found in mixed paper (MP) passively collected for recycling at domestic paper mills between 2020 and 2023. On average, 153 tonnes of UBCs in MP were processed annually at domestic recycling plants, yielding approximately 84 tonnes of recyclable fiber and 46 tonnes of Poly-Alu residue. The recovered paper fiber is subsequently converted into Kraft paper for use in paper container production, while most of the remaining Poly-Alu—mixed with other residues from paper recycling plants—is primarily utilized as an alternative fuel, either internally in boilers or externally in cement and power plants.

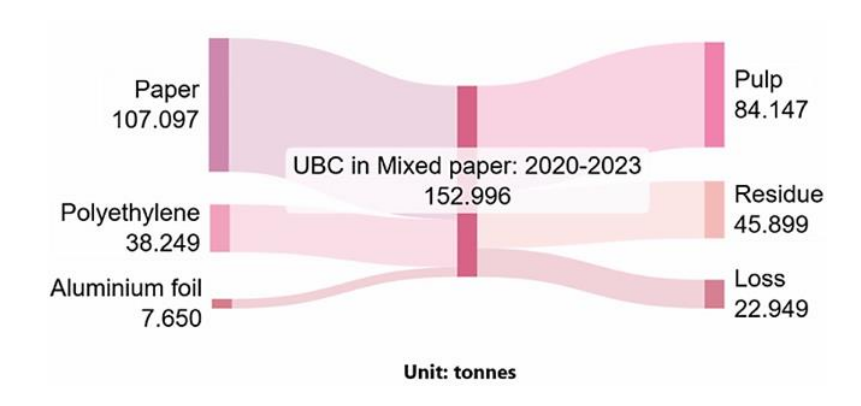


Figure 1 UBCs in MP: domestic collection and recycling (average from 2020 to 2023)

This study reveals that based on annual UBC consumption, Thailand passively recovers less than 1% of UBCs from mixed paper waste, far below European countries that achieve higher recovery rates through source separation or co-collection systems. Although passive collection of used beverage cartons (UBCs) for recycling in conventional paper mills is minimal and presents challenges in terms of efficient material separation and recycling processes, such practices can nonetheless contribute to partial fiber recovery and reintegration into the production cycle, in accordance with circular economy principles. In light of Thailand's current situation, where no legislation mandates source separation of waste by the public, efforts to increase the recovery rate of used beverage cartons (UBCs) should continue to prioritize the strengthening of active collection schemes. In parallel, particular emphasis should be placed on implementing sustained price-based incentives within the informal collection system, alongside ongoing promotion of public participation in source separation—especially at high-generation points such as schools.

Conclusion:

In conclusion, the results of this study provide a clear overview of UBCs embedded in mixed paper streams in Thailand, serving as baseline data supporting their management and recycling potential. The findings highlight that passive collection of UBCs for recycling at paper recovery facilities accounts for only a minimal fraction of national beverage carton consumption, yielding limited fiber recovery and generating significant Poly-Alu residue. These outcomes also contribute to strengthening the national database on UBC recycling and support the advancement of more sustainable waste management practices.

- 1. Pretz T, Pikhard O. Final report Beverage carton recycling. Aachen (Germany): Institut für Aufbereitung und Recycling fester Abfallstoffe; 2010. 44 p.
- 2. 4Evergreen. Fibre-based packaging recyclability evaluation protocol. Brussels (Belgium): 4Evergreen; 2022.
- 3. Alliance for Beverage Cartons and the Environment (ACE), EXTR:ACT. Beverage carton recycling facts & figures. Brussels: ACE; 2024. 15 p.
- 4. Kwonpongsagoon S, Kingphadung K, Limphitakphong N, Wongsoonthronchai M. Practical approach for implementing extended producer responsibility by using Material Flow Analysis, value chain analysis, and Life Cycle Assessment: Case study of beverage carton. Bangkok: National Science, Research and Innovation Fund (NSRF) and Program Management Unit for Competitiveness Enhancement (PMU-C); 2024.
- 5. Green Network Thailand. The green shelter project for friends in need (of "Pa") volunteers foundation [Internet]. Bangkok: Green Network Thailand; 2022 [cited 2025 Aug 21]. Available from: https://www.greennetworkthailand.com/tetra-pak-thai-green-shelter/
- 6. Prognos. End-of-waste criteria for recovered paper: Impact assessment for used beverage cartons. Schuetz N, Birnstengel B, Mevissen N, authors. Düsseldorf (Germany): Prognos AG for Tetra Pak International; 2010.
- 7. The Energy and Resources Institute (TERI). Used Beverage Cartons Management Study 2022. New Delhi (India): TERI; 2022. 94 p.
- 8. The Energy and Resources Institute (TERI). Used Beverage Carton Management Study for Indian Cities. New Delhi (India): TERI; 2019. 134 p.
- 9. Villanueva A, Eder P. End-of-waste criteria for waste paper: Technical proposals (EUR 24789 EN). Ispra (Italy): Joint Research Centre, European Commission; 2011.
- 10. Pivnenko K, Pedersen GA, Eriksson E, Astrup TF. Bisphenol A and its structural analogues in household waste paper. Waste Manag. 2015;44:39-47. doi:10.1016/j.wasman.2015.07.017.
- 11. Brunner PH, Rechberger H. Practical handbook of material flow analysis. 1st ed. Boca Raton (FL): CRC Press; 2003. 311 p.

HEALTH RISK ASSESSMENT OF NICKEL AND CHROMIUM CONTAINING PARTICLES IN ARC WELDING FACTORY

K. Jaikla^{a,b}, T. Neamhom^{a,b*}, C. Jaikanlaya^{a,b} and W. Patthanaissaranukool^{a,b}

^a Department of Environmental Health Sciences, Faculty of Public Health, Mahidol University, 420/1 Rajvithi Rd., Rajchathawee, Bangkok, Thailand ^b Center of Excellence on Environmental Health and Toxicology (EHT), OPS, MHESI, Bangkok, Thailand

* Corresponding author E-mail address: thanakrit.nea@mahidol.ac.th

Abstract:

Welding is an essential process in Thailand's growing industrial sector but generates hazardous metal fumes that pose significant health risks. Of particular concern are nickel (Ni) and chromium (Cr), due to their toxicity and carcinogenicity. This study measured Ni and Cr concentrations in airborne dust from a welding factory in Chonburi Province and assessed associated health risks using personal and area samples. Results showed that personal sampling yielded higher Ni $(1.35\pm0.29-2.74\pm3.43~\mu g/m^3)$ and Cr $(2.30\pm0.60-2.67\pm0.81~\mu g/m^3)$ concentrations than area sampling. In all areas, hazard quotient (HQ) values remained below 1.0, indicating low non–carcinogenic risks. However, carcinogenic risks (CR) greatly exceeded the occupational limit of $1.00~x10^{-4}$. Ni risks ranged from $7.54x10^{-3}\pm0.00$ to $1.68x10^{-2}\pm0.02$, while Cr risks were markedly higher, ranging from $1.75x10^{-1}\pm0.04$ to $2.49x10^{-1}\pm0.08$, suggesting a substantially greater cancer risk from Cr exposure. These CR values exceed acceptable thresholds, indicating residual cancer risk. These findings emphasize the need for improved engineering controls and protective measures to safeguard worker health.

Keywords: Welding fume, nickel, chromium, health risk assessment, occupational exposure

Introduction:

Thailand's rapid industrialization and infrastructure growth have substantially increased metal consumption, reaching 16.39 million tons in 2021, with the automotive sector alone contributing 22% (1). Within this sector, welding is a critical process that supports production efficiency but simultaneously generates hazardous emissions that threaten worker health. For example, a welding factory in Chonburi Province consumed 9,301 tons of metal in 2022, including 28 tons of copper wire, with welding operations producing an estimated 0.14 tons of fumes. Welding activities are recognized sources of airborne pollutants such as particulate matter, toxic gases, and metal fumes, whose composition and levels depend on welding methods, filler materials, and equipment used (2). The metal inert gas (MIG) welding process in this factory, performed on SS400 base metal containing carbon (C), manganese (Mn), silicon (Si), copper (Cu), aluminum (Al), phosphorus (P), sulfur (S), molybdenum (Mo), and notably nickel (Ni) and chromium (Cr), is of particular concern because it releases Ni and Cr in ultrafine particulate form (0.001-100 µm), which are associated with significant toxicity and carcinogenicity. Both metals are present in respirable particulates capable of penetrating the body via inhalation, dermal absorption, or ingestion (3, 4), and are linked to acute effects such as mucosal irritation and dizziness, as well as chronic outcomes including lung fibrosis, allergic dermatitis, and cancers of the lung, larynx (2, 5). Cr(VI) is a Group 1 human carcinogen (3, 4) that can persist in lung tissue and significantly elevate long-term cancer risk. Despite these hazards, routine workplace inspections in the factory have measured only total and respirable dust levels without quantifying individual metals, particularly Ni and Cr, creating a critical data gap for assessing long—term health risks from cumulative exposure to hazardous welding fumes. To address this, the present study analyzed Ni and Cr concentrations in airborne dust from personal and area sampling and evaluated both non—carcinogenic and carcinogenic risks to workers, providing urgently needed evidence to guide exposure control strategies in welding environments.

Materials and Methods:

Study subjects

The study was conducted in a metal arc welding factory located in the Amata City Industrial Estate, Chonburi Province, Thailand (13.4193°N, 101.0176°E). Workers included welders and employees in nearby zones such as spotting, packing, and production areas, all of whom were potentially exposed to welding fumes. Eligibility criteria required participants to be full–time workers who had held the same position for at least one year. A total of 53 air samples were collected, comprising 41 personal samples and 12 area samples (Figure 1(A)).

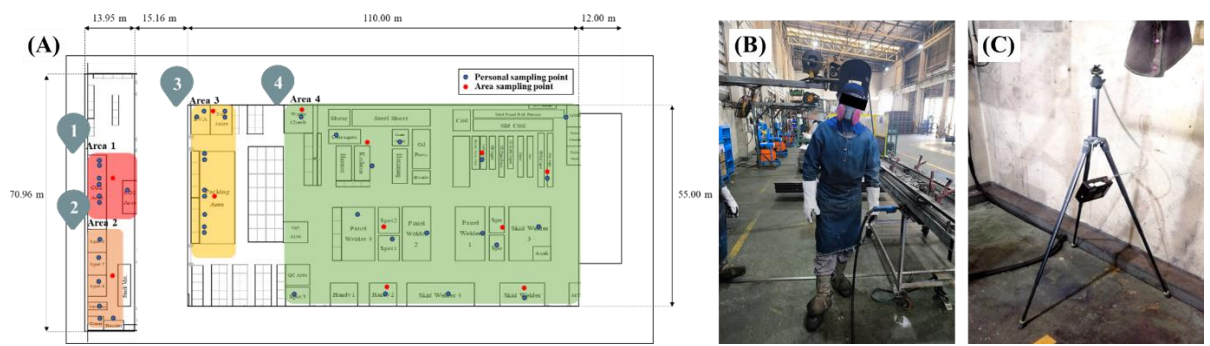


Figure 1 (A) Layout of personal and area sampling points in the factory, (B) personal sampling, and (C) area sampling

Collection and Analysis of Welding Fumes

Study site and survey

The factory covers an area of 6,972 m². A walkthrough survey identified four distinct work areas based on distance from welding sources (Fig. 1(A)): Area 1 – CO₂ welding, Area 2 – Spotting, Area 3 – Packing, and Area 4 – Production. Sampling numbers were determined according to NIOSH (1977) and HKSAR (2019) guidelines, considering both area size and workforce distribution. In total, 41 personal and 12 area samples were obtained) (6).

Sampling procedure and chemical analysis

Airborne fumes were collected using 37 mm mixed cellulose ester (MCE) membrane filters (0.8 µm pore size) (manufacturer, country). For personal sampling, cassettes were clipped to workers' collars in the breathing zone (Fig. 1(B)), while for area sampling, cassettes were mounted on stands at representative locations (Fig. 1(C)). Pumps operated at 1–3 L/min for ~6 h, ensuring a minimum air volume of 480 L per sample. Filter loading was controlled to <2 mg. The collected membrane filters were subsequently digested with hydrochloric acid (HCl) and nitric acid (HNO₃) and analyzed for Ni and Cr concentrations following NIOSH Methods 7303(7) 7024 (8). Metal quantification was performed using inductively coupled plasma mass spectrometry (ICP–MS, NexION® 2000, PerkinElmer, USA).

Health risk assessment

Exposure Assessment

Since personal protective equipment (PPE) was routinely used and hygiene practices were observed, this study focused on inhalation as the primary exposure pathway. The U.S. EPA (2022) framework (9) was applied to calculate the average daily dose (ADD) for non–carcinogenic effects and the lifetime average daily dose (LADD) for carcinogenic risks using Equation (1):

$$ADD/LADD(mg/kg/d) = \frac{C(mg/m^3) \times IR(m^3/hr) \times ET(hr/d) \times EF(d/yr) \times ED(yr)}{365(d/yr) \times AT(yr) \times BW(kg)}$$
(1)

Where: $C = \text{concentration (mg/m}^3)$, $IR = \text{inhalation rate (m}^3/\text{hr})$, ET = exposure time (hr/day), EF = exposure frequency (days/yr), ED = exposure duration (yr), BW = body weight (kg), AT = averaging time (days). For non-carcinogenic effects, $AT = ED \times 365$; for carcinogenic risks, AT = 25,550 days (70 years).

Risk Characterization

■ Non–carcinogenic risk was estimated by hazard quotient (HQ) (9):

$$HQ\ inhalation\ = \frac{ADD\ inhalation}{RfC\ inhalation} \tag{2}$$

Where RfC is the reference concentration for inhalation exposure (mg/kg-day). HQ values >1 indicate potential health concern.

■ Carcinogenic risk (CR) was assessed by multiplying ADD with the inhalation slope factor (SF) (9):

$$CR = ADD \times SF \tag{3}$$

Values exceeding 1x10⁻⁴ are considered unacceptable for occupational exposure.

Results and Discussion:

■ Chemical concentration in total dust

As shown in Fig. 2(A), Ni concentrations in personal were highest in Area 1 (2.74 \pm 3.43 $\mu g/m^3$) and lowest in Area 3 (1.35 \pm 0.29 $\mu g/m^3$), while area concentrations were consistently lower (1.07 \pm 0.00 - 1.22 \pm 0.15 $\mu g/m^3$). For Cr, personal concentrations ranged from 2.30 \pm 0.60 $\mu g/m^3$ (Area 3) to 2.67 \pm 0.81 $\mu g/m^3$ (Area 2), with slightly lower values observed in area samples (1.90 \pm 0.00 - 2.07 \pm 0.68 $\mu g/m^3$). Overall, personal sampling yielded higher Ni and Cr concentrations than area sampling.

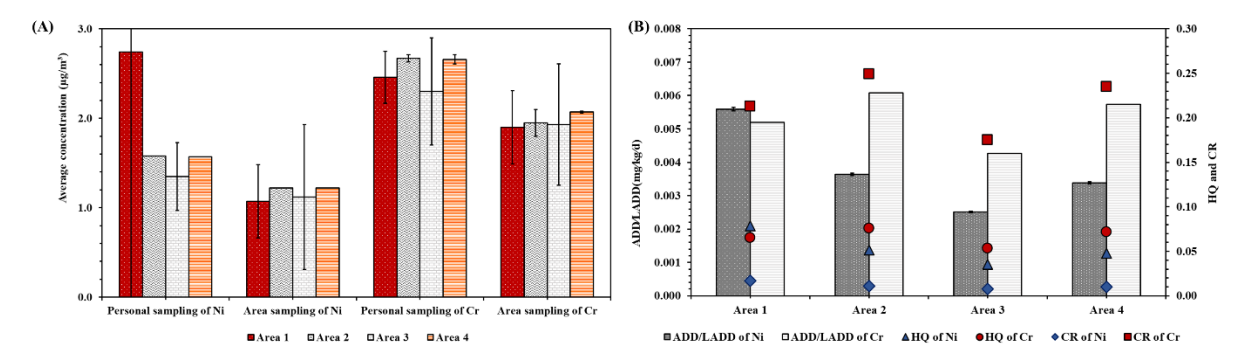


Figure 2 (A) Average concentrations of Ni and Cr in total dust from personal and area sampling across four work areas, and (B) Inhalation risk assessment of Ni and Cr based on personal and area sampling, including HQ and CR

■ Health risk assessment

As shown in Fig. 2(B), HQ values for both Ni and Cr were below 1.00 in all areas, indicating negligible non-carcinogenic risk. In contrast, CR values exceeded the acceptable limit (1.00×10⁻⁴) across all zones. For Ni, CR ranged from 7.54×10⁻³±0.00 (Area 3) to $1.68\times10^{-2}\pm0.02$ (Area 1), while for Cr, values were much higher, from $1.75\times10^{-1}\pm0.04$ (Area 3) to 2.49×10⁻¹±0.08 (Area 2). Overall, carcinogenic risks were significant, especially for Cr, which posed far greater risk than Ni. When compared with prior studies, such as Yang et al. (2018) (10), which reported higher CR values for Ni and Cr(VI) among welders in pipeline construction, the CR values in this study were comparable but still exceeded the acceptable limit. Similarly, Zainal Bakri et al. (2020) (11) reported CR values for Cr and Ni that also substantially exceeded acceptable limits among workers in the Malaysian automotive industry. Although the CR values observed in the present study are comparatively lower than those reported in heavy welding operations, they still indicate a residual cancer risk. Overall, these results underscore that even under relatively lower airborne concentrations, long-term inhalation exposure to Cr (particularly Cr(VI)) can contribute to a significant carcinogenic risk. Implementation of effective exposure control measures, including engineering controls such as local exhaust ventilation, optimized welding practices, and the consistent use of respiratory protection, is therefore crucial to mitigate adverse health outcomes.

Conclusion:

This study quantified Ni and Cr exposure in a welding factory and assessed associated health risks. Personal sampling revealed higher concentration than area sampling, confirming direct worker exposure. Although HQ indicated negligible non-carcinogenic risks, CR exceeded acceptable limits across all zones, with Cr posing markedly higher risks than Ni. These findings align with previous reports of elevated cancer risks among welders and highlight a residual long-term cancer hazard even at moderate airborne concentrations. To mitigate these risks, effective control measures must be implemented in conjunction with continuous monitoring of metal-specific exposures to enhance worker health protection.

- 1. Iron and Steel Institute of Thailand I. Journals and Reports (Annual) 2022 [Available from: https://iiu.isit.or.th/en/reports/Yearly%20Report.aspx.
- 2. OSHA. Controlling Hazardous Fume and Gases during Welding 2013 [Available from: https://www.osha.gov/sites/default/files/publications/OSHA_FS-3647_Welding.pdf.
- 3. ECHA. European Union Risk Assessment report on chromium trioxide, sodium chromate, sodium dichromate, ammonium dichromate and potassium dichromate 2005 [Available from: https://echa.europa.eu/documents/10162/3be377f2-cb05-455f-b620-af3cbe2d570b.
- 4. ECHA. European Union Risk Assessment Report NICKEL 2008 [Available from: https://echa.europa.eu/documents/10162/cefda8bc-2952-4c11-885f-342aacf769b3.
- 5. Pakkarada Sansuksom JS-u. RISK ASSESSMENT OF WORKER EXPOSURE TO METAL FUME PRODUCED IN WELDING PROCESS. 2019.
- 6. The Government of the Hong Kong Special Administrative Region H. A Guide on Indoor Air Quality Certification Scheme for Offices and Public Places (2019) 2019. Available from: https://www.iaq.gov.hk/wp-content/uploads/2021/04/new-iaq-guide_eng.pdf.
- 7. NIOSH. ELEMENTS by ICP METHOD: 7303, Issue 1. 2003.
- 8. NIOSH. CHROMIUM and compounds, as Cr METHOD: 7024, Issue 2 1994.
- 9. Conducting a Human Health Risk Assessment [Internet]. 2022. Available from: https://epa.gov/risk/conducting-human-health-risk-assessment.
- 10. Show-Yi Yang1, Jia-Ming Lin1, Wan-Yu Lin3,4 and Ching-Wen Chang1,4. Cancer risk assessment for occupational exposure to chromium and nickel in welding fumes from pipeline construction, pressure container manufacturing, and shipyard building in Taiwan. J Occup Health. 2018.
- 11. Zainal Bakri S, Hariri A, Ismail M. Occupational Health Risk Assessment of Inhalation Exposure to Welding Fumes. International Journal of Emerging Trends in Engineering Research. 2020;8:90-7.

INFECTIOUS WASTE GENERATION, KNOWLEDGE, ATTITUDE AND PRACTICE OF PERSONNELS TO THE INFECTIOUS WASTE MANAGEMENT IN SUB-DISTRICT HEALTH PROMOTION HOSPITAL OF THE RAYONG PROVINCIAL ADMINISTRATIVE ORGANIZATION

 $\underline{\text{T. Ouengsakuncharoen}}^{a,b},$ C. Warodomrungsimun a,b , N. Khansakorn a,b , and T. Prechthai a,b

^aDepartment of Environmental Health Sciences, Faculty of Public Health, Mahidol University, 420/1 Rajvithi Rd., Rajchathawee, Bangkok, Thailand ^bCenter of Excellence on Environmental Health and Toxicology (EHT), OPS, MHESI, Bangkok, Thailand

* Corresponding author. E-mail address: tawach.pre@mahidol.ac.th

Abstract:

This study aimed to determine the generation rate of infectious waste as well as knowledge, attitude, and practices of personnel to manage the infectious waste in Sub-district Health Promoting Hospitals (SHPHs) of the Rayong Provincial Administrative Organization (Rayong PAO). The amount of infectious waste and number of patients were collected from 85 SHPHs whereas questionnaire was used to evaluate the level of knowledge, attitude and practice of personnels. The average infectious waste generation rate was 0.88 kg/SHPHs/day while the average number of patient was 32.00 persons/SHPH/day. The significant correlation between the amount of infectious and number of patients (p-value<0.05) was observed in this study. The positive correlation coefficient (r = 0.703) indicates the influence of number of patients to the amount of infectious waste of SHPHs. The average infectious waste generation rate of patients was 0.0284 kg/person/day. Regarding to the regulation on infectious disposal in Thailand, the approximately 96.47% of personnels have relatively high knowledge, attitude and practice to manage the infectious waste in SHPHs.

Keywords: Infectious waste, Sub-district Health Promoting Hospital, knowledge, attitude, practice

Introduction:

Rayong Province covers an area of 3,552 Km² which is divided into eight districts. The total population is about of 759,400 persons. This area is served as an industrial business hub following the Eastern Seaboard Development Project as well as a hub for technology, education, and research services. Because of high industrial investment, rapid urban expansion and population growth due to labor migration can be found in this province. This increasing of population also lead to increase of medical health care facilities and amount of infectious waste to be managed in this province. It has been reported that the amount of infectious waste generation in Rayong Province has increasing from 538.6 tons in 2019 to 1,087.1 tons in 2023 (Rayong PAO, 2023).

The Sub-district Health Promoting Hospitals (SHPHs) are considered as primary healthcare units in Rayong Province. The activities of SHPHs are not only medical treatment and health rehabilitation but also health promotion, disease prevention and control and management of health risk factors in the community. Currently, there are totally 95 sites of SHPHs in Rayong Province, which 85 sites are under the supervision of the Rayong Provincial Administrative Organization (Rayong PAO), whereas 10 sites are under the supervision of other local administrative organizations in Rayong Province. It was found that the total amount of infectious

waste generation from the 85 SHPHs of the Rayong PAO in 2023 was 19.07 tons (Rayong PAO, 2023). This may be related to number of patients seeking services at these facilities. This infectious waste generally needs to be managed properly to prevent environmental contamination and health impact from pathogenic microorganism such as infectious waste separation, collection, transportation, disinfection and disposal. In Thailand, the infectious waste management system of SHPHs have to follow to Ministerial Regulation on Infectious Waste Disposal B.E.2545 (2002). The previous studies on infectious waste management shows the correlation between knowledge, attitude and practice in the infectious waste management of personals in healthcare units (Husna Romin, 2017; Suphacha KamKhien, 2020). The objective to study, therefore, is to determine the infectious waste generation rate as well as the level of knowledge, attitude and practice in infectious waste management of personals in SHPHs of the Rayong PAO.

Materials and method:

This study was designed as cross-sectional survey research. The amount of infectious waste and the number of patients of 85 SHPHs in 2024 were available from the Rayong PAO. In addition, the general characteristics, knowledge, attitude and practice in infectious waste management of personnels were collected by using questionnaire. There are totally 45 items for knowledge, attitude and practice assessment and 13 items for general characteristics of respondent.

In this study, the questionnaire was reviewed for content validity by expert. It was then be pre-tested with personnels from SHPHs which are not under the Rayong PAO. The Kuder–Richardson formula and Cronbach's alpha were than used to assess the reliability of results. The Kuder–Richardson coefficient of knowledge for infectious waste management was 0.838. In addition, Cronbach's alpha coefficient for attitude and practice was 0.809 and 0.845, respectively. These results indicate the suitability of this questionnaire to be used in data collection in this study.

The criteria for interpreting the scores of knowledge, attitude, and practice of personnels SHPHs in regard to the ministerial regulation on infectious waste disposal of Thailand were determined by classifying the respondents' total scores into three levels as shown in Table 1.

Table 1: Criteria for interpreting scores of knowledge, attitude, and practice of personnels in regard to the ministerial regulation on infectious waste disposal of Thailand

C-4	Score Level (points)					
Category	High	Moderate	Low			
Knowledge	11–15	6–10	0–5			
Attitude	21–30	11–20	0–10			
Practice	21–30	11–20	0–10			

Results and discussion:

Generation rate of infectious waste in SHPHs

The infectious waste generation and patients of 85 SHPHs under the Rayong PAO in 2024 are shown in Table 2. The infectious waste generation ranged from 0.03 to 4.14 kg/SHPH/day with average of 0.880 kg/SHPH/day. In addition, the number of patients varied from 5 to 142 persons/SHPH/day. The average number of patients was 32 persons/SHPH/day. The calculation result of infectious waste generation rates of SHPHs under the Rayong PAO, therefore, were in range of 0.004 to 0.160 kg/person/day.

Table 2: Infectious waste generation and number patients of SHPHs in 2024

Data	Minimum	Maximum	Mean	Std. Deviation
Infectious waste (kg/ SHPH/day)	0.030	4.140	0.880	0.720
Number of patients (persons/ SHPH/day)	5.000	142.00	32.00	22.00
Infectious waste generation rate (kg/person/day)	0.004	0.160	0.028	0.019

The correlation analysis between the amount of infectious waste and the number of patients is presented in Table 3. The analysis of Pearson's correlation coefficient shows a significant correlation between the amount of waste and number of patients (P-value < 0.05). Moreover, the positive correlation coefficient (r = 0.703) indicates that the amount of infectious waste was increased to the number of patients. Based on the result of study, the average infectious waste generation rate of SHPHS was 0.028 kg/person/day. This is comparable to Lampang Province where the average infection waste generation rate was found at 0.030 kg/person/day (Khamjira Saiwongpia, 2016).

Table 3: Pearson's correlation coefficients between infectious waste and number of patients

Variable		Amount of infectious waste	Number of patients
Amount of infectious waste	Correlation coefficient P-value	1	.703**
Number of patients	Correlation coefficient P-value	.703** .000	1

Note: Correlation is statistically significant at the 0.01 level (2-tailed).

Knowledge, attitude, and practice of personnels on SHPHs

The scores of knowledge, attitudes, and practices of personnels in SHPHs in regard to the ministerial regulation on infectious waste disposal of Thailand are presented in Table 4. The average score of knowledge, attitude and practice of personnels to the infectious waste management system were 13.40, 27.92 and 28.22 points, respectively. It was found that personnels in SHPHs have relatively high knowledge, attitudes, and practices in infectious waste management. As shown in Table 5, the approximately 96.47% of personnels in SHPHs have high knowledge, attitude and practice in regard to regulation on the infectious waste disposal This result is consistent with the studies of Husna Romin (2017) and Angsumalee Arkornsakul and Yaowalak Amrumpai (2014), which examined the relationships between knowledge, attitudes, and infectious waste management among personnel in non-inpatient healthcare facilities. The distribution of knowledges, attitudes, and practices level of personnel in SHPHs under the Rayong PAO are presented in Table 5.

Table 4: Scores of knowledge, attitudes, and practices of personnels in SHPHs

Category	Mean	Standard Deviation	Maximum	Minimum
Knowledge	13.40	1.51	15	6
Attitudes	27.92	2.66	30	18
Practices	28.22	2.55	30	15

Table 5: Distribution of knowledge, attitudes, and practices level of personnel in SHPHs

Category	High (%)	Moderate (%)	Low (%)
Knowledge	96.47	3.53	0.00
Attitudes	96.47	3.53	0.00
Practices	96.47	3.53	0.00

Conclusion:

The amount of infectious waste generated by Subdistrict Health Promoting Hospitals (SHPHs) of the Rayong Provincial Administrative Organization (Rayong PAO) ranged from 0.03 to 4.14 kg/SHPHs/day with an average of 0.88 kg/SHPHs/day. There was significant correlation between the amount of infectious and number of patient (P-value<0.05) with correlation coefficient (r) of 0.703. The number of patients in SHPHs is in range of 5 to 142 persons/SHPHs with an average of 32 persons/SHPHs/day. In this study, the average infectious waste generation rate was 0.0284 kg/person/day. Regarding to the regulation on infectious disposal in Thailand, most of personnels in SHPHs (96.47%) have high knowledge, attitude and practice in the infectious waste management.

- 1. Angsumalee Arkornsakul and Yaowalak Amrumpai. (2014). Relationships between knowledge, attitude and infectious waste segregation among employees in clinics: A case study of Amphoe Pakkret, Nonthaburi Province. Thai Pharmaceutical and Health Science Journal, 9(3), 129–136.
- 2. Husna Romin. (2 0 1 7). A study of knowledge, attitude, and practice of personnel regarding infectious waste management in clinics, Phuket Province (Master's thesis, Prince of Songkla University).
- 3. Khamjira Saiwongpia. (2016). Infectious waste management model, Lampang Province (Master's thesis, Thammasat University).
- 4. Rayong Provincial Administrative Organization. (2023, August 18). Project for managing infectious waste disposal system using incineration technology. Rayong Provincial Administrative Organization. Retrieved [2 0 25, Jun 1 0], from https://www.rayong-pao.go.th/web/th/agencies/12/detail-news/N0001059.html.
- 5. Suphacha KamKhien. (2020–2021). Factors related to the infectious waste management behavior of personnel in Phichit Hospital. Academic Journal of Mahasarakham Provincial Public Health Office, 5(9), October 2020–March 2021.

MICROPLASTICS IN EVERYDAY DIET: QUANTIFYING CONTAMINATION IN SOFT DRINKS AND SEAFOOD IN THAILAND

Anh Tuan Ta¹

¹Department of Sanitary Engineering, Faculty of Public Health, Mahidol University, Bangkok, 10400, Thailand

Abstract:

Microplastic (MP) contamination in human food and beverages is an increasing concern, but evidence from Southeast Asia remains limited. This study examines MP presence in two main dietary sources in Thailand: soft drinks and seafood. A total of 378 soft drink samples from nine popular brands were analyzed across different packaging types (plastic, aluminum, and glass). MPs were found in all brands, with concentrations ranging from 2 ± 3 to 39 ± 12 items per liter. Surprisingly, glass bottles showed higher MP loads than plastic or aluminum packaging, likely due to frequent reuse and the high surface energy of glass that attracts particles. MPs were mainly small (50–100 µm), with fragments (41–82%) and spheres (especially in cans) as the predominant forms. Micro-FTIR analyses identified PET in plastic bottles, while PP and PE were common in glass-bottled drinks, reflecting the materials used for packaging and sealing. Seafood analysis included blood cockles (Tegillarca granosa) and green mussels (Perna viridis) collected from aquaculture farms and local markets. MPs were found in all specimens, with commercial samples showing higher loads than farmed ones, suggesting additional contamination during packaging and transportation. Polypropylene, polyethylene, polyester, and nylon were the most frequently detected polymers. Smaller size fractions dominated, raising concerns due to their bioavailability and persistence in human diets. These findings confirm that MPs infiltrate both beverages and seafood commonly consumed in Thailand. Estimated consumer exposure from soft drinks alone could reach up to 1,600 MPs per person annually, while seafood contributes an additional dietary route. Given MPs' potential to penetrate biological tissues and carry hazardous chemicals, this study highlights an urgent need for stricter food packaging regulations, safer supply chain practices, and further assessment of health implications for Thai consumers.

Keywords: Microplastics, soft drinks, seafood, human exposure, Thailand

Introduction:

Plastic pollution has become one of the leading environmental challenges of the 21st century, with global plastic production surpassing 380 million tons annually and increasing by 4% each year (PlasticsEurope, 2023). While much research has focused on marine debris and environmental impacts, the contamination of food and drinks by microplastics (MPs; <5 mm) has recently emerged as a major concern. MPs can be ingested directly by humans through daily consumption of packaged beverages and seafood, both of which are dietary staples in Thailand.

Thailand is the sixth largest global contributor to plastic leakage into the oceans, and its high reliance on plastic packaging further increases the likelihood of MP exposure (Thompson et al., 2004). Soft drinks, consumed at an average of 41 liters per person per year, and seafood, which forms a key protein source, are particularly relevant (Ta et al., 2025).

MPs not only persist in these products but also have the potential to carry hazardous additives and adsorbed contaminants such as heavy metals and persistent organic pollutants. Furthermore, small MPs ($<150~\mu m$) are of particular concern as they may penetrate gastrointestinal barriers, circulate in the bloodstream, and accumulate in tissues (Li et al., 2023). Despite these risks, there has been little systematic investigation of MP contamination in soft drinks and seafood in Thailand. This study therefore, aims to quantify MP concentrations in these commonly consumed products, characterize the particles by size, morphology, and polymer type, identify the role of packaging and supply chain processes in contributing to contamination, and assess the potential implications for human health and food safety in the Thai context.

Methodology:

Soft drink samples (n = 378) were collected from supermarkets in Pathum Thani in October 2023, covering nine popular brands and three packaging types: plastic bottles, aluminum cans, and glass bottles. Each sample was vacuum filtered through 0.45 μ m cellulose nitrate membranes, and the filters were dried at 60°C for 24 hours. Quantification of MPs was performed using Nile Red fluorescence microscopy, while polymer identification was confirmed by micro-FTIR spectroscopy. MPs were categorized by size into four ranges (50–100 μ m, 100–500 μ m, 500–1000 μ m, 1000–2000 μ m) and by morphology as fragments, fibers, spheres, or films. For seafood, blood cockles and green mussels were obtained from both aquaculture farms in Chonburi and Samut Prakan and from markets in Pathum Thani and Samut Prakan. Samples were digested with oxidizing solutions, subjected to density separation using sodium iodide, and analyzed under optical microscopy and FTIR to enumerate MPs and determine their polymer composition.

Results, Discussion and Conclusion:

MPs were detected in all soft drink samples across brands and packaging types. Concentrations ranged from 2 ± 3 to 39 ± 12 items/L, with glass bottles showing unexpectedly higher contamination than plastic and aluminum cans. This result is likely due to the frequent reuse of glass containers in Thailand and their higher surface energy, which enhances particle adhesion. MPs in soft drinks were dominated by the smallest size fraction, with particles between $50-100~\mu m$ accounting for nearly half to three-quarters of the total count. Morphologically, fragments were the most common (41–82%), followed by spheres, which were especially prevalent in aluminum cans. Polymer analysis revealed PET as the dominant polymer in plastic bottles, while PE and PP were more common in glass-packaged drinks, reflecting contributions from sealing and cap materials.

Seafood samples also revealed widespread MP contamination. Both mussels and cockles contained MPs, with market specimens consistently showing higher counts than those collected directly from aquaculture farms. For green mussels, the larger commercial individuals (25.4 g/individual) contained more MPs than smaller farmed specimens (3.5 g/individual), averaging 3.2 ± 1.6 items per individual in market mussels compared with 1.2 \pm 0.2 items per individual in farmed mussels. For blood cockles, market specimens (6.1 g/individual) also showed slightly higher MP levels than aquaculture farm cockles (5.8 g/individual). Polymer analysis identified polypropylene, polyethylene, polyester, and nylon as the dominant types, with nylon appearing only in market cockles, suggesting contamination during packaging and transport. Small particles dominated across all seafood samples, particularly those smaller than $100 \, \mu m$, echoing the trend observed in soft drinks and raising concern due to their higher potential for tissue uptake and persistence in the human body (Ta et al., 2022).

The findings confirm that both soft drinks and seafood are significant pathways of human exposure to microplastics in Thailand. The higher contamination observed in glass-bottled soft drinks challenges common perceptions of glass as a safer packaging material and highlights the risks associated with container reuse and post-processing. The predominance of small MPs is of particular concern, as these particles are more likely to be ingested and retained in the human body, potentially leading to oxidative stress, inflammation, and transport of hazardous chemicals into tissues. Seafood results further suggest that contamination is not only derived from the aquatic environment but also introduced during supply chain processes, including packaging and transportation.

Estimated exposure levels suggest that consuming soft drinks alone may lead to up to 1,600 MPs annually per person, with seafood adding a substantial dietary source. Although only a small portion of MPs are likely to be retained in the human body, lifelong exposure could increase health risks. This study provides the first baseline data on MP contamination in soft drinks and seafood in Thailand and highlights the need for regulatory measures, including better packaging standards, stricter hygiene practices during food handling, and systematic monitoring of MPs in dietary sources. Public awareness campaigns are also vital to decrease reliance on problematic packaging materials and to educate consumers about potential risks. Ultimately, these findings stress the importance of addressing MPs as a food safety concern and lay a foundation for future policies to safeguard public health in Thailand.

- 1. Li, Y., Tao, L., Wang, Q., Wang, F., Li, G., Song, M., 2023. Potential health impact of microplastics: a review of environmental distribution, human exposure, and toxic effects. Environment & Health 1, 249-257.
- 2. Plastics Europe, 2023. Plastics the fast Facts 2023. Plastics Europe, Brussels, Belgium.
- 3. Ta, A.T., Babel, S., Wang, L.P., 2025. Prevalence and characteristics of microplastic contamination in soft drinks and potential consumer exposure. Journal of Environmental Management 373, 123810.
- 4. Ta, A.T., Pupuang, P., Babel, S., Wang, L.P., 2022. Investigation of microplastic contamination in blood cockles and green mussels from selected aquaculture farms and markets in Thailand. Chemosphere 303, 134918.
- 5. Thompson, R.C., Olsen, Y., Mitchell, R.P., Davis, A., Rowland, S.J., John, A.W., McGonigle, D., Russell, A.E., 2004. Lost at sea: where is all the plastic? Science 304, 838-838.

THE ASSESSMENT OF HEALTH RISKS FROM CHEMICAL AND MICROBIOLOGICAL CONTAMINATION IN WATER USE: A CASE STUDY OF HUAI SO MUNICIPALITY, CHIANG KHONG DISTRICT, CHIANG RAI PROVINCE

A. Khanmee a, S.Sreesai*a,b, C.Warodomrungsimn a,b, C.Singhakant a,b, A. Phosri a,b

^a Department of Environmental Health Sciences, Faculty of Public Health, Mahidol University, 420/1 Rajvithi Rd., Rajchathawee, Bangkok, Thailand ^b Center of Excellence on Environmental Health and Toxicology (EHT), OPS, MHESI, Bangkok, Thailand

* Corresponding author E-mail address: siranee.sre@mahidol.ac.th

Abstract:

Access to clean water and adequate sanitation is a fundamental human right under Sustainable Development Goal 6 (SDG 6), which aims to ensure universal access to safe drinking water by 2030. This study aimed to assess health risks associated with chemical and microbiological contamination in water use (village tap water and coin-operated drinking water from vending machines) in Huai Xo Subdistrict Municipality, Chiang Khong District, Chiang Rai Province. This research employed a cross-sectional analytical study design, consisting of two phases. Phase 1 Water quality results were analyzed, and the drinking water consumption behaviors of 150 residents were surveyed for the calculation of the Hazard Quotient (HQ). Phase 2 focused on health risk assessment, employing the Hazard Quotient (HQ) approach for chemical contaminants and Quantitative Microbial Risk Assessment (QMRA) for microbiological contamination. The findings indicated that water quantity and quality had the lowest scored (mean = 2.61). Laboratory analysis fond contamination of coliform bacteria (90.48%) and E.coli (66.67%). The most frequently detected chemical contaminants were arsenic (61.90%) and fluoride (33.33%). The health risk assessment showed that fluoride levels exceeded HQ > 1 in some place specifically in Ban Chaipattana (HQ = 4.769), Ban Kaen Nuea (HQ = 2.733), and Ban Kieng Tai (HQ = 1.536). Arsenic contamination presented unacceptable cancer risks such as in Ban Kaen Nuea (1.57×10^{-2}) and Ban Kieng Tai (1.10×10^{-2}) . Regarding coin-operated water vending machines, most samples had HQ < 1, however, Ban Kieng Tai exhibited a fluoride HQ of 1.968, while arsenic was detected in 40% of the samples. Although E.coli was not found, coliform bacteria were still detected in 30% of the samples. In conclusion, the primary health risks associated with drinking water in the study area stemmed from fluoride and arsenic contamination, resulting in both non-carcinogenic risks (HQ > 1) and carcinogenic risks (Cancer Risk > 10⁻⁴), coupled with high rates of coliform contamination. Therefore, integrated measures for water quality improvement, continuous monitoring, and effective risk communication to the public are recommended to ensure long-term access to safe and sustainable drinking water.

Keywords: Water use, chemical and biological contaminants, health risk assessment, Chiang Rai Province

Introduction:

Access to clean water and adequate sanitation is a fundamental human right, as outlined in the United Nations' Sustainable Development Goal 6 (SDG 6) (1), which aims to ensure universal access to safe drinking water by 2030 (2). However, in 2022, more than 2.2 billion people worldwide still lacked access to safe drinking water, and 703 million people did not even have access to basic water services (1). In Thailand, although approximately 98% of the population has access to clean water, only 88% of households consume good-quality

tap water. According to surveillance conducted by the Department of Health over the past ten years, only 38.4% of household water supplies met the required standards (3). This issue is associated with the entire water supply chain, including production, distribution, and storage systems, as well as contamination from both chemical substances and microorganisms, which may result in gastrointestinal diseases or long-term health effects. Within the study area, Huai Xo Subdistrict Municipality, Chiang Khong District, Chiang Rai Province, is an agricultural zone where chemical substances are extensively used. Furthermore, the area lies along a gold mineral belt, posing a risk of heavy metal contamination in raw water sources. Consequently, this region warrants close monitoring. Therefore, the present study aims to assess the health risks posed by chemical and microbiological contamination in local water supply systems. The findings are expected to provide essential information for public risk communication and to support the development of strategies for improving water supply quality at the local level.

Methodology:

research cross-sectional analytical This was a study conducted Huai Xo Subdistrict Municipality, Chiang Khong District, Chiang Rai Province. The study was divided into two phases: (1) data collection and (2) health risk assessment. In Phase 1, data collection involved the evaluation of water qualities Water samples were collected from 21 village water supply systems, covering 21 villages, consisting of 16 groundwater-based systems and 5 surface water-based systems. In addition, 10 water samples were collected from coin-operated drinking water vending machines within the study area. All water samples were analyzed for chemical and microbiological quality at the Public Health Laboratory Division, Department of Health, Ministry of Public Health, Thailand. The analyses followed the criteria of the Thai Drinking Water Quality Standard (Department of Health, 2020). Parallel to the sampling, data on community water consumption behavior were obtained through a structured questionnaire designed to capture information on water sources and the daily volume of water intake. Phase 2 involved a health risk assessment based on data obtained from Phase 1, water quality analyses, and community water consumption behaviors. The health risk assessment for chemical contaminants was performed using the Hazard Quotient (HQ) method, in accordance with the United States Environmental Protection Agency (USEPA) guidelines (4). The HQ was calculated by dividing the Average Daily Dose (ADD) of a chemical by its Acceptable Daily Intake (ADI), as shown in Equation (1) and (2):

$$ADD = \underbrace{C \times IR \times EF \times ED}_{BW \times AT}$$
 (1)

$$HQ = ADD \over ADI$$
 (2)

Here, C denotes the concentration of the chemical in water; IR represents the daily water ingestion rate; EF indicates the frequency of exposure; ED refers to the duration of exposure; BW is the body weight of the individual; and AT corresponds to the averaging time applied for exposure assessment. An HQ value greater than 1 indicates that the average daily intake of the contaminant exceeds the acceptable safe level and is therefore considered a potential health risk. For microbiological risk assessment, the Codex Alimentarius Commission (5) guidelines were applied, employing the Quantitative Microbial Risk

Assessment (QMRA) approach with exponential dose–response modeling, as expressed in Equations (3)–(5):

$$P_i = 1 - \exp(-rd) \tag{3}$$

$$P_E = P (1 - e^{-mc})$$
 (4)

$$R - P_i x P_E \tag{5}$$

In these equations, Pi represents the probability of illness, while r denootes the parameter in the exponential model. The variable d refers to the ingested dose, expressed in MPN per day. PE corresponds to the probability of exposure, and P indicates the probability value or the exposure factor. m represents the daily volume of drinking water consumed, measured in milliliters, whereas C denotes the concentration of microorganisms, expressed in MPN per milliliter. Finally, R represents the overall risk of illness resulting from microbial infection.

Results and Discussion:

The results of the laboratory analyses revealed that contamination in the 21 village water supply systems was considerably high in terms of both microbiological and chemical parameters. Coliform bacteria were detected in 19 samples (90.48%), while E. coli was found in 14 samples (66.67%), reflecting insufficient effectiveness of disinfection practices. For chemical parameters, arsenic was detected in 13 samples (61.90%) and fluoride in 7 samples (33.33%), indicating that water quality remained inconsistent with the established standards. In contrast, the 10 coin-operated drinking water vending machines showed lower levels of contamination. The most prominent contaminant was arsenic, detected in 4 machines (40.00%), followed by coliform bacteria in 3 machines (30.00%) and fluoride in 1 machine (10.00%). Notably, E. coli was not detected in any of the vending machine samples. (Figure 1 and 2).

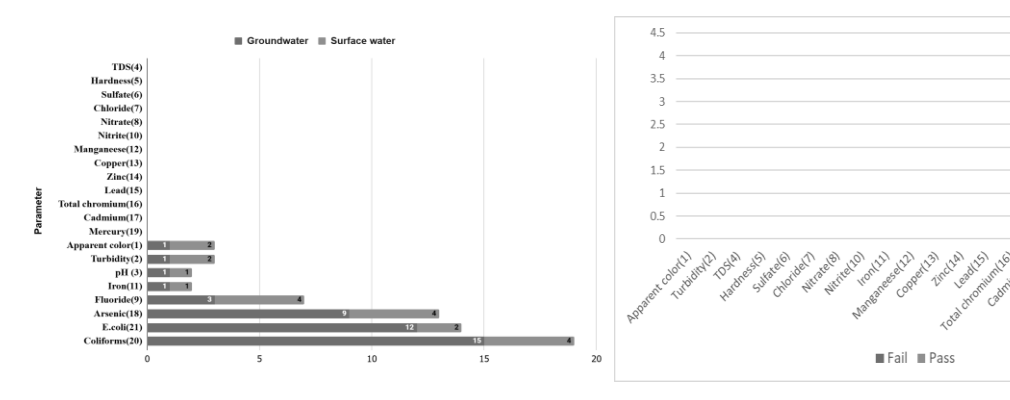


Figure 1. Drinking Water Samples with Detected Contamination Classified by Water Source Type

Figure 2. Drinking Water Samples with Detected Contamination in Coin-Operated Vending Machines

The chemical risk assessment revealed that fluoride levels in some systems had HQ values greater than 1, including Ban Chaipattana (HQ = 4.769), Ban Kaen Nuea (HQ = 2.733), and Ban Kieng Tai (HQ = 1.536). These findings indicate potential health risks, such as dental fluorosis and skeletal fluorosis, if consumption continues over time. In addition, arsenic contamination showed Cancer Risk values exceeding the acceptable standard. For instance, Ban Kaen Nuea reported a value of 1.57×10^{-2} and Ban Kieng Tai 1.10×10^{-2} , both of which are higher than the acceptable range (10^{-6} to 10^{-4}), suggesting a long-term carcinogenic risk.

Regarding the 10 coin-operated drinking water vending machines, most had HQ values below 1. However, risks from fluoride were still evident, particularly in the vending machine at Ban Kieng Tai, which recorded an HQ of 1.968, exceeding the safety threshold. Furthermore, arsenic was detected in some samples, with Cancer Risk values ranging from 10⁻³ to 10⁻², and coliform bacteria were present in 30% of the vending machines. Although E. coli was not detected, the presence of coliform bacteria still highlights a microbiological risk that cannot be overlooked. The study revealed high levels of arsenic and fluoride contamination, which is consistent with the findings of Rodtim et al. (2016), who assessed health risks from arsenic exposure in five types of domestic water sources: surface water supply, groundwater supply, mine pit water supply, mountain water supply, and shallow wells. The cancer risk assessment indicated that the overall risks from all water types ranged from 1.20E-04 to 7.23E-03 for children and from 4.58E-05 to 2.75E-03 for adults. (6) These results also align with Khair et al. (2011), who found that a large proportion of groundwater samples in China contained arsenic and fluoride concentrations exceeding WHO standards (As $> 10 \mu g/L$; F⁻ > 1.5 mg/L) (7), emphasizing that such contamination is closely linked to geological conditions. In terms of microbiological contamination, the high detection rates of coliform bacteria and E. coli in village water supply systems are in agreement with Yamasamit et al. (2020), who conducted a quantitative microbial risk assessment of drinking water dispensers at Thammasat University, Rangsit Campus. Their study found that individuals consuming water from dispensers located near cafeterias and lecture halls had higher probabilities of exposure and infection from total coliform and fecal coliform compared to those drinking from dispensers located in student dormitories. Specifically, the probabilities of exposure and infection from total coliform in all dispensers were 0.3529 and 3.69347E-05, respectively (8). These findings highlight the microbial risks associated with inadequately controlled water supply systems.

Conclusion:

The findings of this study indicate that the primary risks stem from fluoride and arsenic, which pose both non-carcinogenic effects (HQ > 1) and carcinogenic effects (Cancer Risk $> 10^{-4}$). In addition, the high rate of coliform contamination in village water supply systems and coin-operated vending machines further highlights microbiological risks. Therefore, addressing these issues requires an integrated approach, including the development of effective filtration and disinfection systems, continuous water quality monitoring, and public education on safe water consumption. Such measures are essential to ensure that village water supply systems can sustainably meet the demand for safe drinking water in the long term.

- 1. United Nations. Goal 6: Ensure access to water and sanitation for all [Internet]. 2023 [cited 2025 Jul 10]. Available from: https://www.un.org/sustainabledevelopment/water-and-sanitation/
- 2. United Nations Thailand. Sustainable Development Goals: Goal 6 Clean water and sanitation [Internet]. 2023 [cited 2025 Jul 10]. Available from: https://thailand.un.org/th/sdgs/6
- 3. Department of Health. Summary report on household drinking water quality surveillance, fiscal year 2022 [Internet]. Nonthaburi: Department of Health; 2022 [cited 2025 Jul 10]. Available from: http://foodsan.anamai.moph.go.th

- 4. United States Environmental Protection Agency (USEPA). Risk assessment guidance for superfund. Volume I: Human health evaluation manual, Part A. Interim final report. Washington, DC: Office of Solid Waste and Emergency Response; 1989. Report No.: EPA/540/1-89/002.
- 5. Haas CN, Rose JB, Gerba CP. Quantitative microbial risk assessment. 2nd ed. Hoboken, NJ: John Wiley & Sons; 2014.
- 6. Mutathip Rodtim, Mallika Panyakapo, & Panupong Prommarat. (2016). Health risk assessment from arsenic exposure in domestic water sources in the former tin mining area of Surat Thani Province. Veridian E-Journal Science and Technology, Silpakorn University, 3(1), 34–47.
- 7. Khair, A. M., Li, C., Hu, Q., Gao, X., & Wanga, Y. (2014). Fluoride and arsenic hydrogeochemistry of groundwater at Yuncheng Basin, Northern China. Geochemistry International, 52(10), 868-881.
- 8. Nattapong Yamasamit, Woranee Mungkalasiri, Kanjana Changkaew, & Jitti Mungkalasiri. (2020). Quantitative microbial risk assessment of total coliform and fecal coliform from drinking water dispensers at Thammasat University, Rangsit Campus. Thai Science and Technology Journal, 28(8), 1428–1436.

THE EFFECTIVENESS OF FOOD HANDLER TRAINING COURSES ON HYGIENE AND SANITATION COMPETENCIES OF FOOD HANDLERS IN NONTHABURI MUNICIPALITY

J. Duangsonsaeng a,c*, S. Sreesai a,c*, C. Singhakant a,c, J. Sillabutra b

a Department of Environmental Health Sciences, Faculty of Public Health, Mahidol University

b Department of Biostatistics, Faculty of Public Health, Mahidol University

420/1 Rajvithi Rd., Rajchathawee, Bangkok, Thailand

c Center of Excellence on Environmental Health and Toxicology (EHT), OPS, MHESI, Bangkok, Thailand

* Corresponding author E-mail address: Siranee.sre@mahidol.ac.th

Abstract:

This survey research was aimed to compare the effectiveness of a food handler training program on hygiene and sanitation competencies between two training formats: training at the training venue (onsite training) and training via digital technology (online training). The sample consisted of 180 food handlers from food establishments in Nonthaburi Municipality, which equally divided into 9 0 participants per group. Data collection tools included a knowledge test, an attitude questionnaire, a practice questionnaire, and a sanitation standard assessment checklist based on the Department of Health's criteria (Clean Food Good Taste). Data were analyzed using descriptive and inferential statistics such as Chi-square test, and Independent Sample t-test at a significance level of 0.05.

Results of the study revealed that both training formats significantly improved knowledge, attitudes, and practices regarding food hygiene and sanitation (p < 0.05). After the training, all participants in both formats demonstrated good levels of knowledge, attitudes, and practices (100.00%). No statistically significant difference was found in knowledge scores between the groups (p = 0.657). The online training group had a significantly higher mean attitude score than the onsite training group (p = 0.039), whereas the onsite training group showed a significantly higher mean practice score compared to the online training group (p < 0.001). Chi-square test results indicated that knowledge and attitude were not significantly associated with the training format (p > 0.05). On the contrary, practices were significantly associated with the onsite training format (p < 0.001). Clear improvements after both training formats were observed in the individual and environmental domains. Food establishments that met food sanitation standards were proportionally higher in the onsite training group (44.19%) compared to the online training group (3 5 . 0 0 %). In conclusion, both training formats were effective in enhancing the competencies of food handlers. However, onsite training was more suitable for developing actual practices and compliance with sanitation standards. The findings suggest that continuous training should be promoted among food handlers, particularly those with less experience or who have never attended food sanitation training. Online training through video presentations should be further developed and integrated with instructor-led teaching to enhance learning effectiveness. Training content should emphasize personal hygiene as a priority, and a long-term follow-up system should be implemented to assess whether improvements in knowledge and attitudes translate into actual hygienic practices in food establishments. Relevant authorities should establish strategies to diversify and adapt training content to be more suitable for specific target groups.

Keywords: Food handlers, training formats at the training venue (onsite training), training formats via digital technology (online training), food handler courses, sanitation competency level of food handlers

Introduction:

Quality and safe food is a critical determinant of national health, economic stability, and social well-being. Thailand continues to encounter challenges related to food- and waterborne diseases, such as diarrhea and food poisoning (1), which persist as recurrent public health concerns. A key contributing factor is the unhygienic practices of food handlers. Accordingly, training food handlers has become a vital strategy to mitigate risks, enhance knowledge and understanding, and promote proper practices, thereby strengthening the quality standards of food establishments. Nonthaburi Province, characterized by rapid economic and social growth, has witnessed an expansion in food-related businesses, particularly food outlets. This expansion has, however, reduced the degree of regulatory oversight in food hygiene and sanitation due to competitive pressures arising from increasing consumer demand. As a result, food establishments face a heightened risk of microbial contamination, which may subsequently lead to food- and waterborne illnesses (2). To address these challenges, both training formats at the training venue (onsite training) programs and training formats via digital technology (online training) have been adopted as key approaches to develop food handler competencies in line with technological advancements and emerging lifestyles (3).

Materials and Methods:

This study employed a survey research design. The sample was divided into two groups. Group 1 consisted of food handlers who received onsite training, delivered in three different formats: (1) onsite training conducted by instructors, (2) onsite training through video presentations, and (3) onsite training combining video presentations with instructor-led teaching. Group 2 consisted of food handlers who received online training, also delivered in three different formats: (1) online training conducted by instructors, (2) online training through video presentations, and (3) online training via an e-learning system. Purposive sampling was applied, and measurements were taken before and after the training. The population consisted of food handlers from various types of food establishments in Nonthaburi Municipality, with a total sample size of 180 participants. They were divided into two groups: onsite training (n = 90) and online training (n = 90). Research instruments included (1) a knowledge test, (2) an attitude questionnaire, (3) a practice questionnaire, and (4) a sanitation standard evaluation form based on the Clean Food Good Taste criteria. Data were analyzed using descriptive and inferential statistics (Chi-square test and Independent Sample t-test).

Results and Discussion:

The study found that after the training, both onsite training and online training groups demonstrated significantly higher levels of knowledge, attitudes, and practices (p < 0.05). All participants achieved good levels of knowledge, attitudes, and practices (100.00%). However, some differences were observed: the online training group had significantly higher attitudes compared to the onsite training group (p = 0.039), whereas the onsite training group demonstrated significantly higher practices than the online training group (p < 0.001). Clear post-training improvements were evident in both formats, such as personal aspects (e.g., proper hygienic attire) and place aspects (e.g., having a trash can with a tight-fitting lid and a grease trap before releasing wastewater into the public sewer). Correlation analysis revealed that knowledge and attitudes were not associated with the type of training, while practices were significantly associated with the training format (p < 0.001) (Table 1). Furthermore, food establishments meeting the Clean Food Good Taste sanitation standards were higher in the onsite group (44.19%) compared to the online group (35.00%) (Table 2). These findings suggest that both training formats were effective in enhancing

the competencies of food handlers. However, onsite training had a greater impact on actual practices, as hands-on activities under the supervision of trainers facilitated learning and fostered sustainable behavioral changes (4). In contrast, although online training offered greater convenience and accessibility, it still faced limitations in monitoring and practical engagement (5).

Table 1 Relationship between knowledge, attitudes, and practices in food hygiene and sanitation among food handlers across onsite and online training formats (N = 180)

Food handler	Knowledge		lge Attitudes		Practices		
competency	onsite	online	onsite	online	onsite	online	
level	(%)	(%)	(%)	(%)	(%)	(%)	
Good level	100.00	100.00	100.00	100.00	100.00	100.00	
Fair level	0	0	0	0	0	0	
Improved level	0	0	0	0	0	0	
df	5		17		23		
x^2	7.450		23.806		168.267		
p-value	0.189		0.125		<0.001		

Table 2 Assessment of food establishment quality based on food sanitation criteria (Clean Food Good Taste), including physical and biological aspects, between onsite and online training formats

	Onsite training (n = 43)				Online training (n = 40)			
Quality of food establishment	Before training		After training		Before training		After training	
	Number (of places)	%	Number (of places)	%	Number (of places)	%	Number (of places)	%
Passed Clean								_
Food Good	5	11.63	19	44.19	5	12.50	14	35.00
Taste standards								
No passed								
Clean Food	38	88.37	24	55.81	35	87.50	26	65.00
Good Taste	36	00.37	24	.4 33.61	33	67.50	20	05.00
standards								
Total	43	100.00	43	100.00	40	100.00	40	100.00

Conclusion:

Onsite training demonstrates greater potential to promote sustainable behavioral changes among food handlers, while online training remains valuable for enhancing accessibility and knowledge acquisition. Integrating both formats could maximize training effectiveness, combining the convenience of online learning with the practical reinforcement of onsite instruction. The findings suggest that continuous training programs, particularly targeting inexperienced food handlers or those who have never undergone training. Online training should be enhanced by incorporating interactive video materials alongside

instructor-led sessions to increase effectiveness. Additionally, a long-term monitoring system should be implemented to assess whether improved knowledge and attitudes translate into actual hygienic practices in food establishments.

- 1. Bureau of Epidemiology Department of Disease Control. National Disease Surveillance (Report 506). [cited 2022 Sep 10]. Available from: http://doe.moph.go.th/surdata/index.php
- 2. Todd ECD, Greig JD, Bartleson CA, Michaels BS. Outbreaks where food workers have been implicated in the spread of foodborne disease. Part 11. Use of antiseptics and sanitizers in community settings and issues of hand hygiene compliance in health care and food industries. J Food Prot. 2010;73(12):2306–2320
- 3. Salas E, Tannenbaum SI, Kraiger K, Smith-Jentsch KA. The science of training and development in organizations: What matters in practice. Psychol Sci Public Interest. 2012;13(2):74–101.
- 4. Insfran-Rivarola A, Tlapa D, Limon-Romero J, Baez-Lopez Y, Miranda-Ackerman M, Arredondo-Soto K, Ontiveros S. A systematic review and meta-analysis of the effects of food safety and hygiene training on food handlers. Foods (Basel). 2020 Aug 25;9(9):1169.
- 5. Lee J. Impact of hands-on training methods on food safety practices among food handlers. J Food Prot. 2021;84(4):716–24.



Center of Excellence on Environmental Health and Toxicology (EHT)

Faculty of Science, Mahidol University K Building, 5th Floor, K 514, Rama VI Road Bangkok 10400, Thailand

Tel: 0-2201-5913-14

Website - eht.sc.mahidol.ac.th